Charles University in Prague

Faculty of Natural Sciences

Department of Physical and Macromolecular Chemistry

Study Program: Macromolecular Chemistry

Nanostructured conducting polymer composites

Doctoral Thesis by

Islam Mohamed Mohamed MINISY

Supervisor: Patrycja Magdalena Bober, PhD.
Institute of Macromolecular Chemistry, Czech Academy of Sciences

Prague 2022

Univerzita Karlova v Praze

Přírodovědecká Fakulta

Katedra fyzikální a makromolekulární chemie

Studijní program: Makromolekulární chemie

Nanostrukturované vodivé polymerní kompozity

Doktorská disertační práce

Mgr. Islam Mohamed Mohamed MINISY

Školitel: Ing. Patrycja Magdalena Bober, PhD.
Ústav makromolekulární chemie, Akademie věd České republiky, v.v.i.

Praha 2022

Declaration:

This Thesis describes my original work except where acknowledgment is made in the text. It is not substantially the same as any work that has been or is being submitted to any other University for any degree, diploma or any other qualification.

Prague, 1 March 2022

Islam M. MINISY

Dedicated to the soul of my beloved father

Acknowledgment

It has been four years of hard research work to accomplish my thesis, I have learned a lot, not just in science and research but also to be an effective member of a working team. Scientific research is not an easy task, without persistence and long-term undertaking, nothing can be achieved. For all of that, I am grateful to who I lean on, and who have made this work reach the finish line.

I owe thanks to Dr. Patrycja Bober, my supervisor, for her continuous support and guidance. I was lucky to get such an active, motivative and supportive supervisor. Without her support, this work cannot have been finished during this time.

Also, I would thank all people I worked with, single out Dr. J. Stejskal for his support and deep knowledge in the field of conducting polymers. I acknowledge that most of the characterization techniques used in this thesis are in cooperation with researchers who co-authored the published papers; I would like to thank Mrs. J. Hromádková for electron microscopy, Mr. U. Acharya for electrical conductivity measurements, Dr. M. Trchová, O. Taboubi and others for FTIR and Raman spectroscopies, and many others for their significant contributions to fulfill this thesis.

My sincere gratitude and respect go to my laboratory co-workers for their cooperation and assistance, and to everyone who helped me to accomplish this work, who are not explicitly named, whose enthusiasm, interest and support have motivated me to realize this achievement. I am grateful for their time which they shared with me and made my stay in Prague enjoyable.

Very special thanks and pure love go to my family, especially my beloved mother, my sisters and my brother, for their unconditional support, love, and prayers.

Table of Contents

List of the publications constituting the Thesis

1. **I.M. Minisy**, P. Bober, U. Acharya, M. Trchová, J. Hromádková, J. Pfleger, J. Stejskal, Cationic dyes as morphology-guiding agents for one-dimensional polypyrrole with improved conductivity, *Polymer*, 174 (2019) 11–17. DOI: 10.1016/j.polymer.2019.04.045 IF 4.231

2. **I.M. Minisy**, N. Gavrilov, U. Acharya, Z. Morávková, C. Unterweger, M. Mičušík, S.K. Filippov, J. Kredatusová, I.A. Pašti, S. Breitenbach, G. Ćirić-Marjanović, J. Stejskal, P. Bober, Tailoring of carbonized polypyrrole nanotubes core by different polypyrrole shells for oxygen reduction reaction selectivity modification, *Journal of Colloid and Interface Science*, 551 (2019) 184–194. DOI: 10.1016/j.jcis.2019.04.064 IF 7.489

3. **I.M. Minisy**, B.A. Zasońska, E. Petrovský, P. Veverka, I. Šeděnková, J. Hromádková, P. Bober, Poly(*p*-phenylenediamine)/maghemite composite as highly effective adsorbent for anionic dye removal, *Reactive and Functional Polymers*, 146 (2020) 104436. DOI: 10.1016/j.reactfunctpolym.2019.104436 IF 3.975

4. P. Bober, **I.M. Minisy**, U. Acharya, J. Pfleger, V. Babayan, N. Kazantseva, J. Hodan, J. Stejskal, Conducting polymer composite aerogel with magnetic properties for organic dye removal, *Synthetic Metals*, 260 (2020) 116266:1–6. DOI: 10.1016/j.synthmet.2019.116266 IF 3.266

5. **I.M. Minisy**, P. Bober, I. Šeděnková, J. Stejskal, Methyl red dye in the tuning of polypyrrole conductivity, *Polymer*, 207 (2020) 122854:1–9. DOI: 10.1016/j.polymer. 2020.122854116266 IF 4.430

6. **I.M. Minisy**, U. Acharya, L. Kobera, M. Trchova, C. Unterweger, S. Breitenbach, J. Brus, J. Pfleger, J. Stejskal, P. Bober, Highly conducting 1-D polypyrrole prepared in the presence of safranin, *Journal of Materials Chemistry C*, 8 (2020) 12140–12147. DOI: 10.1039/D0TC02838J IF 7.393

7. **I.M. Minisy**, P. Bober, Frozen-state polymerization as a tool in conductivity enhancement of polypyrrole, *Macromolecular Rapid Communications*, 41(17) (2020) 2000364:1–5. DOI: 10.1002/marc.202000364 IF 5.734

8. **I.M. Minisy,** U. Acharya, S. Veigel, Z. Morávková, O. Taboubi, J. Hodan, S. Breitenbach, C. Unterweger, W. Gindl-Altmutter, P. Bober, Sponge-like polypyrrole–nanofibrillated cellulose aerogels: Synthesis and application, *Journal of Materials Chemistry C*, 9 (2021) 126151–12623. DOI: 10.1039/D1TC03006J IF 7.393

List of publications not included in the Thesis

1. M.M. Ayad, W.A. Amer, S. Zaghlol, **I.M. Minisy**, P. Bober, J. Stejskal, Polypyrrole-coated cotton textile as adsorbent of methylene blue dye, *Chemical Papers*, 7 (2018) 1605–1618. DOI: 10.1007/s11696-018-0442-6 IF 1.246

2. **I.M. Minisy**, N.A. Salahuddin, M.M. Ayad, Chitosan/Polyaniline hybrid for the removal of cationic and anionic dyes from aqueous solutions, *Journal of Applied Polymer Science*, 136 (2019) 47056:1–12. DOI: 10.1002/app.47056 IF 2.520

3. M.M. Ayad, N.L. Torad, **I.M. Minisy**, R. Izriq, E.M. Ebeid, A wide range sensor of a 3D mesoporous silica coated QCM electrodes, *Journal of Porous Materials*, 26 (2019) 1731–1741. DOI: 10.1007/s10934-019-00765-3 IF 2.183

4. M. Kumorek, **I.M. Minisy**, T. Krunclová, T. Krunclová, M. Voršiláková, K. Venclíková, E. M. Chánová, O. Janoušková, D. Kubies, pH-responsive and antibacterial properties of self-assembled multilayer films based on chitosan and tannic acid, *Materials Science and Engineering C*, 109 (2020) 110493:1–13. DOI: 10.1016/j.msec.2019.110493 IF 7.328

5. **I.M. Minisy**, N.A. Salahuddin, M.M. Ayad, In vitro release study of ketoprofen-loaded chitosan/polyaniline nanofibers, *Polymer Bulletin*, 78 (2021) 5609–5622. DOI: 10.1007/s00289-020-03385-z IF 2.870

6. **I.M. Minisy**, N.A. Salahuddin, M.M. Ayad, Adsorption of methylene blue onto chitosan–montmorillonite/polyaniline nanocomposite, *Applied Clay Science*, 203 (2021) 105993:1–10. DOI: 10.1016/j.clay.2021.105993 IF 5.467

7. Z. Moravkova, O. Taboubi, **I.M. Minisy**, P. Bober, The evolution of the molecular structure of polypyrrole during chemical polymerization, *Synthetic Metals*, 271 (2021) 116608:1–6. DOI: 10.1016/j.synthmet.2020.116608 IF 3.266

8. D.V. Tumacder, Z. Morávková, **I.M. Minisy**, J. Hromádková, P. Bober, Electropolymerized polypyrrole-safranin films: capacitance enhancement, *Polymer*, 230 (2021) 124099:1–9. DOI: 10.1016/j.polymer.2021.124099 IF 4.430

9. N.L. Torad, **I.M. Minisy**, H. Sharaf, J. Stejskal, Y. Yamauchi, M.M. Ayad, Gas sensing properties of polypyrrole/poly(*N*-vinylpyrrolidone) nanorods/nanotubes-coated quartz-crystal microbalance sensor, *Synthetic Metals*, 282 (2021) 116935:1–8. DOI: 10.1016/j.synthmet.2021.116935 IF 3.266

10. K. Milakin, U. Acharya, I.M. Minisy, D.V. Tumacder, Z. Morávková, O. Taboubi, T. Syrový, L. Syrová, J. Pfleger, P. Bober, Tuning of surface properties of conducting films cast from polyaniline-phytic acid-poly(N-vinylpyrrolidone) dispersions, *Progress in Organic Coatings*, 163 (2022) 106666:1–9. DOI: 10.1016/j.porgcoat.2021.106666

IF 5.161

Scientometric data of I.M. Minisy:

Publications 22, *h*-Index: 11, Total number of citations: 332, according to SCOPUS.

Publications 22, *h*-Index: 10, Total number of citations: 297, according to Web of Science.

records were collected on 01.03.2022.

The results of the Thesis presented by I.M. Minisy at scientific meetings

1. **I.M. Minisy,** P. Bober, U. Acharya, M. Trchova, J. Stejskal, Effect of safranin on the polymerization of pyrrole: morphology and conductivity control, Career in Polymers X, Book of Abstracts. Prague: Institute of Macromolecular Chemistry, CAS, P-4. ISBN 978-80-85009-90-3, 22–23.6.2018 (Poster Presentation).

2. **I.M. Minisy,** N. Gavrilov, U. Acharya, C. Unterweger, J. Stejskal, P. Bober, Carbonized polypyrrole nanotubes covered with globular, nanofibrilar or nanotubular polypyrrole, 3rd International Meeting on Materials Science for Energy Related Applications, Belgrade, Serbia, 25–26.9.2018 (Poster Presentation).

3. **I.M. Minisy,** P. Bober, U. Acharya, J. Pfleger, M. Trchová, J. Stejskal, Polypyrrole prepared in the presence of safranin or phenosafranin: the tuning of morphology and conductivity, lectures and oral communications for the 6th Young Polymer Scientists Conference & Short Course, San Sebastian, Spain, 1–3.10.2018 (Oral presentation).

4. **I.M. Minisy,** P. Bober, U. Acharya, J. Pfleger, M. Trchová, J. Stejskal, Polypyrrole prepared in the presence of safranin or phenosafranin: the tuning of morphology and conductivity, ECNP International Conference on Nanostructured Polymers and Nanocomposites /10/. San Sebastian, Spain, 3–5.10.2018 (Poster Presentation).

5. **I.M. Minisy**, U. Acharya, M. Trchová, L. Kobera, J. Brus, J. Pfleger, J. Stejskal, P. Bober, Highly electrically conductive 1D-polypyrrole prepared in the presence of safranin, 6th Nano Today Conference, Lisbon, Portugal, 16–20.6.2019 (Poster Presentation).

6. **I.M. Minisy**, U. Acharya, J. Hodan, J. Hromádková, P. Bober, Polypyrrole-nanofibrillated cellulose cryogels: synthesis and application, Career in Polymers XI, Book of Abstracts. Prague: Institute of Macromolecular Chemistry, Czech Academy of Sciences, 2019. P-2. ISBN 978-80-85009-94-1, 28–29.6.2019 (Poster Presentation).

7. **I.M. Minisy**, U. Acharya, S. Veigel, Z. Morávková, O. Taboubi, J. Hodan, S. Breitenbach, C. Unterweger, W. Gindl-Altmutter, P. Bober, Removal of hexavalent chromium ions by sponge-like polypyrrole-nanofibrillated cellulose aerogels, 7th Young Polymer Scientists Conference and Short Course, Lodz, Poland (online), 27–28.9.2021 (Poster Presentation).

The results of the Thesis presented by co-authors of research papers at scientific meetings

1. U. Acharya, **I.M. Minisy**, B. Zasońska, J. Pfleger, Syntheses and electrical properties of poly(p-phenylenediamine)/maghemite composites, Career in Polymers XI, Book of Abstracts. Prague: Institute of Macromolecular Chemistry, Czech Academy of Sciences, 2019. P-6. ISBN 978-80-85009-94-1, Workshop "Career in Polymers XI". Prague, CR, 28–29.6.2019

2. P. Bober, **I.M. Minisy**, U. Acharya, J. Hodan, B. Zasońska, J. Pfleger, J. Stejskal, Macroporous conducting polypyrrole cryogels, Book of abstracts. Birmingham: Royal Society of Chemistry, 2019. P-154, International Conference on Materials Chemistry /14/ MC14. Birmingham, UK, 8–11.7.2019

3. U. Acharya, P. Bober, **I.M. Minisy**, B. Zasońska, J. Pfleger, Electrical impedance spectroscopy of poly(*p*-phenylenediamine)/maghemite composites Book of abstracts. Birmingham: Royal Society of Chemistry, 2019. P-94, International Conference on Materials Chemistry /14/ MC14. Birmingham, UK, 8–11.7.2019

4. P. Bober, **I.M. Minisy**, U. Acharya, K. Milakin, M. Trchová, J. Pfleger, J. Hodan, J. Hromádková, J. Stejskal, Conducting polymers cryogels, aerogels and carbogels, Career in Polymers XI, Book of Abstracts. Prague: Institute of Macromolecular Chemistry, Czech Academy of Sciences, 2019. ML-1. ISBN 978-80-85009-94-1, Workshop "Career in Polymers XI". Prague, CR, 28–29.6.2019

5. P. Bober, **I.M. Minisy**, U. Acharya, J. Pfleger, J. Stejskal, Polypyrrole composites-enhancement of electrical conductivity, ECNP Workshop on Progress in Nanostructured Polymers, Lodz: Lodz University of Technology, Faculty of Chemistry, Department of Molecular Physics, Program and Abstracts. 2020, s. 20, /1./. Lodz, Polsko, 14.12.2020

List of abbreviations and notations

AB	Acid Blue 25
APS	Ammonium peroxydisulfate
Cr(VI)	Chromium hexavalent ion
CPs	Conducting polymers
DC	Direct current
FTIR	Fourier transform infrared spectroscopy
MO	Methyl orange
MR	Methyl red
NMP	*N*-methyl-2-pyrrolidone
NFC	Nanofibrillated cellulose
ORR	Oxygen reduction reactions
PA	Polyacetylene
PANI	Polyaniline
PEDOT	Poly(3,4-ethylenedioxythiophene)
PPDA	Poly(*p*-phenylenediamine)
PPDA–γ-Fe_3O_4	Poly(*p*-phenylenediamine)–maghemite nanocomposite
PPy	Polypyrrole
PVAL	Poly(vinyl alcohol)
RB	Reactive black 5
SEM	Scanning electron microscopy
TEM	Transmission electron microscopy
TGA	Thermogravimetric analysis
UV-Vis	Ultraviolet–visible spectroscopy

Abstract

Conducting polymers (CPs) combine the electrical properties of semiconductors and material properties of organic polymers. Polypyrrole (PPy) and polyaniline (PANI) are the most studied CPs due to their relatively high electrical conductivity (typically several units S cm^{-1}), environmental stability, ease of preparation, good processability and low cost.

Organic dyes have similar properties as surfactants, with an interesting ability to form various organized templates in water that could during synthesis tailor PPy morphologies to various nanostructures with high yield and improved electrical conductivity.

Herein, PPy was prepared in the presence of cations dyes, safranin and phenosafranin, and anionic dye, methyl red, to obtain various nanostructures. The effect of dye concentration, oxidant-to-pyrrole mole ratio and other polymerization conditions on the physicochemical properties of the produced PPy was carefully investigated. Pyrrole was polymerized in the frozen reaction media at −24 °C in the presence of safranin, Acid Blue 25 (AB) or methyl orange (MO). Prepared one-dimensional nanostructures exhibited high yield and improved conductivity; the highest conductivity of 175 S cm^{-1} was obtained when safranin was used.

Polypyrrole nanotubes prepared in the presence of MO were carbonized at 650 °C in an inert atmosphere followed by coating with pristine PPy or PPy prepared in the presence of MO or AB. The obtained products with high specific surface area and conductivity were used as electrochemical catalysts for the oxygen reduction reaction.

Poly(*p*-phenylenediamine) (PPDA) was prepared by the oxidative polymerization of *p*-phenylenediamine in the presence of various contents of maghemite. PPDA/maghemite composites have been used as adsorbents for the removal of Reactive Black 5 (RB) from water. The incorporation of magnetic nanoparticles provides easy separation of composites by applying a magnetic field and it improves the adsorption capacity. The adsorption isotherms and kinetics were analyzed by using various models.

Polyaniline/poly(vinyl alcohol) (PANI/PVAL) macroporous aerogels were prepared by the *in-situ* cryopolymerization of aniline in the presence of PVAL and Ni_2SrCr_xW hexaferrite, followed by freeze-drying. Aerogel with high coercivity was used as an adsorbent for the removal of RB from water, with a removal efficiency of 99%.

Polypyrrole–nanofibrillated cellulose (NFC) cryogels were prepared under frozen conditions in the presence of low contents of NFC (0.2 – 2 wt%). The sponge-like, lightweight aerogels prepared by freeze-drying, possess excellent mechanical properties and high conductivity. Moreover, PPy–NFC aerogels have high adsorption capacities towards Cr(VI) ions, due to their high specific surface area and excellent ion-exchange capability.

Within this study, for all the prepared materials, the DC electrical conductivity was determined by the van der Pauw method, morphology and supramolecular structures were examined by scanning and transmission electron microscopies, molecular structures were confirmed by Fourier-transform infrared, Raman and nuclear magnetic resonance spectroscopies and thermal stabilities were studied by thermogravimetric analysis.

Keywords

Conducting polymers;

Conductivity;

Cryopolymerization;

Dye adsorption;

Magnetic composites;

Morphology;

Organic dyes;

Poly(*p*-phenylenediamine);

Polyaniline;

Polymerization temperature;

Polypyrrole.

Abstrakt

Vodivé polymery kombinují elektrické vlastnosti polovodičů s materiálovými vlastnostmi organických polymerů. Polypyrrol (PPy) a polyanilin (PANI) jsou nejvíce studovanými polymery díky relativně vysoké elektrické vodivosti (několik jednotek S cm^{-1}), dobré stabilitě v běžném prostředí, jednoduchosti přípravy, dobré zpracovatelnosti a nízké ceně.

Organická barviva mají podobné vlastnosti jako surfaktanty se zajímavou schopností vytváření různých organizovaných struktur ve vodě, které mohou při přípravě upravovat morfologii PPy do různých nanostruktur, a to ve vysokém výtěžku a se zlepšenou vodivostí.

V této práci, PPy byl připraven v přítomnosti kationtových barviv, safraninu a fenosafraninu, a aniontového barviva, methylčerveně, s cílem získat různé nanostruktury. Byl pečlivě zkoumám vliv koncentrace barviva a molárního poměru oxidant/pyrrol na fyzikálně chemické vlastnosti vytvářeného PPy. Pyrrol byl polymerován ve zmrzlém reakčním mediu při −24 °C v přítomnosti safraninu, Acid Blue 25, a methyloranže. Připravené jednorozměrné nanostruktury vykázaly vysoký výtěžek a zlepšenou vodivost, kdy nejvyšší vodivost 175 S cm^{-1} byla získána při použití safraninu.

Polypyrrolové nanotrubky připravené v přítomnosti methyloranže byly karbonizovány při 650°C v inertní atmosféře a následně pokryty polypyrrolem nebo polypyrrolem připraveným v přítomnosti methyloranže či Acid Blue 25. Získané produkty s vysokým specifickým povrchem a vodivostí pak byly použity jako elektrochemické katalyzárory pro redukci kyslíku.

Poly(*p*-fenylendiamin) (PPDA) byl dále připraven oxidativní polymerací *p*-fenylendiaminu v přítomnosti různého množství maghemitu. Kompozity PPDA/maghemit byly použity k adsorptivnímu odstranění barviva Reactive Black 5 z vody. Přítomnost magnetických nanočástic umožňuje jednoduchou separaci kompozitu aplikací magnetického pole a zvyšuje adsorpční kapacitu. Adsorpční izotermy a kinetika byly analyzovány pomocí různých modelů.

Makropórézní aerogely polyanilin/polyvinylalkohol (PANI/PVAL) byly připraveny kryopolymerací anilinu v přítomnosti PVAL a Ni_2SrCr_xW hexaferitu, následovanou vymražováním ve vakuu. Aerogel s vysokou koercivitou by použit pro adsorptivní odstraňování barviva Reactive Black 5 z vody, s účinností 99%.

Kryogely na bázi PPy a nanovláknité celulózy (NFC) byly připraveny ve zmrzlém stavu v přítomnosti nízkých obsahů NFC (0,2–2 váh.%). Houbovité nedýchané aerogely připravené

vymražováním mají výborné mechanické vlastnosti a vysokou vodivost. Komposity PPy/NFC navíc vykazují vysokou adsorpční kapacitu vzhledem k chromanovým iontům díky vysokému specifickému povrchu a výborné schopnosti výměny iontů.

V průběhu těchto studií, stejnosměrná vodivost všech vodivých polymerů a jejich kompozitů byla stanovována metodou van der Pauwa. Morfologie a supramolekulární struktura byly zkoumány pomocí skenovací a transmisní elektronové mikroskopie. Molekulární struktura byla potvrzena spektroskopií infračervenou, Ramanovou a NMR. Konečně teplotní stabilita byla prověřena pomocí termogravimetrické analýzy.

Klíčová slova

Vodivé polymery;

Vodivost;

Kryopolymerace;

Adsorpce barviv;

Magnetické kompozity;

Morfologie;

Organická barviva;

Poly(p-fenylendiamin);

Polyaniline;

Polymerační teplota;

Polypyrrol.

1. INTRODUCTION

1.1. Conducting polymers

Conducting polymers (CPs) are a special class of polymers that are intrinsically conducting [1]. Their main feature is the presence of π-conjugated system (*i.e.*, alternating single/double bonds) along their backbone chain. The overlapping of the neighboring π-orbitals (p_z orbitals) in a conjugated system facilitates the delocalization of π-electrons along the molecule backbone, which is responsible for the electrical conductivity. In some cases, a double bond in the conjugated system can be replaced by a hetero atom with a lone pair of non-bonding electrons *e.g.,* N or S atoms as in the case of pyrrole or thiophene aromatic heterocycles. The delocalized π-electron along the backbone chain and the weak interchain interactions create a quasi-one-dimensional nature and allow anisotropy [2]. CPs show the electrical and optical properties associated with semiconductors; however, they still retain the other physical properties of conventional polymers [2]. Typical examples of CPs are polyacetylene (PA), polyaniline (PANI), polypyrrole (PPy), polythiophene, *etc*. (Figure 1).

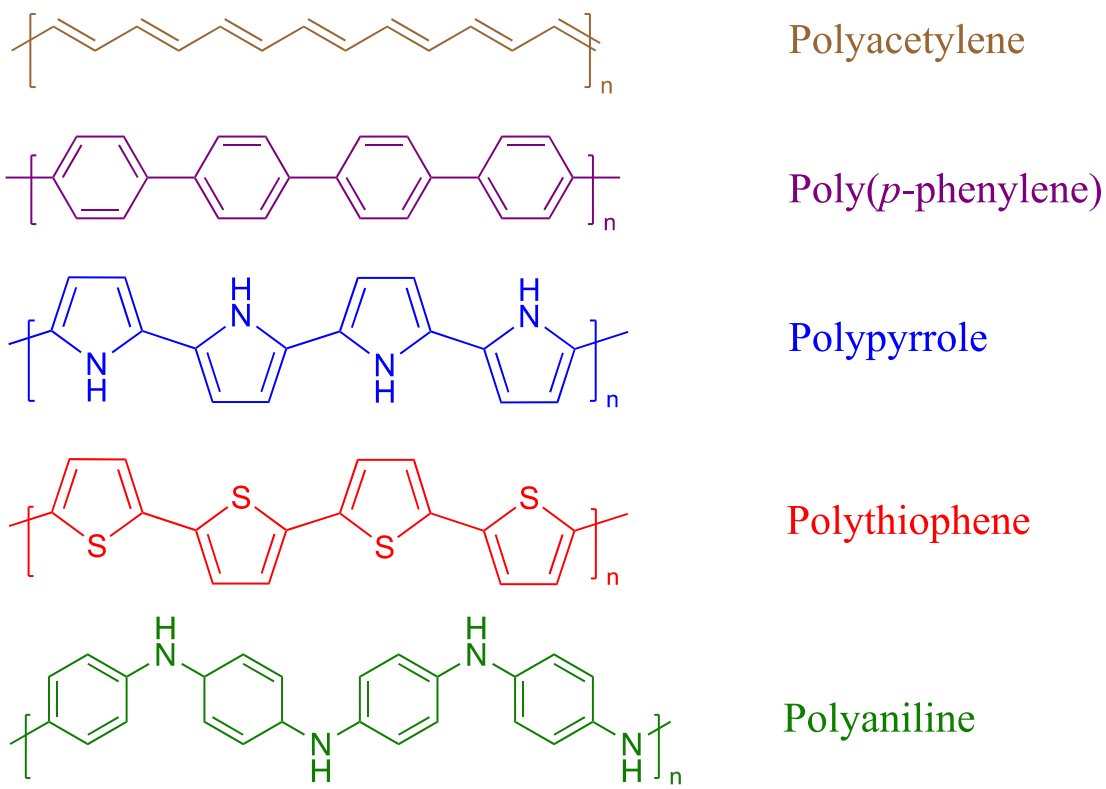

Figure 1. Most common conducting polymers.

Although acetylene was polymerized for the first time in 1958 by Natta et al. [3,4], PA did not attract considerable attention due to its poor processability and low environmental stability. Berets and Smith were the first who reported the electrical properties of PA in 1968 [5]. Later, Shirakawa et al. in 1977 [6] reported the doping behavior of PA with halogen gases *e.g.,* Cl_2, I_2 and Br_2, which significantly enhanced the conductivity. The *trans*-PA conductivity increased over seven orders of magnitude (from 4.4×10^{-5} to 38 S cm^{-1}) at room temperature when doped with iodine. This interesting finding revealed an attractive type of polymers with the electrical properties of metals or semiconductors [7]. The importance of this discovery was awarded the Nobel Prize in chemistry "*for the discovery and development of conductive polymers*" in 2000 shared by the pioneers of CPs: Alan J. Heeger, Alan G. MacDiarmid and Hideki Shirakawa [8]. Since then, the exponential growth of research has been noticed in this field to develop new types of CPs.

Conducting polymers possess unique electronic and optical behavior, side by side with other polymers' properties *e.g.,* low density, optical transparency and high environmental stability [9]. Moreover, they can be easily prepared at a relatively low cost. CPs show a great ability to respond to various stimuli by a change in their optical, electrical, chemical and/or mechanical behavior [10]. On the basis of electrical conductivity, materials are classified as: insulators (with conductivity less than 10^{-7} S cm^{-1}), semiconductors (with conductivity in the range 10^{-7} to 10^{0} S cm^{-1}), and conductors (with conductivity greater than 10^{0} S cm^{-1}). CPs can behave as insulators, semiconductors and conductors based on their doping level as illustrated in Figure 2.

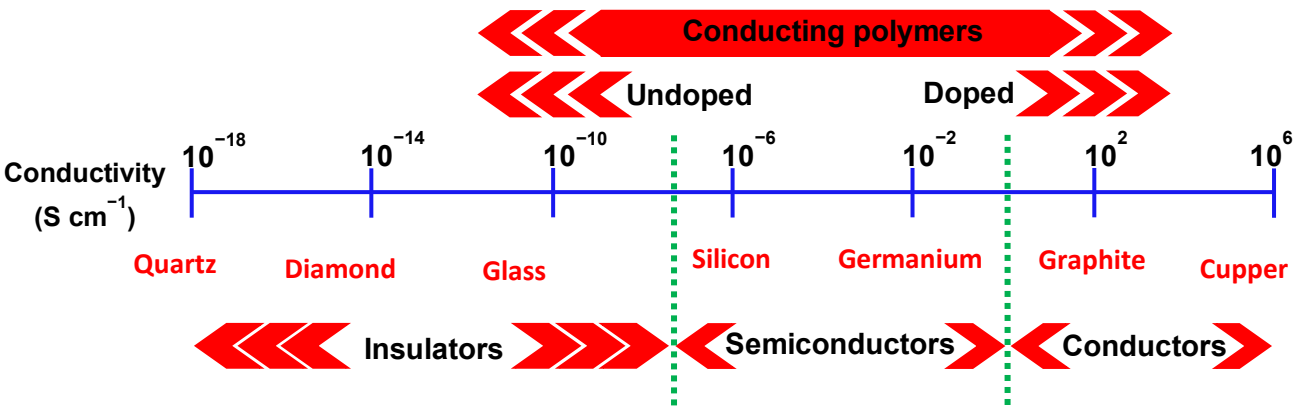

Figure 2. Electrical conductivity of conducting polymers compared to other materials [11].

1.2. Synthesis of the conducting polymers

Conducting polymers are synthesized by the oxidative polymerization of their monomers, except PA, which is polymerized from acetylene by the addition polymerization in the presence of Ziegler catalyst [12]. Chemical and electrochemical polymerization routes are the main approaches that can be used for the preparation of CPs [13–15], where chemical oxidants or electric potential are applied, respectively. In both cases, the main step is the oxidation of the monomers to their radical cations followed by coupling to prolongate the polymer chains (Figure 3). Each polymerization method (chemical or electrochemical) has its own advantages over the other. The chemical route is more suitable for mass production with low cost, while, large-scale production of CPs is still not possible to be obtained electrochemically [16, 17]. On the other side, electrochemical polymerization allows for the easy control of thin-film thickness and roughness, while bulk powders and uncontrolled thick films are typically obtained by the chemical polymerization route [17].

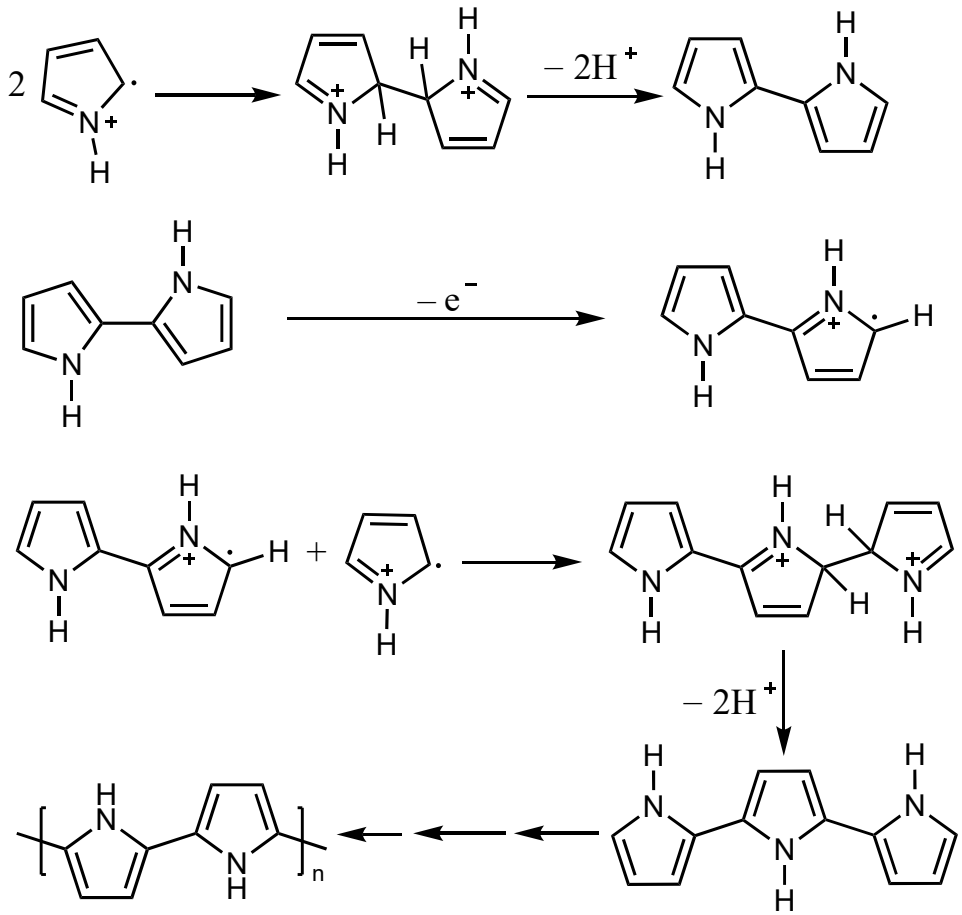

Figure 3. Mechanism of the oxidative polymerization of pyrrole [18].

In addition to the oxidative chemical and electrochemical major polymerization routes of CPs, there are other routes that are not commonly used, such as mechanochemical polymerization [19], solid-state polymerization [20], photo-induced polymerization [21], and radiation polymerization [22]. Within this Thesis, chemical polymerization only is considered.

1.2.1. Chemical Polymerization

Among a long list of CPs, PPy comes as the most frequently studied polymer [23]. PPy was synthesized chemically for the first time in 1916 [24] when pyrrole was treated with acidified H_2O_2 to form insoluble black powder called "*pyrrole black*". A large number of oxidants have been used for the oxidative polymerization of pyrrole such as ammonium peroxydisulfate (APS) [25], cerium(IV) sulfate [26], iron(III) nitrate [27], silver nitrate [28], potassium hexacyanoferrate(III) [29], *etc*. Iron(III) chloride is the most common oxidant for the preparation of highly conductive PPy [30]. Generally, the oxidants are consumed stoichiometrically [31]. Theoretically, two moles of iron(III) chloride are needed to polymerize one mole of pyrrole [26], however, the optimal mole ratio of iron(III) chloride to pyrrole is 2.5 to obtain doped PPy (Figure 4) [32].

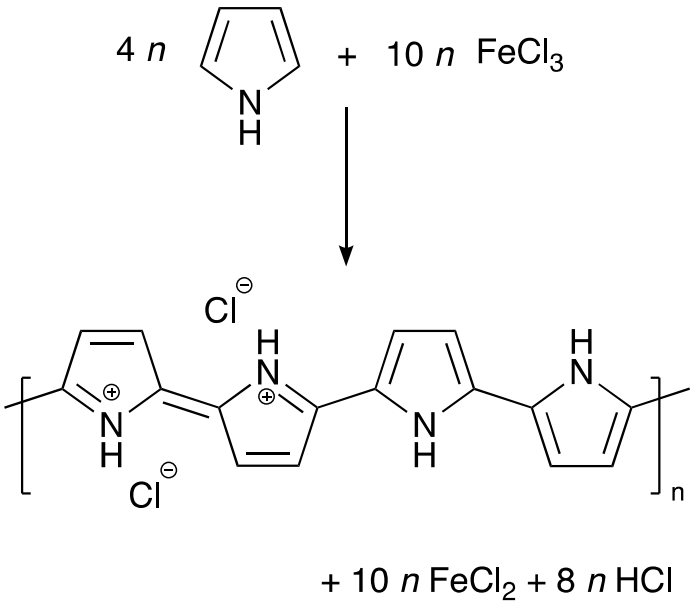

Figure 4. The chemical oxidation of pyrrole with iron(III) chloride to polypyrrole hydrochloride.

Moreover, lower and higher mole ratios can still be used to prepare PPy with different properties. The optimal mole ratio of APS to pyrrole is 1.25 [25], however, PPy with the highest conductivity was obtained at a mole ratio of 1–1.1 [25]. The higher APS concentrations lead to overoxidation of the produced PPy, accompanied by a decrease in its conductivity and yield [33].

In a very similar way to PPy preparation, PANI can be synthesized chemically by the oxidative polymerization of aniline with APS, as the most used oxidant [34] (Figure 5). Also, many other oxidants can be used as well, such as iron(III) chloride [35], silver nitrate [36] [28,37], cerium(IV) sulfate [26], potassium permanganate and potassium dichromate [38].

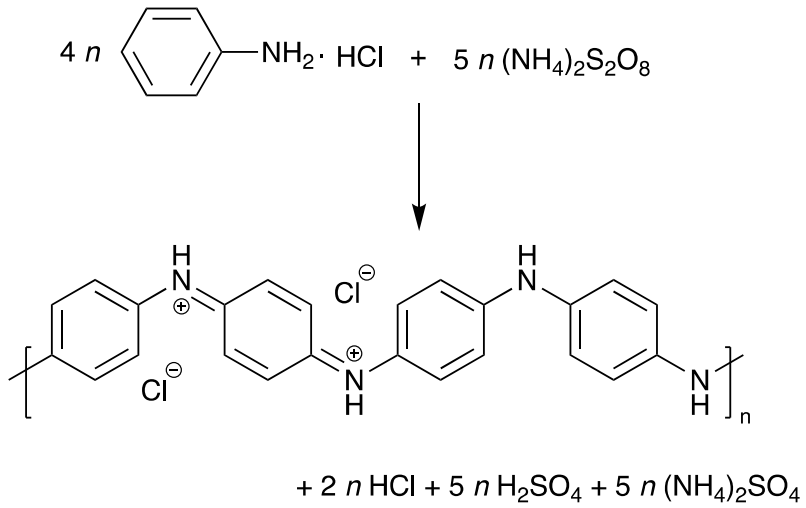

Figure 5. Chemical oxidation of the aniline hydrochloride with ammonium peroxydisulfate to polyaniline emeraldine salt.

The aniline derivative, *p*-phenylenediamine, was polymerized for the first time as an additive to the aniline polymerization to enhance the polymerization rate and yield of PANI [39]. The addition of a small amount of *p*-phenylenediamine (1 mole%) to aniline was found to accelerate its polymerization with silver nitrate [40,41]. Also, *p*-phenylenediamine was solely polymerized with various oxidizing agents such as sodium disulfate [42], potassium disulfate [43] and APS [44]. In addition, silver nitrate was used to prepare poly(*p*-phenylenediamine) (PPDA)–silver nanocomposites [45]. PPDA is proposed to form ladder-like or ladder (phenazine) molecular structures [46] (Figure 6), such rigid chain structures improved the thermal stability [42,47].

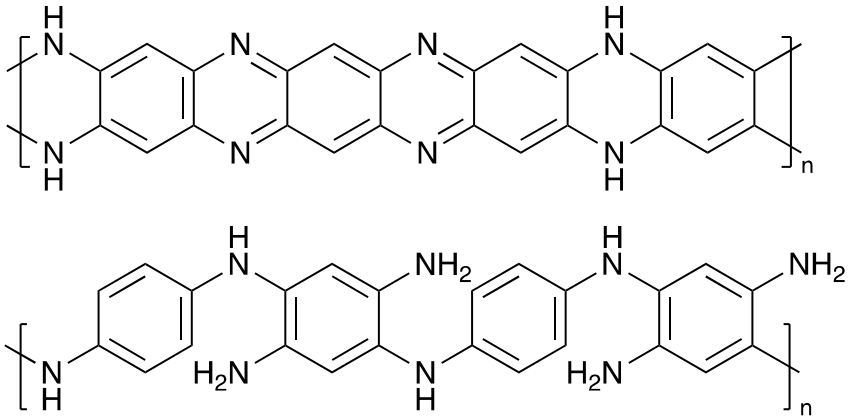

Figure 6. Ladder and ladder-like structures of poly(*p*-phenylenediamine).

Polymerization conditions of CPs *e.g.,* pH, temperature, oxidant to monomer mole ratio and polymerization medium were found to significantly affect the physicochemical properties of the produced CPs such as conductivity and their morphology [48–50]. For instance, granular and nanofibrillar PANI structures are formed in strongly acidic conditions, mild acidic conditions are preferred for the preparation of PANI nanotubes, while alkaline medium forms oligomeric PANI with micro- and nanospheres structures [51]. Low polymerization temperature leads to molecular weight increase and hence, higher conductivity is expected [41,52]. The conductivity of PPy was highly improved by decreasing the polymerization temperature, the conductivity of ~26 S cm^{-1} was obtained at 0 °C compared to 0.04 S cm^{-1} obtained at 60 °C [50]. The rate of the CPs chemical polymerization can be controlled by the mole ratio of the monomer to oxidant and the pH of the polymerization medium [38,53].

The chemically prepared CPs are mainly produced as powders along with the ability to coat the surfaces of different materials immersed into the polymerization medium *e.g.,* glass, textiles or metals [54–57]. Additionally, vapor phase polymerization, a special case of chemical polymerization [58], is carried out by coating a substrate surface with the oxidant and exposing it to the monomer vapors under vacuum conditions [59]. It is considered a very effective tool for the preparation of CPs thin-film coatings. Moreover, modification of the chemical polymerization approach allows the production of CPs in other forms such as colloids, hydrogels, cryogels, and free-standing films [60–63]. Colloids of CPs can be prepared in the presence of surfactants [64] or suitable steric stabilizing agents such as poly(*N*-vinylpyrrolidone) [65,66] or poly(vinyl alcohol) (PVAL) [66,67], poly(2-acrylamido-2-methyl-1-propanesulfonic acid) (PAMPSA) [68], and carboxymethylcellulose [69]. CPs cryogels are

obtained by the freezing of their colloidal dispersions [60]. CPs hydrogels are prepared by combining CPs with hydrophilic polymer matrix *e.g.,* polyacrylamide [70,71], chitosan [72], PVAL [73] and phytic acid [74]. Free-standing films of pristine CPs can be prepared by liquid-liquid or gas-liquid interfacial polymerization method [75–77].

The main disadvantage of the use of harsh oxidants in the oxidative chemical polymerization can be overcome by the alternative enzymatic polymerization [78,79]. Enzymatic polymerization is a green chemistry approach, where various eco-friendly and non-toxic biocatalysts are used for the synthesis of CPs in moderately acidic conditions [80]. Soybean peroxidase [81] and horseradish peroxidase [82] are the most used enzymatic systems for the oxidative polymerization of aniline.

1.2.2. Electrochemical Polymerization

Electrochemical polymerization route uses electrical potential to oxidize the monomers to CPs. Pyrrole and aniline can be electrochemically polymerized in various protonic acid solutions *e.g.,* hydrochloric acid, sulfuric acid, nitric acid [83,84] or proton-free organic solvents *e.g.,* acetonitrile, dichloromethane and nitrobenzene [85] with/without electrolytes such as *n*-$(Bu)_4NBF_4$ or $LiClO_4$ [86–88], under an inert atmosphere (solution is purged with nitrogen or argon). Electrochemical polymerization can be carried out galvanostatically by applying constant current [89–91], potentiostatically, where constant potential is applied [92], or potentiodynamically (cyclic voltammetric scanning), where potential is ramped linearly versus time in opposite directions [93,94]. As a result, PPy or PANI are produced as coherent and stable films coating the working electrode. Film properties such as morphology, thickness and conductivity can be tailored by deposition time, electrolyte used, type of electrodes and the applied potential [16]. Generally, potentiostatic conditions are preferred to prepare thin films, while galvanostatic conditions are used to prepare thick films [95].

Far apart from aniline, electrochemical polymerization of *p*-phenylenediamine is not as easy as the case of aniline monomer. Studies show that electrochemical cyclic voltammetric procedure produces only low molecular weight oligomers in the aqueous solution of perchloric acid [43] or non-aqueous solvents [96]. Reports demonstrate that no films stick to the electrode surface but insoluble product flows away into the solution [43], or in the best electrochemical

polymerization conditions, only thin passive films of *p*-phenylenediamine oligomers coat the working electrode [97].

Predominantly, electrochemical polymerization techniques provide an effective tool for online monitoring and controlling CPs film thickness and roughness [98]. Also, it is considered an eco-friendly approach, where harsh oxidants are not used [99]. In addition, electrochemical polymerization approach is limited by using conducting substrates *e.g.,* carbonaceous [100,101], metallic [86] or conducting glass [102] electrodes.

1.3. Morphology control

The physicochemical properties of the CPs *e.g.,* specific surface area, conductivity, thermal and mechanical properties are highly dependent on the morphology. Nanostructured CPs show improved electrical and electrochemical activities, with enhanced optical properties and better biocompatibility [103] compared to typical granular morphology [104,105]. CPs have been prepared in various nanostructures such as zero-dimensional (nanoparticles) [106,107], one-dimensional *i.e.,* nanowires, nanofibers, *etc*. [108], two-dimensional nanostructures [109], and three-dimensional networks [110–112]. Diverse nanostructures have been prepared to fit special requirements for specific applications. One-dimensional CPs with a high aspect ratio exhibit high conductivity due to their better macromolecular chain ordering and the effective distribution of dopants [113]. They are highly preferred for the preparation of conducting composites from CPs dispersed into nonconducting matrices [113]. One-dimensional CPs nanostructures form percolation networks at lower concentrations compared to globular ones, for instance, PANI nanowires approach the percolation threshold in epoxy resin matrix at 1 wt%, compared to 5 wt% of PANI particles [114]. Similarly, PPy nanofibers reached the percolation threshold with 10 wt%, while PPy nanospheres needed at least 20 wt% in epoxy resin composites [115]. Lowering the percolation threshold is advantageous for decreasing the cost and enhancing the thermal and mechanical properties of the composites [116].

Nanostructured CPs can be formed either by the assistance of morphology guiding templates or by template-free approaches. CPs tend to coat objects that exist in the reaction medium during their polymerization [117]. Consequently, many additives have been added to the polymerization media as templates (or seeds) to influence and orchestrate their morphology formation [118]. Templates can be classified into (1) soft templates *e.g.,* micellar aggregates [119–122] or liquid crystals [123,124], (2) hard templates *e.g.,* solid porous materials [125],

anodic aluminum oxide membranes [126], or cuprous oxide [127], and (3) reactive templates or *in-situ* generated solid organic dye templates [108,128].

The template-free strategy for the preparation of CPs nanostructures uses self-assembly or supramolecular complexes of dopant or dopant–monomer as morphology guiding agents, without the need for additional template [129]. PANI nanostructures (nanotubes and nanorods) were prepared using substituted aminobenzene sulfonic acids, which have both doping and surfactant functions. The self-assembled aniline/dopant aggregates act as templates, which can guide the growth of PANI nanostructures [130]. Similarly, PANI nanofibers and nanotubes have been prepared by a self-assembled strategy in the presence of β-naphthalene sulfonic acid as a dopant [131]. PANI nanotubes diameter and conductivity were found to decrease with decreasing dopant/aniline mole ratio, due to reducing the doping level of the formed PANI [131]. In the same way, PPy micro/nanotubes were prepared chemically or electrochemically in the presence of β-naphthalene sulfonic acid or *p*-toluenesulfonic acid as dopants [132].

Soft templates are formed mainly based on the self-assembly of the surfactants such as sodium dodecylsulfate and dodecyl benzenesulfonic acid [133]. The morphology of formed CPs depends on the micellar aggregates state *i.e.,* PPy nanospheres were produced at low azobenzene sulfonic acid concentrations, while coral-like PPy is obtained at higher surfactant concentrations [134]. PANI prepared in the presence of *n*-dodecylbenzene sulfonic acid [135] produces interconnected networks of PANI nanofibers that form separated hollow PANI nanotubes after washing free *n*-dodecylbenzene sulfonic acid molecules. Various PANI nanoforms *e.g.,* particles or fibers with high conductivity of 20 S cm^{-1} were prepared in the presence of sodium dodecylsulfonate as a surfactant [136], where the morphology was controlled by the concentration of the surfactant. PPy nanoparticles prepared with sodium dodecyl sulfate showed much higher conductivity (47 S cm^{-1}) than PPy prepared with dodecylbenzene sulfonic acid (0.8 S cm^{-1}) [137].

Recently, the *in-situ* generated dye templates [108] have attracted the most attention among the various types of templates. Organic dyes self-assembly in aqueous solutions forms various templates that could guide the formation of organized supramolecular structures of CPs, especially PPy [138]. Such templates are generated based on various mechanisms:

(1) Soluble salt–insoluble acid transition in most organic dyes (acid-generated dye template), where the drop in the pH induces the template formation. For example, methyl orange (MO) produces insoluble needle-like templates by increasing the solution acidity [32] (Figure 7).

The decrease in solubility is due to the dimerization by electrostatic attraction between the formed MO zwitterions [139]. Acid Blue 25 (AB) has similar behavior, it forms acid-generated template at pH 1 due to the formation of the insoluble dimer [140].

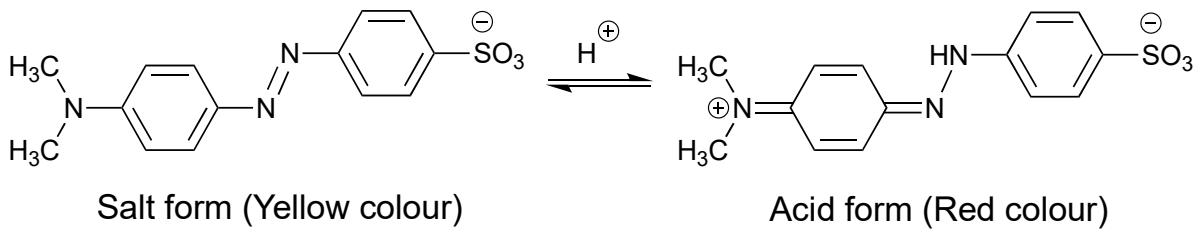

Figure 7. Soluble salt–insoluble acid transition of methyl orange.

(2) Organic dyes may behave as surfactants [113]. Dye molecules have a similar chemical structure to surfactants, they possess ionic groups (act as head in surfactant), and large aromatic moiety ensures hydrophobicity (act as a tail). Dyes could assemble in one-dimensional micelles by π–π interactions between their aromatic rings forming template-like aggregates [113].

(3) Dyes may produce insoluble complexes when interacting with the oxidant (iron(III) ions) [141]. Acid Red 1 was proposed to complex with iron ions which guide the formation of PPy rectangular nanotubes [138,142].

(4) Some dyes may oxidatively oligomerize with the addition of oxidants, forming solid aggregates. Safranin, the aromatic diamine organic dye, could oxidize with APS forming insoluble safranin oligomers [143]. Such oligomers could serve as seeds for the growth of one-dimensional PPy [113].

(5) In addition, other types of organic dyes assemble based on J-aggregates [113,144]. Porphyrin and phthalocyanines dyes tend to form J-aggregates of one-dimensional rod-like structure [145], which act as templates to prepare one-dimensional nanoforms of various CPs [146,147].

The addition of various organic dyes into pyrrole polymerization media induces the formation of various PPy nanostructures (Figure 8) and significantly improves their conductivity. Anionic dyes such as MO were found to guide the formation of PPy nanotubes and the conductivity was remarkably enhanced from ~1 (with the absence of dyes) to 68 S cm^{-1} [139]. Acid Red 1 was

used for the preparation of aligned PPy nanotubes with conductivity up to 28.6 S cm^{-1} [142]. Using Acid Red B leads to PPy micro/nanofibers with the conductivity of 8.6 S cm^{-1} [148], while AB forms PPy nanofibers with 60 S cm^{-1} [140]. Sunset Yellow FCF, another anionic dye, was proved to produce three-dimensional barrel-like PPy nanostructures, however, it has almost no impact on the conductivity [138]. Similarly, some cationic dyes such as rhodamine B [149], acriflavine [150] and safranin [113], have been reported as morphology guiding agents for the preparation of one-dimensional PPy nanostructures. Acriflavine was found useful to prepare PPy nanofibers with conductivity up to 14 S cm^{-1} and interesting antimicrobial activity towards Gram-positive and negative bacteria [150].

Organic Dye	SEM	TEM	Reference
Methyl orange 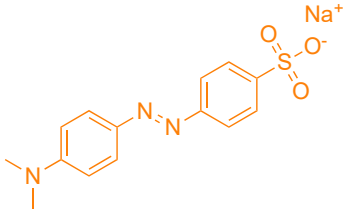	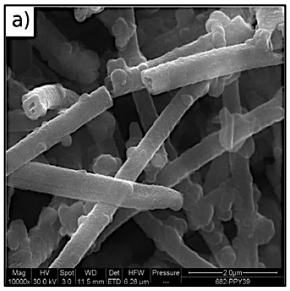	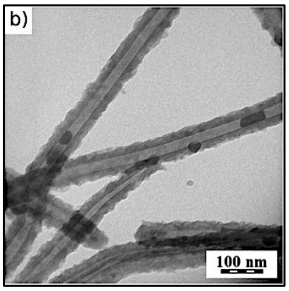	[139]
Acid Red 1 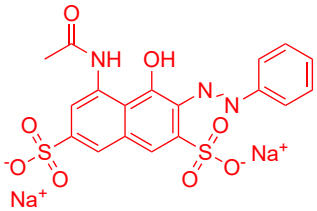	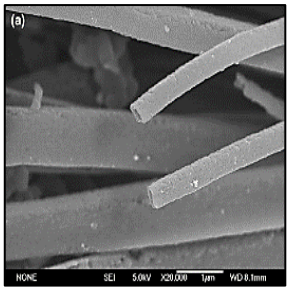	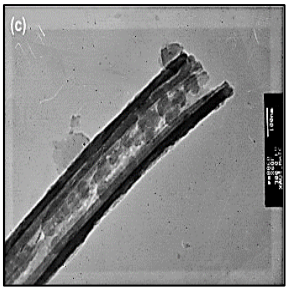	[142]
Acid Red B 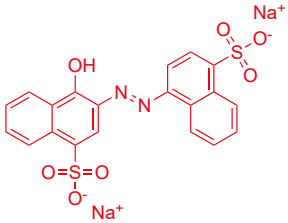	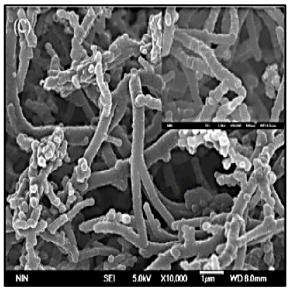	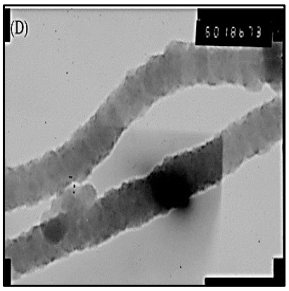	[148]

Acid Blue 25

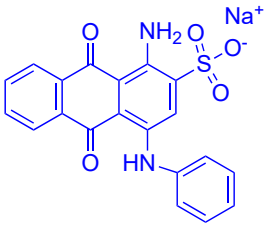

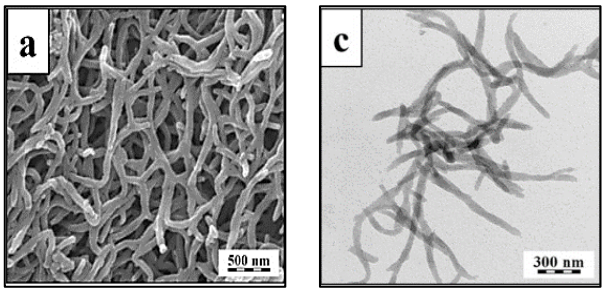

[140]

Rhodamine B

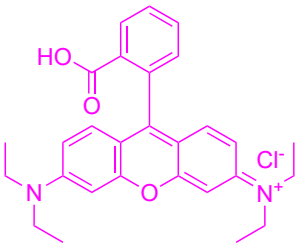

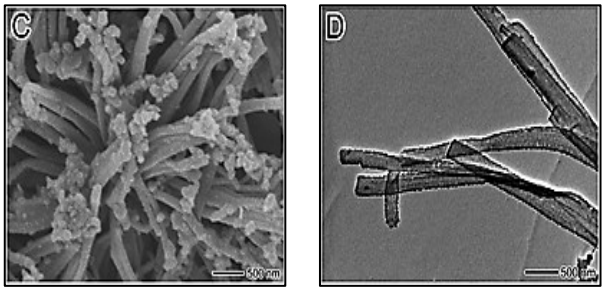

[149]

Acriflavine

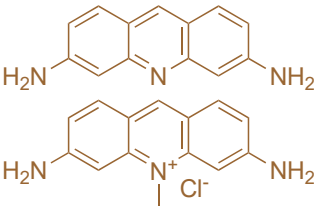

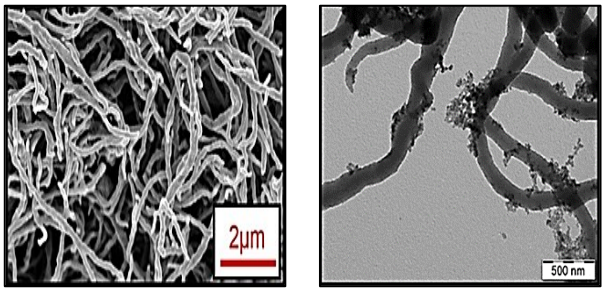

[150]

Figure 8. Effect of various organic dyes on the morphology of polypyrrole.

Not all organic dyes have a positive impact on the conversion of PPy morphology, for instance, Acid Blue 129, which has a closely related chemical structure to AB showed no effect on the PPy morphology, however, it still improves the conductivity to 40 S cm^{-1} [140]. The same was in the case of ethyl orange, which has a similar structure to MO, however, it has no effect on the PPy morphology while the conductivity increases to 27 S cm^{-1} [32].

Only a few dyes were reported to assist one-dimensional PANI formation. Sunset yellow was used to prepare PANI with coral-like nanostructures accompanied with conductivity increase from 2 S cm^{-1} to 15 S cm^{-1} [151]. Crosslinked PANI nanofibers were prepared with the aid of Acid Red 27, with a specific capacitance of 463 F g^{-1} compared to 280 F g^{-1} for conventional PANI [152].

1.4. Conducting polymer composites

The pristine forms of CPs have shown difficulties to achieve satisfying features needed for practical applications, they are in form of infusible powders with poor mechanical properties and low specific surface area [153]. The preparation of CPs composites is a well-known approach to improve the processability, conductivity, mechanical properties and specific surface area, due to the synergistic effect of the individual components. The composites of CPs have been widely prepared with various additives, which could be categorized as:

(1) Inorganic components: The combination of CPs with inorganic materials could enhance the electrical conductivity, electrochemical performance, catalytic properties and mechanical integrity [154]. A variety of inorganic nanoparticles can be combined with CPs such as:

- Metal oxides *e.g.*, TiO_2 [155], Nb_2O_5 [156], ZnO [157], MnO_2 [158], V_2O_5 [159], $BiVO_4$ [160], *etc*. composites with CPs have been widely used in electrode material for supercapacitors. PANI/TiO_2 composite was used as a stable electrode material for a supercapacitor with an excellent retention capacity of 83 % after 30000 cycles at 3.3 A g^{-1} current density [161]. Additionally, PPy/TiO_2 composite showed specific capacitance of 459 F g^{-1} and capacity retention of 92.6% after 1000 cycles [155]. Free-standing and flexible electrode of PPy/V_2O_5 composite exhibited high specific capacitance of 334 F g^{-1} with superior cycling stability (retention capacity of 82.5% after 2000 cycles) [162]. $BiVO_4$/PANI composite has shown specific capacitance of 701 F g^{-1} and capacity retention of 95.4% after 5000, at 1 Ag^{-1} current density [160].

- Noble metals *e.g.*, Au [163], Pd [164], Pt [165], Ag [166], *etc*. The deposition of Au has greatly enhanced the sensitivity of PEDOT towards detection of DNA in PEDOT/Au biosensor [167]. Composites of PANI with Ag nanoparticles showed enhanced antimicrobial, antifungal and anti-yeast activity compared to individual PANI and Ag nanoparticles [168]. PEDOT/Pt nanocomposites have shown greatly enhanced electrocatalytic activity compared to bulk Pt or pristine PEDOT electrodes in the oxidation of methanol [169]. PPy nanotubes/Au nanoparticles were used as highly efficient electrocatalysts for oxygen reduction reactions (ORR) and in the catalytic reduction of 4-nitrophenol [170]. Composites of CPs with magnetic nanoparticles *e.g.,* γ-Fe_2O_3, Fe_3O_4, and NiO, merge both magnetic and electrical properties. This allows for a wide range of applications as electromagnetic shielding [171] and microwave absorbing materials

[172,173]. In addition, such composites can be used as adsorbents for water treatment due to the easy removal of adsorbents by an external magnetic field [174,175].

- Clays *e.g.,* montmorillonite, mica, zeolites [176]. CPs/clay composites can enhance the anticorrosion protection by improving their adhesion, mechanical properties and decreasing the porosity of their pristine forms [176]. Homogenous and adhered PANI/montmorillonite coatings on aluminum alloy 3004 prepared by direct electrochemical polymerization showed 190 times lower corrosion rate than uncoated aluminum alloys [177]. Chemically polymerized mica/PPy composites were used for corrosion protection of cold-rolled steel [178], by decreasing current density and increasing corrosion potential values. Ternary composites of PPy/montmorillonite or PANI/ montmorillonite with epoxy resin enhance the corrosion protection of epoxy coatings for carbon steel [179] and aluminum alloys [180,181]. The incorporation of CPs/MMT nanocomposites inside the epoxy resin was found to significantly increase the corrosion resistance in comparison to the neat epoxy resin.

(2) Carbon-based materials: composites of CPs with various carbonaceous materials *e.g.,* MWNT, graphene, graphene oxide [182,183] are aimed to improve CPs' capacity and poor cycle stability [184]. Carbon-based materials exhibit very attractive properties such as high conductivity, high surface area, high chemical and thermal stability, in addition to their low cost [185]. An *in-situ* prepared PANI/graphene nanosheets composite showed very high specific capacitance of 1046 F g^{-1} compared to 115 F g^{-1} for pristine PANI, at a scan rate of 1 mV s^{-1} [186]. Similarly, homogenous PPy/graphene nanosheets composite showed high specific capacitance (482 F g^{-1} at a current density of 0.5 A g^{-1}) with excellent capacity retention of 95% after 1000 cycles [187].

(3) Metal-organic frameworks (MOFs): Metal-organic frameworks are supramolecular assemblies that consist of inorganic metal ions connected to organic linkers through strong coordination bonds. MOFs have attracted great interest owing to their excellent properties *e.g.,* very large surface area, ultrahigh porosity (up to 90% free volume), high chemical and thermal stability, and high sorption capacity. The majority of MOFs are nonconductive [188,190], enhancing their conductivity by integrating with different CPs can open tremendous applications based on their synergistic effect [191]. The conductivity of Cd-based three-dimensional MOF (10^{-12} S cm^{-1}) has increased by 9 orders of magnitude when PPy was hosted into its one-dimensional nanochannels [190]. High-performance

supercapacitors were prepared by combining PANI with different MOFs. PANI/ carbonized Zn-MOF composite showed specific capacitance of 477 F g^{-1} [192], while PANI/Zr-MOF showed 1015 F g^{-1} [193], at a current density of 1 A g^{-1}. In addition, the incorporation of electro-inactive MOF *e.g.,* ZIF-8 onto electropolymerized substituted aniline has significantly enhanced its ORR electrocatalytic efficiency in neutral solutions [194].

(4) Organic materials: Composites of CPs with natural polymers such as cellulose [195], chitosan [196], chitin [197], lignin [198], gelatin [199], and others have been prepared in various forms *e.g.,* hydrogels, aerogels, films, colloids or powders. Conductive PPy/agarose hydrogel showed self-healing and thermoplastic properties due to thermal stimuli reversible liquefaction/gelation [200]. It exhibited Young's modulus of 46 kPa and conductivity of 0.35 S cm^{-1}. Three-component polyacrylamide/chitosan/PPy hydrogels with a conductivity of 0.003 S cm^{-1} showed superior mechanical properties (compression modulus of 136.3 MPa) and good biocompatibility [201]. Also, the combination of CPs with synthetic polymers such as PVAL, polystyrene, poly(methyl methacrylate), and poly(vinyl acetate) [202] enhance the plasticity and mechanical integrity. The incorporation of PPy into polyacrylamide matrix forms electroconductive biocompatible hydrogels, and allows the electrochemically controlled release of loaded risperidone (an antipsychotic drug) [203].

1.5. Chemical and Physical properties

The physicochemical properties of the CPs were found to be highly controlled by their oxidation state.

Polyaniline has various reversible oxidation states with alternative optical and conducting properties (Figure 9). The oxidative polymerization of aniline in an acidic medium produces the protonated emeraldine salt [204], which is the most conductive PANI form [205]. Emeraldine salt is characterized by the green color and conductivity of a few units S cm^{-1}. It can be easily deprotonated to the emeraldine base [206], which is nonconductive. Emeraldine salt can be further oxidized to pernigraniline form [207]. The emeraldine froms can be reduced to the colorless leucoemeraldine, which is the fully reduced form of PANI [205,207]. The reversible acid/base transition of conducting emeraldine salt to the non-conducting emeraldine

base is located at pH 6–7 [204]. However emeraldine salt is insoluble in organic solvents, emeraldine base is partially soluble in highly polar aprotic solvents such as NMP [208,209], tetrahydrofuran (THF), dimethylformamide (DMF) [210] and N,N′-dimethylpropylene urea [208]. PANI insolubility is attributed to its stiff backbone in addition to strong hydrogen bonding interactions between the adjacent polymer chains [211]. The better solubility of the deprotonated PANI is due to the higher disordering in the polymer chains [212].

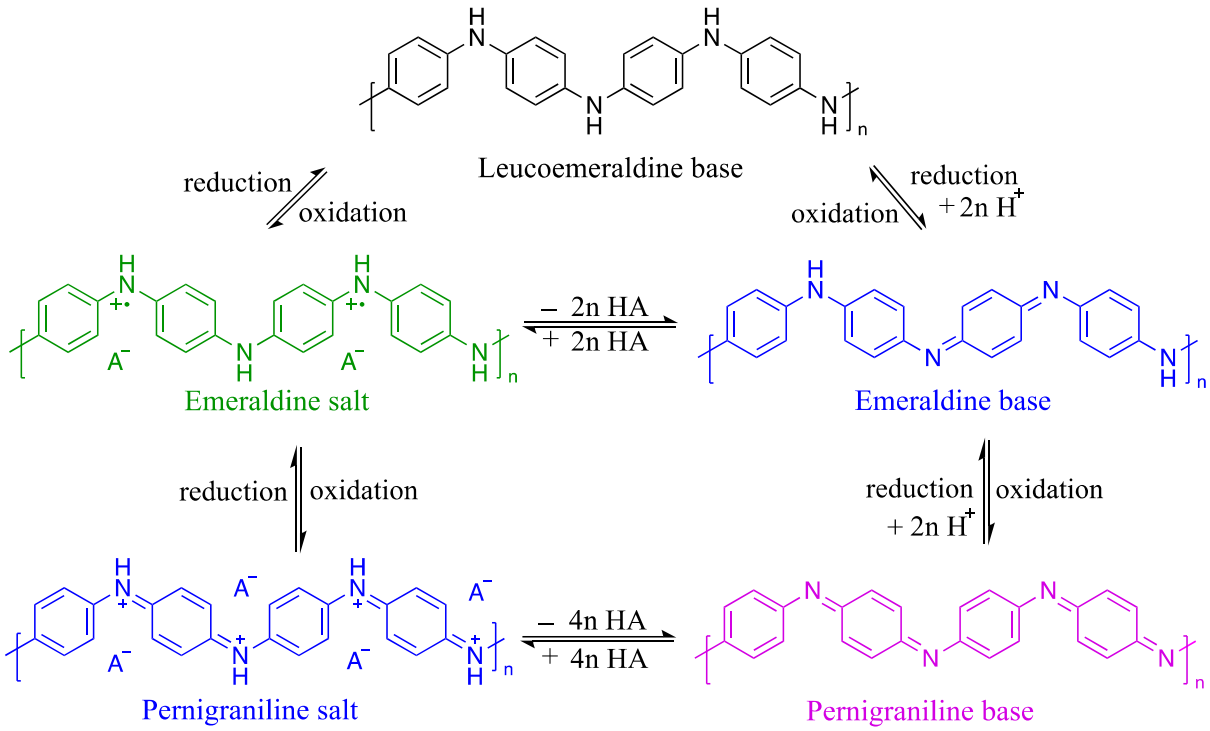

Figure 9. Oxidation states of polyaniline.

In a similar manner, oxidation state and/or pH changes highly affect the physical, chemical and electrical properties of PPy [213]. The as-prepared protonated PPy undergoes deprotonation when treated with basic solutions (pH > 9) to its nonconducting form [213,214]. Convertibly, treating the deprotonated PPy with strong acidic solutions (pH < 3) leads to a protonation process with a significant increase in conductivity. Simple protonation/deprotonation process is reversible (Figure 10) [215]. However, the prolonged treatment with strong alkaline solutions (pH > 11) introduces hydroxyl and carbonyl groups into the PPy chain and leads to an irreversible reaction, and the initial conductivity cannot be regained after re-protonation with acidic solutions [214]. Chemically or electrochemically

prepared PPy is neither fusible nor soluble in common organic or polar solvents [216], due to long conjugation, strong inter/intramolecular interactions and crosslinking of polymeric chains [217,218].

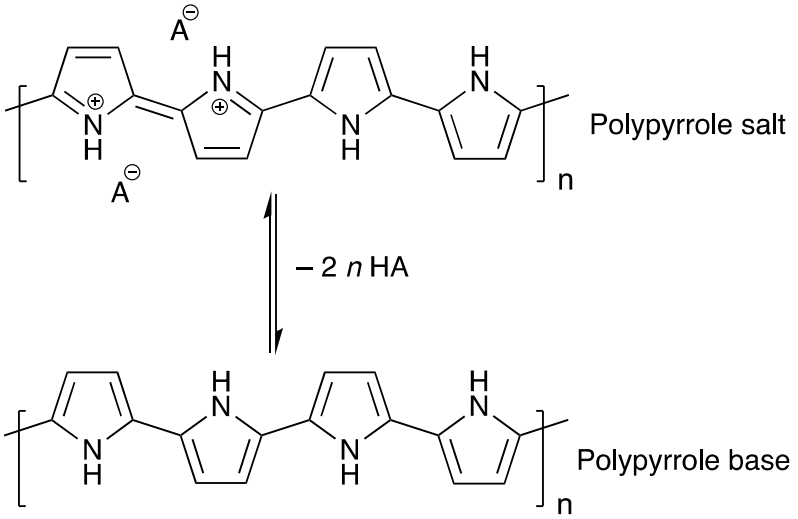

Figure 10. Protonation-deprotonation of polypyrrole.

Conducting polymers lack of solubility, fusibility and poor processability have limited studying their chemical structure [219] and their industrial applications [220]. Various approaches have been used to produce soluble or dispersible forms of CPs. This can be achieved by doping with bulky functionalized organic acids or preparation of colloids using steric stabilizers. PPy prepared chemically with APS as oxidant and dodecylbenzene sulfonic acid [221] or butylnaphthalene sulfonic acid [222] as dopants exhibited good solubility in common organic solvents *e.g., m*-cresol, chloroform, dichloromethane. Similarly, PANI doped with dodecylbenzene sulfonic acid is soluble in common organic solvents [223]. The incorporation of large dopants impedes the inter- and intra-molecular interactions of the polymeric chains, and consequently improves their solubility [217,224]. Another strategy for the preparation of soluble CPs is the chemical modification of the monomers [15] by introducing substituents. Appropriate alkyl substituents on the thiophene ring improve the solubility of polythiophenes in common organic solvents [225]. In addition, the introduction of bulky substituents *e.g., N*-(benzylideneamino) to pyrrole ring produces highly soluble PPy based polymer [219]. Also, sulfonic acid group substituent on the benzene ring of aniline prepares water-soluble self-doped PANI [220].

1.6. Conducting polymers applications

Conducting polymers have shown high environmental, chemical and electrochemical stability [226], as well as biocompatibility [227]. CPs have small band gaps (1.5–3.0 eV) [228], low density [229] along with reversible switch between conductive–insulating states through doping/dedoping processes [230]. Consequently, they have attracted massive interest in a broad spectrum of applications in various fields (Figure 11).

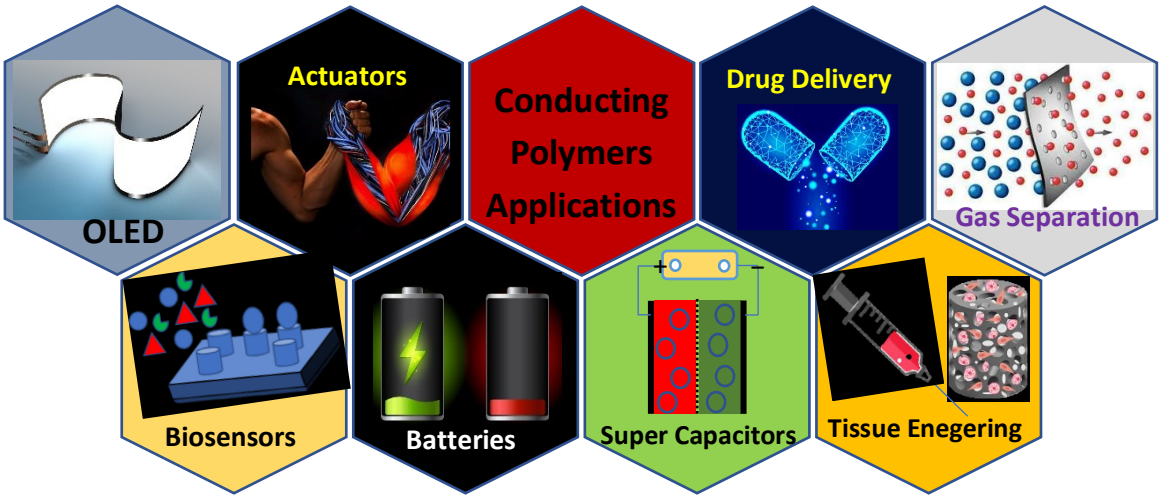

Figure 11. Conducting polymers applications.

CPs have been used in electronic and optoelectronic devices [231], energy storage and energy conversion applications *e.g.,* rechargeable battery electrodes [232–235], solar cells with a high energy-harvest factor [231], light-emitting diodes [236] and electrical heating elements [237]. Various CPs have been utilized in chemical, electrochemical and bio-sensors [238], and analytical electrodes [239]. Also, they have been utilized in electromagnetic shielding to avoid electromagnetic interference [240], and antistatic- [241] and anti-corrosion coatings [242,243]. CPs can be used in gas separation membranes [244], ion selective electrodes [245–247], electrocatalysis [248] and the removal of various wastewater contaminants [249], in addition to potential applications in drug delivery systems [250] and tissue engineering [251].

Among the plenty of previously mentioned applications, CPs have been widely used in sensors. Various CPs were utilized as chemical sensors that can be used in aqueous or gaseous systems for the detection of hazardous pollutants *e.g.,* ammonia vapors, and volatile organic

compounds [252–254]. Also, CPs were used for the detection of organic and inorganic species *e.g.,* ascorbic acid [255], dopamine, uric acid [256] and metal ions [257]. CPs due to their excellent ability to immobilize biomolecules have been used as biosensors for the recognition and quantification of various biological analytes such as glucose, urea, cholesterol, lactate and some enzymes [258,259].

Due to the electrochemo-mechanically active properties of CPs [260], they were found very useful for the application in actuators or artificial muscles [260]. CPs doping/dedoping process is accompanied by reversible volume (swell/shrink) changes [261]. This process can be controlled by electric signals (current or potential). The mechanism of CPs actuators is very similar to natural muscles, which are triggered by nervous pulses that increase the concentration of Ca^{2+} in the surrounding muscles fibers [250]. Similarly, in CPs the electric pulses enforce doping/dedoping reactions, which involve ionic interactions/dissociation between the CPs chains and ions from solutions. Bilayer or multilayer actuator systems prepared from different CPs and nonconducting polymers [262–265] can bend reversibly in 360° by electrochemical oxidation/reduction in electrolytes. Results showed that electrochemically prepared PPy films have a very large actuation strain (~30%) compared to the film cast from solutions of chemically prepared PPy (~2.5%), due to the more diffusible molecular structures and higher conductivity of electrochemically prepared film, allowing easier charge transfer [266].

One of the most attractive properties of CPs is their catalytic activity. CPs were used widely in catalytic and electrocatalytic applications for decomposing toxic inorganic or organic compounds [248]. Reduced PPy films were found useful for the catalytic reduction of toxic hexavalent chromium Cr(VI) to Cr(III) [267]. Also, PANI-coated ITO electrode showed a continuous electrocatalytic reduction of Cr(VI) [268]. CPs (*e.g.,* PANI, PPy and polythiophene) composite electrodes with Pt or Pb particles were used in the electrocatalytic oxidation of formic acid [269]. In addition, various CPs have shown high activity as catalysts for ORR. Very early, Jakobs et al. used PPy as a rotating ring-disc electrode for the ORR in acidic solutions [270]. Composite of PPy/carbon black has been used as an alternative of Pt electrocatalyst for ORR in microbial fuel cells [271]. PPy/carbon black electrode showed 15 times higher power per cost than Pt. Carbonized PPy/mesoporous silicate nanocomposite has shown enhanced electrocatalytic activity in ORR, exceeding the commercial Pt catalyst in an alkaline solution [272]. Similarly, carbonized two-dimensional PANI/mesoporous silica and mesoporous titania have shown high electrocatalytic activity towards ORR in alkaline solutions [273]. Composites

of PANI with graphene prepared by *in-situ* polymerization followed by carbonization were used as electrochemical ORR catalysts with higher activity than the benchmarked Pt/C catalyst [274].

Various CPs, in their pristine or composite forms, have been commonly used in environmental applications, for the removal of organic dyes, pharmaceutical, personal care products, pesticides and heavy metals from aqueous solutions through adsorption [249] or photocatalytic [275] or electrocatalytic [276] degradation. CPs due to their functional groups and high specific surface area can adsorb large amounts of organic or metallic contaminants. Also, they show high thermal stability and ease of functionalization with environmental sustainability [249]. The fundamental interaction mechanisms between CPs and different organic pollutants are based on: π–π interaction between the aromatic rings, electrostatic interactions between oppositely charged groups, hydrogen bonding and hydrophobic interactions [277]. Adsorptive removal of water contaminants is the most preferred approach compared to the other techniques, it is considered as the most economically feasible and highly effective method, also it is a fast and clean process, where no byproducts are formed [278]. In addition, the adsorption approach allows the regeneration and reusability of the adsorbents [279,280]. Table 1 presents the use of CPs and their composites for the adsorptive removal of water contaminants. Various CPs composites were applied to enhance the adsorption capacity by increasing specific surface area or/and in favor of the easy separation of adsorbents from solution. CPs aerogels have shown high adsorption capacity due to their large specific surface area, in addition, they are mechanically stable adsorbents [281,282]. The incorporation of magnetic nanoparticles allows the magnetic separation of the CPs composites with the aid of an external magnetic field [283–286].

Table 1. The adsorption capacity and specific surface area of various CPs and their composites used for the adsorptive removal of heavy metals and organic dyes from wastewater

Material (Adsorbent)	Contaminant	Capacity, mg g^{-1}	Surface area, m^2 g^{-1}	Reference
PANI/PVAL aerogels	Cr(VI)	41.2	N/A	[281]
PPy/Fe_3O_4/attapulgite	Cr(VI)	53.37	N/A	[283]
Chitosan/PPy	Cr(VI)	78.6	3.07	[287]

PANI/cellulose	Cr(VI)	86.74	5.89	[288]
PPy/Fe_3O_4	Cr(VI)	169.5	N/A	[285]
PANI nanotubes	Cr(VI)	182	37.6	[289]
Fe_3O_4/PANI	Cr(VI)	200	N/A	[284]
PPy-PANI nanofibers	Cr(VI)	227		[290]
PPy/Fe_3O_4	Cr(VI)	243.9	N/A	[285]
PPy-PANI/Fe_3O_4	Cr(VI)	434.78	56.52	[291]
γ-Fe_2O_3/chitosan/PPy	Cr(VI)	301.2	61.7	[292]
PPy/TiO_2	Zn(II) Pb(II) Cu(II)	77.81 140.27 9.01	140	[293]
Thiol-functionalized PPy	Hg(II)	1736.8	12.86	[294]
Poly(aniline-*co*-sulfophenylenediamine)	Hg(II)	497.7	N/A	[295]
PANI	Hg(II)	600	35.4	[296]
PPy	As(III)	23	N/A	[297]
PANI/Fe^0	As(III) As(V)	232.5 227.3	N/A	[298]
Polythiophene/Sb_2O_3	Pb(II)	18.94	N/A	[299]
Poly(*o*-phenylenediamine)	Pb(II)	103.20	N/A	[300]
Polythiophene/TiO_2	Pb(II)	173.6	229.66	[301]
Poly(*m*-phenylenediamine)	Pb(II)	242.7	N/A	[302]
PPDA	Pb(II)	253.2	N/A	[302]
PEDOT aerogel	Pb(II) Hg(II) Basic fuchsin	79.6 184.1 170	216	[282]
PPy hydrogel	Rhodamine B	22.6	71	[303]

PANI/graphene oxide	Methylene blue	14.2	N/A	[304]
PANI/reduced graphene oxide	Methylene blue	19.2	N/A	[304]
PANI hydrogel	Methylene blue	71.2	35.3	[305]
Chitosan–montmorillonite/PANI	Methylene blue	111	N/A	[279]
PANI hollow nanotubes	Methylene blue Acid green 25	69.4 57.8	39.18	[306]
PANI/chitosan	Methylene blue Acid Green 25	81.3 240.4	12.34	[280]
PANI/carbon aerogel	Acid Green 25	518	61.27	[307]
PANI/chitosan	Congo Red Coomassie blue	322.58 357.14	N/A	[308]
PPy/carbon nanotubes-$CoFe_2O_4$	Methyl blue MO Acid Fuchsin	137 116.1 132.15	150.41	[309]
ZnO-$ZnFe_2O_4$-PPy	Congo red	74	N/A	[310]
CuFe@PANI	MO	345.9	20.37	[311]
PANI microspheres	MO	154.56	N/A	[312]
Cellulose/Fe_3O_4/PPy	RB	62.31	12.2	[313]
PANI nanofibers	RB	312.5	38.99	[314]
PPy nanofiber/Zn-Fe	Safranin	63.4	24.13	[315]
PANI emeraldine salt	Eosin Yellow	335	N/A	[316]
Fe_3O_4/TiO_2/PPy	Acid Red G	161.8	57.26	[286]
poly(*m*-phenylenediamine)	Orange G	469.5	284.5	[317]

2. AIMS OF THE WORK

The main goal of this work is to enhance the conductivity of the CPs, particularly PPy.

The following approaches were used to obtain highly conductive PPy with high yield:

- Preparation of PPy nanostructures in the presence of various organic dyes.
- Frozen-state polymerization of PPy in the presence/absence of organic dyes.
- Cryopolymerization of PPy in the presence of nanofibrillated cellulose (NFC).

The other goal of this work is to utilize various CPs and their composites in the field of environmental treatment, for the removal of organic dyes and heavy metals from solutions. Magnetic nanoparticles were introduced into CPs matrix to provide a magnetic property that facilitates their separation from solutions by applying an external magnetic field. Additionally, highly porous PPy–NFC aerogel can be easily separated after the adsorption process. The following points were fulfilled:

- PPDA/γ-Fe_3O_4 nanocomposites with various wt% of maghemite content were used to remove RB from aqueous solutions.
- The *in-situ* preparation of PPy–NFC aerogels with different NFC contents.
- PPy–NFC aerogels were used for the removal of heavy metals, Cr(VI), from aqueous solutions.
- PANI/hexaferrite aerogels supported by PVAL were tested for the efficient removal of RB from aqueous solutions.

The physicochemical properties of the PPy, PANI and PPDA and their composites, prepared by the previously mentioned approaches were fully studied and discussed. FTIR and Raman spectroscopies were carried out to confirm their chemical structures. Scanning and transmission electron microscopies (SEM, TEM) were used to study the morphologies. Thermal gravimetric analysis (TGA) was performed to study the thermal stability, and specific surface area was estimated using BET analysis. Conductivity was determined using the van der Pauw method. Also, the adsorption capacities of CPs toward the colored pollutants were estimated using UV-Vis spectroscopy.

The current Thesis consists of eight scientific papers published in international journals (Appendices 1–8) with a general introduction and a discussion of the papers' contents.

3. EXPERIMENTAL AND CHARACTERIZATION TECHNIQUES

Chemicals, reagents, preparation procedures, in addition to instrumentations and measurements techniques are described in detail in the published papers (Appendices 1–8). Herein, the basic theories of the different characterization techniques are briefly discussed.

- **Ultraviolet-visible spectroscopy**

Ultraviolet-visible (UV-Vis) spectroscopy is a basic characterization technique, which is used in qualitative and quantitative analysis. It measures the absorbance spectra of chemicals in solution or as a solid. Absorption spectra reflect the molecules' electronic transitions from the ground state (bonding and non-bonding electrons) to the excited state (anti-bonding) in the range of 1.5–6.2 eV region of energy (wavelength range of 200–800 nm). There are four possible types of transitions: π–π*, n–π*, σ–σ*, and n–σ*. Organic dyes and Cr(VI) heavy metal ions have well-defined characteristic absorption bands, and hence their concentrations by the aid of Beer-Lambert law (Eq. 3) can be estimated and followed by the UV-Vis spectra.

$$A = \log(I_0 \,/\, I) = \varepsilon l C \qquad (3)$$

Where A is the absorbance, I_0 is the incident light intensity at a given wavelength, I is the transmitted light intensity, ε, L and C represent the molar extinction coefficient (constant, characteristic of the material), the path length of the light through the sample and the absorbing species concentration, respectively.

- **Fourier transform infrared (FTIR) spectroscopy**

FTIR spectroscopy is an analytical technique used for the identification of the molecular structures of the organic, inorganic, and polymeric materials based on their functional groups infrared absorption frequencies. The FTIR spectra are collected by allowing infrared radiation to pass through the sample/potassium bromide (KBr) mixture pellets. Infrared radiation interacts with vibrational excitations of CPs and with their charge carriers. [318]. FTIR was proven to be useful for the identification and quantification of the various oxidation states of CPs, level of doping and polaron/bipolaron ratio. Herein, the FTIR spectra of the prepared CPs and their composites were recorded in the range 400–4000 cm^{-1}. CPs powders were dispersed

in KBr with a ratio of 1 mg of finely ground sample to ~100–150 mg of KBr then compressed into pellets.

- **Raman spectroscopy**

Raman spectroscopy is a non-destructive analytical technique and is considered as complementary vibrational spectroscopy to FTIR. It is used to determine the vibrational modes which result in changes in the polarizability of the molecules. It depends on the inelastic Raman scattering of monochromatic (laser) light in the visible, near-infrared, or near UV region. The monochromatic light interacts with molecular vibrations, resulting in an energy shift. This energy shift provides information about the vibrational modes of the molecules, which help for sample identification and quantitation.

In this study, NIR diode laser emitting at 785 nm, HeNe 633 nm laser and Ar-ion 514 nm laser were used. Spectra recorded using laser line 785 nm is in resonance with the electronic transitions (polaron absorption band) in PPy, and laser line 633 nm resonantly enhances polarons and bipolarons absorption bands. The 514 nm laser excitation energy is close to the electronic absorption in the used dyes and hence, the spectra of the dyes are enhanced.

- **Scanning electron microscopy (SEM)**

Scanning electron microscopy allows direct observation of surfaces morphology and topography of the CPs with 10–30 nm resolution. The contrast of the SEM images arises from the dependence of the secondary electrons' numbers on the angle between the specimen surface and the primary electron beam. Also, EDX analysis was performed for CPs composites with high atomic number atoms *e.g.,* Fe, Ag, *etc*.

- **Transmission electron microscopy (TEM)**

Transmission electron microscopy operates based on the same principles as the optical microscopy, however, an electron gun is used instead of a light source and electrostatic or magnetic electron lenses corresponding to glass lenses in optical microscopes. TEM provides images for the specimen with a significantly higher resolution (1–0.2 nm). Electrons transmitted

through thin specimens are used for image formation. TEM was used as a useful tool to distinguish between PPy nanofibers and nanotubes.

- **Conductivity**

Electrical conductivity or specific conductance is a fundamental material property, which represents the ability to conduct electric current. Conductivity (σ) is the reciprocal of electrical resistivity (ρ) which is defined as:

$$\rho = R\,A/l \tag{4}$$

And hence,

$$\sigma = 1/\rho \tag{5}$$

where R is the electrical resistance of a uniform specimen, l is the length and A is the cross-sectional area of the specimen of the material. The electrical conductivity unit was calculated as siemens per centimeter (S cm^{-1}).

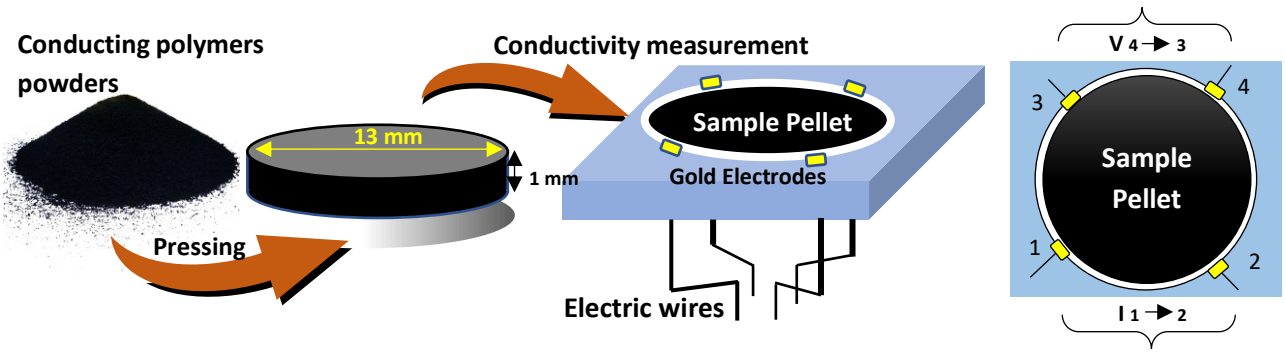

Figure 12. Powder samples preparation and electrodes arrangement for van der Pauw conductivity measurement.

For the bulk conductivity measurements, homogeneous conducting polymers powders (dried over silica gel at room temperature and finely ground) were pelletized in a 13 mm diameter evacuable die under 70 kN (527 MPa) using a manual hydraulic press. A cylindrical shape pellet with a flat surface and uniform thickness (1±0.05 mm) was obtained. The conductivities were measured in the ambient conditions at room temperature by the van der Pauw method [319]. Four electrodes are placed on the edges of the sample perimeter as shown

in Figure 12, this configuration allows the van der Pauw method to estimate the average resistivity of the sample.

The van der Pauw resistivity of a sample is calculated as follows:

$$\rho = \frac{\pi d}{\ln(2)}\left(\frac{R_1+R_2}{2}\right)f(R_1/R_2) \quad (6)$$

For symmetrical samples (disks with contacts at 90°), $R_1=R_2$ then,

$$\rho = \frac{\pi d}{\ln(2)}R \quad (7)$$

where d is the sample thickness and $\pi/\ln(2)$ is the van der Pauw constant. Resistance (R) is calculated from the linear section of the current-voltage plot, $R=V/I$. Hence the conductivity is calculated as follows:

$$\sigma = \frac{\ln(2)I}{\pi dV} \quad (9)$$

- **Thermogravimetric analysis**

Thermogravimetric analysis (TGA) is a great method to study the thermal stability, thermal decomposition, combustions, oxidation or reduction reactions of the materials. TGA monitors the mass changes of a material as a function of temperature (to perform dynamic thermogravimetry with a constant temperature change rate) or time (to perform isothermal analysis, temperature is constant) in a controlled atmosphere (in the air or under inert gases). In this study, the weight change of CPs was measured as a function of temperature in air or under nitrogen. TGA plots of CPs and their composites were recorded in a heating rate of 10 °C min^{-1} and 50 mL min^{-1} of air or nitrogen flow.

- **Specific surface area (BET) analysis**

The specific surface area of a solid is the total surface area of a unit mass of the material. Brunauer–Emmett–Teller (BET) isotherms method is the most common method used to calculate the specific surface area which is an adsorption-based method. It is based on the physical adsorption of inert gas molecules (N_2 or He) on a solid surface to quantify the number of binding sites (specific surface area).

4. RESULTS AND DISCUSSION

4.1. Dyes in the tuning of polypyrrole morphology

Conventional PPy is prepared by the oxidation of pyrrole with a suitable oxidant *e.g.,* iron(III) chloride as a powder with globular morphology [113]. When the oxidation takes place in the presence of suitable organic dyes, one-dimensional morphologies, such as nanotubes or nanofibers are obtained [108]. Organic dyes can form various templates by various assembly mechanisms *e.g.,* J-aggregates stabilized by π–π interactions [144], soluble salt–insoluble acid transition of most of the organic dyes [32] or by oligomerization of certain dyes [143].

4.1.1. Effect of cationic dyes

Safranin and phenosafranin, the cationic dyes, were used as morphology-guiding agents for the conversion of PPy morphology (Appendix 1). However, safranin and phenosafranin have similar chemical structures, they form two different types of insoluble precipitates when mixing with iron(III) chloride (Figure 13). Safranin forms tiny fibrillar aggregates (Figure 13A), while phenosafranin generates relatively large microcubes (Figure 13B). Such precipitates can work as morphology-guiding agents to control the morphology of the PPy. Those precipitates are formed by the oxidation of safranin or phenosafranin dyes to corresponding insoluble oligomers [143].

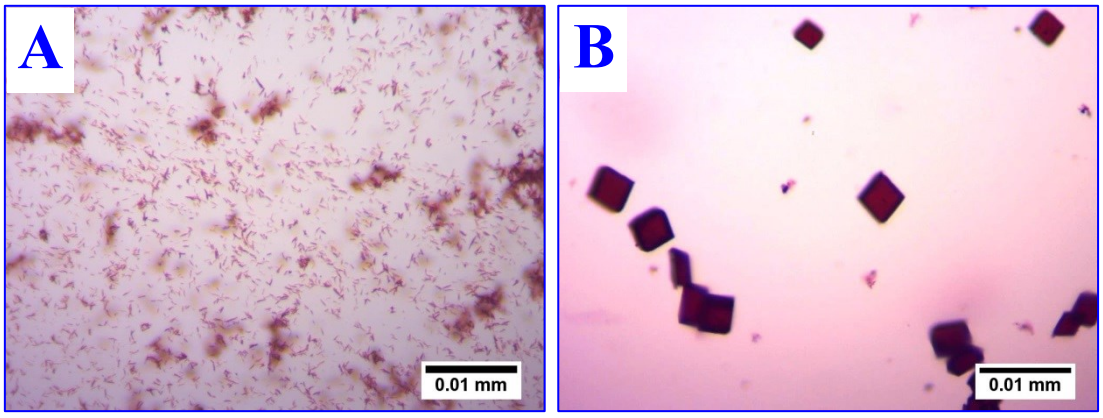

Figure 13. Optical microscope images of formed templates by mixing 4 mM of (A) safranin and (B) phenosafranin with 0.25 M iron(III) chloride. (Appendix 1)

Effect of safranin concentration on PPy morphology

The SEM analysis of a series of PPy prepared in the presence of various concentrations of safranin shows a significant effect of the safranin on the PPy morphology (Appendix 1). At the lowest concentration, 0.5 mM of safranin, a mixture of globules and nanorods was formed (Figure 14). At low safranin concentration, the formed templates population is low, and hence template content is consumed faster than pyrrole polymerization. By increasing the safranin concentration, exclusively nanofibers were obtained with different dimensions.

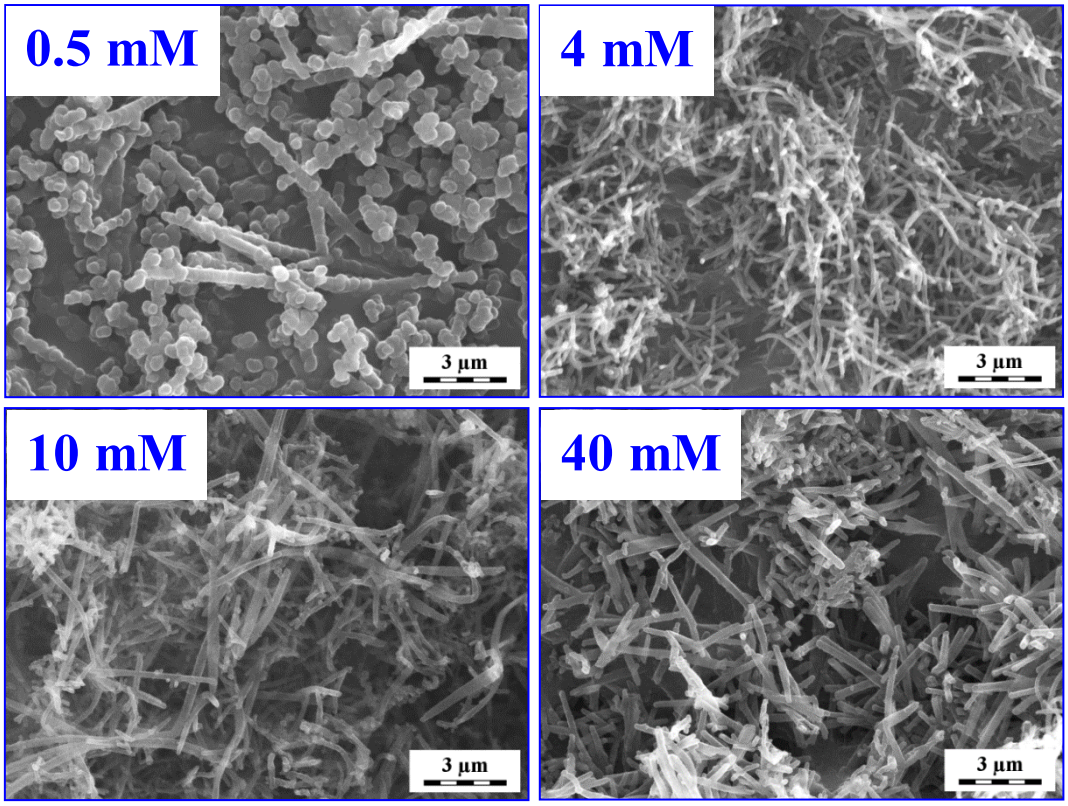

Figure 14. SEM micrographs of polypyrrole prepared in the presence of 0.5 mM, 4 mM, 10 mM, and 40 mM of safranin at room temperature.

The TEM analysis (Figure 15) confirmed the formation of the mixture of nanotubes/nanofibers. At low safranin concentrations, PPy nanofibers were formed while at higher safranin concentrations, hollow nanofibers (nanotubes) were produced. However, no exclusive nanotubular morphology has been observed even at the highest safranin concentration.

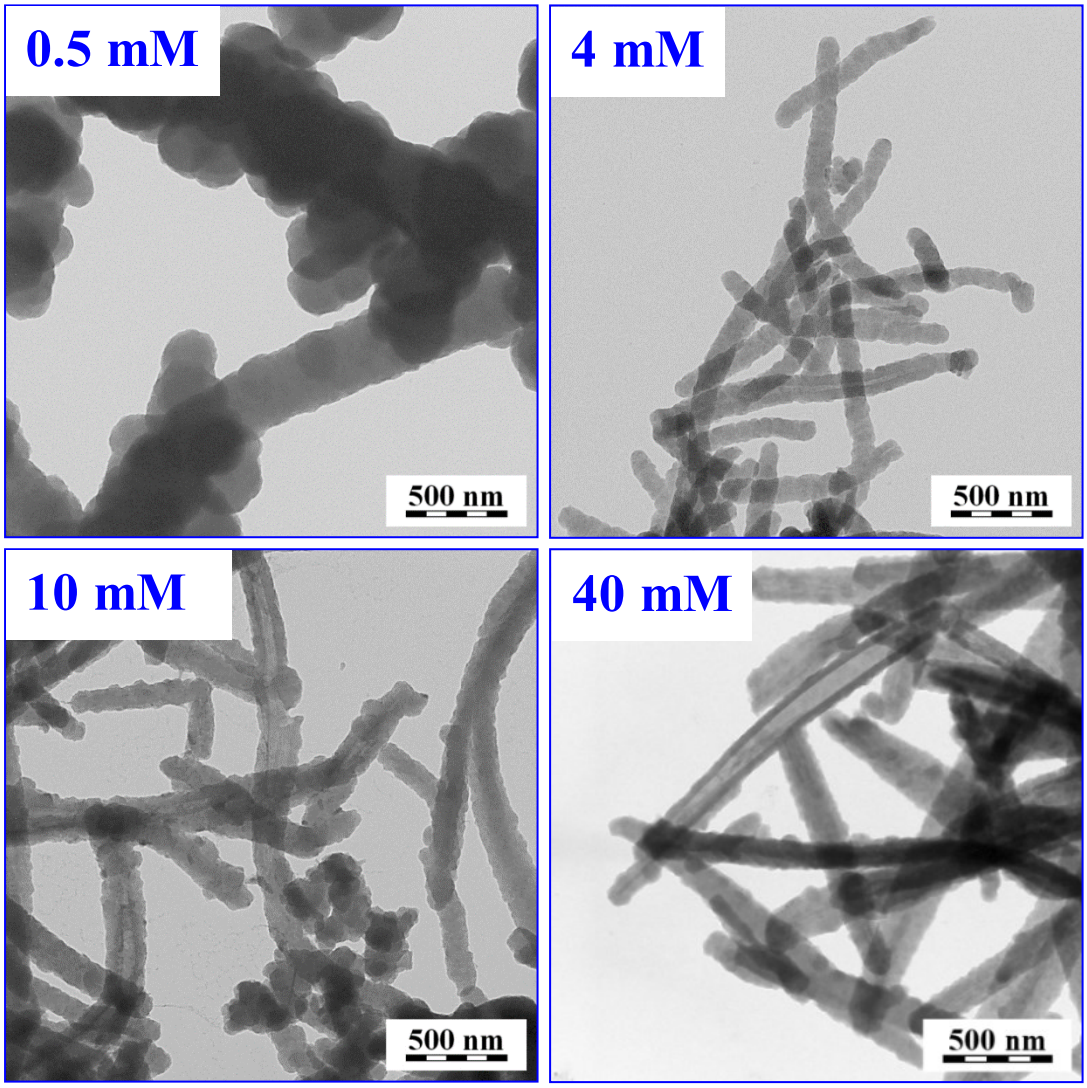

Figure 15. TEM micrographs of polypyrrole prepared in the presence of 0.5 mM, 4 mM, 10 mM, and 40 mM of safranin at room temperature.

Effect of phenosafranin concentration on PPy morphology

The SEM micrographs of PPy prepared in the presence of phenosafranin show that all produced fibers are accompanied by globules (Appendix 1). Phenosafranin is producing robust cubic templates with a low population (Figure 13B), hence, the phenosafranin templates deplete sooner from the polymerization mixture and globular PPy are therefore produced as the polymerization proceeds. The aspect ratio of the formed fibers is smaller compared to fibers prepared with safranin. TEM micrographs confirm the formation of nanotubes with rough

surfaces (Figure 16). The dimensions of the formed PPy nanotubes did not markedly change with the change of phenosafranin concentration.

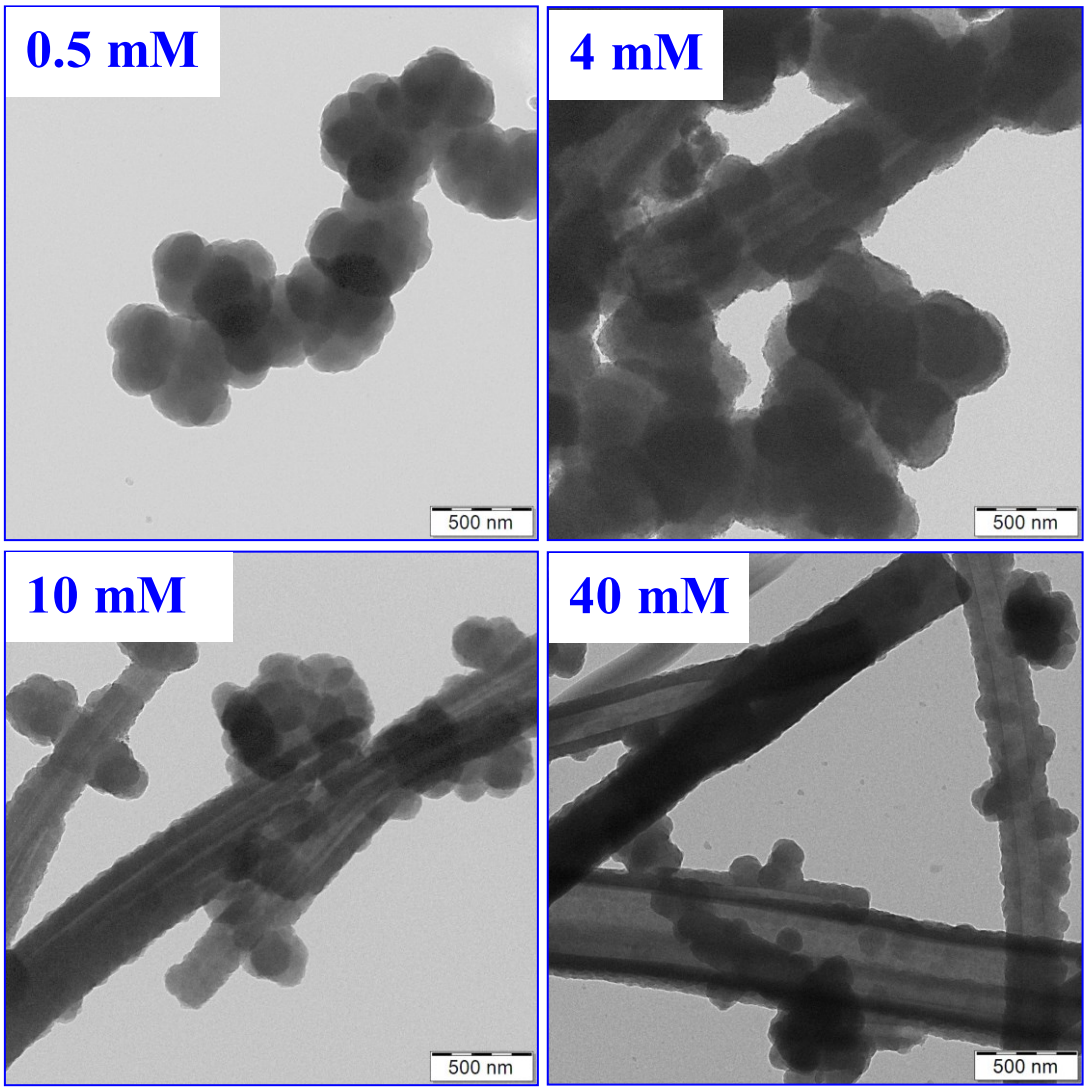

Figure 16. TEM micrographs of polypyrrole prepared in the presence of 0.5 mM, 4 mM, and 40 mM of phenosafranin at room temperature.

4.1.2. Effect of oxidant-to-monomer mole ratio (in the presence of safranin)

A series of PPy was synthesized with variable oxidant-to-monomer mole ratios, at fixed pyrrole (0.2 M) and safranin (4 mM) concentrations, to study the effect on the morphology and conductivity of PPy. However, the optimum stoichiometric mole ratio of iron(III) chloride to pyrrole equals 2.5 [32], lower and higher mole ratios produce PPy with varied properties. At a

low oxidant-to-monomer mole ratio (1:1), the morphology of PPy was a mixture of fibers and globular particles (Figure 17), due to the less template's population in the polymerization medium. By increasing the mole ratio up to 2:1, exclusively nanofibers were formed. At high mole ratios (3.5:1 and 5:1), a mixture of globular and fibrillar morphology is formed, due to the very high rate of polymerization at high oxidant concentrations which does not allow the PPy chain to organize into nanostructured morphology.

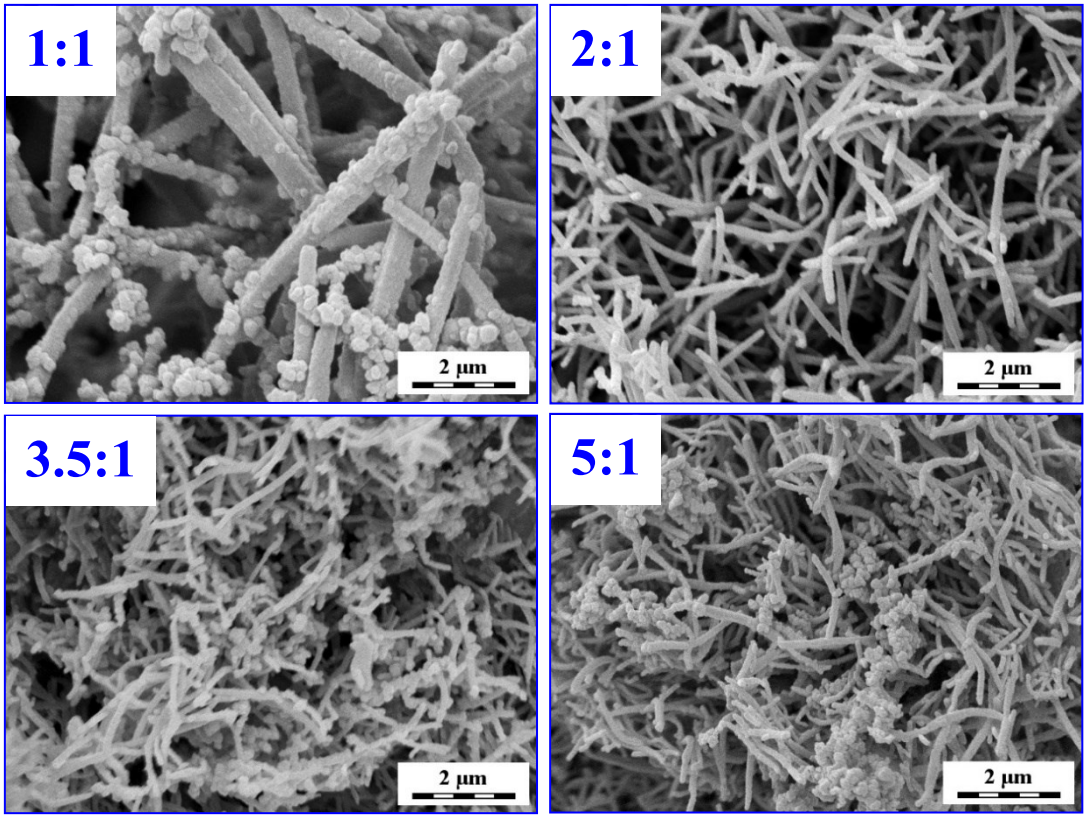

Figure 17. Effect of oxidant-to-monomer mole ratio on the morphology of polypyrrole prepared in the presence of safranin.

4.1.3. Effect of methyl red (anionic dye)

Although, the preparation of PPy in the presence of methyl red (MR) acid form had no effect on PPy properties, either morphology or conductivity, surprisingly, when the preparation of PPy is carried out in the presence of MR sodium salt the morphology and conductivity of the produced PPy are strongly influenced.

Methyl red acid form is insoluble in the reaction medium and when introduced in the reaction mixture, it has no effect on the PPy formation; the morphology and conductivity remain unchanged. Water-soluble MR sodium salt precipitates when the strongly acidic oxidant ($FeCl_3$) is added to the dye-containing pyrrole solution (Appendix 2). The forming MR precipitate simultaneously acts as an adsorption site for pyrrole oligomers, which is followed by the growth of PPy chains [320]. Such a template-supported growth of PPy is believed to produce better organized PPy chains, providing in addition to the morphology changes, the conductivity enhancement.

The presence of MR salt, even at a low concentration (1 mM), influences the morphology by reducing the size of PPy globules (Figure 18). At 2 mM or higher MR salt concentration PPy with irregular flakes morphology is produced (Appendix 2).

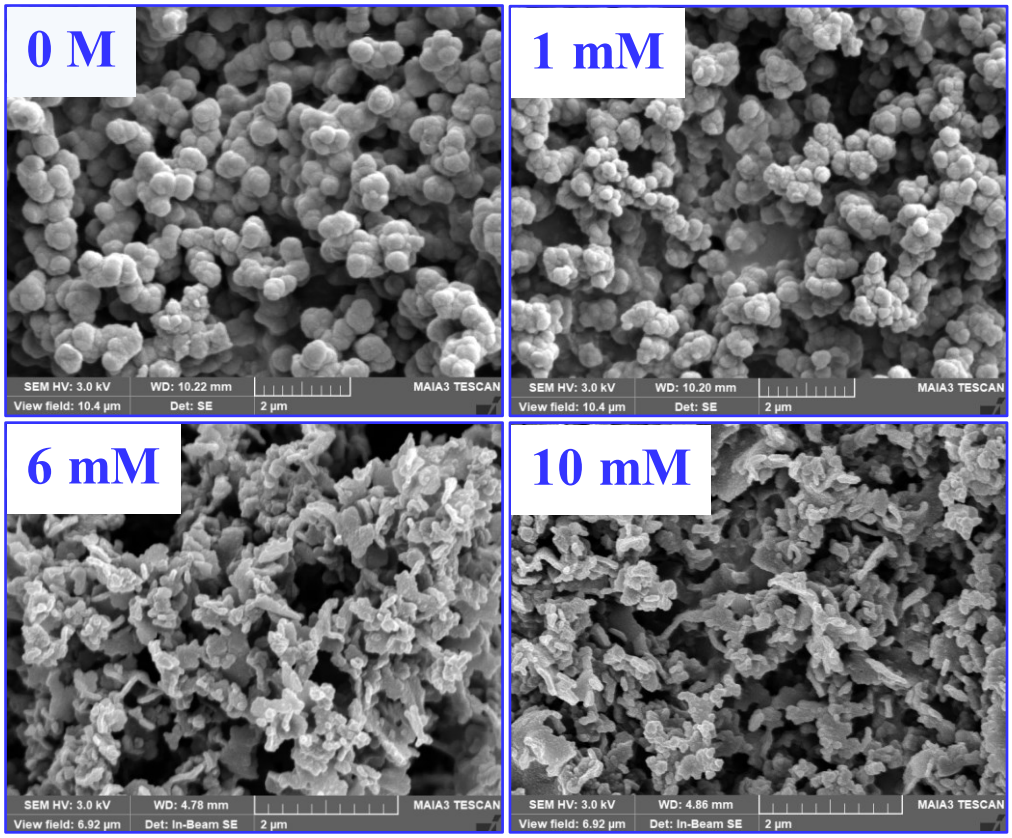

Figure 18. Morphology of polypyrrole prepared at room temperature in the absence and the presence of methyl red salt at 1 mM, 6 mM and 10 mM concentration at room temperature. (Appendix 2)

The TEM investigation reveals that the PPy morphology is composed of irregular aggregates of tiny PPy particles (Appendix 2), which is obviously different than the conventional globular morphology prepared in the absence of dyes. By increasing the MR dye concentration, PPy particle size decreases, based on the fact that some dyes tend to behave as surfactants [321], with the tendency of the reduction of the PPy particle size with increasing dye concentration.

4.2. Dyes in the enhancement of polypyrrole conductivity

Polypyrrole conductivity was found to be dependent on its morphology to a certain extent (however, there is no direct correlation between the PPy conductivity and morphology). Conventional PPy has a typical globular morphology with the conductivity of few units (1–5) S cm^{-1} [32]. The introduction of organic dyes into the polymerization media, even at very low concentration, either converts PPy globular morphology into various one-dimensional nanostructures or decrease the size of the globules. This is based on the various dyes' ability to form templates under certain conditions *e.g.*, dyes pK_a, hydrophobicity and aggregation rate (Appendices 1 and 2).

4.2.1. Effect of cationic dyes

The DC conductivity of PPy prepared with various concentrations of safranin was studied (Appendix 1). The conductivity of oligomeric safranin templates is low ~10^{-9} S cm^{-1} [143]. PPy prepared in the presence of safranin has much higher conductivity than the globular PPy (5 S cm^{-1}) prepared in the dye absence. The PPy conductivity increased linearly with increasing the safranin concentration, reaching the maximum value of 35 S cm^{-1} at 4 mM of dye, then decreased again (Figure 19).

Phenosafranin has a similar effect on the PPy conductivity, the conductivity reached its maximum value of 10.5 S cm^{-1} when 2 mM of phenosafranin was used (Figure 19). The conductivity enhancement is assigned to the better ordering of PPy chains in the nanotubular morphology compared to the less ordering chains in the globules. Also, nanotubular morphology is more favorable for the dopant distribution, which enhance the conductivity. At

high dyes concentrations, the fraction of non-conducting content (dye) is increased, which subsequently leads to decreasing of the conductivity.

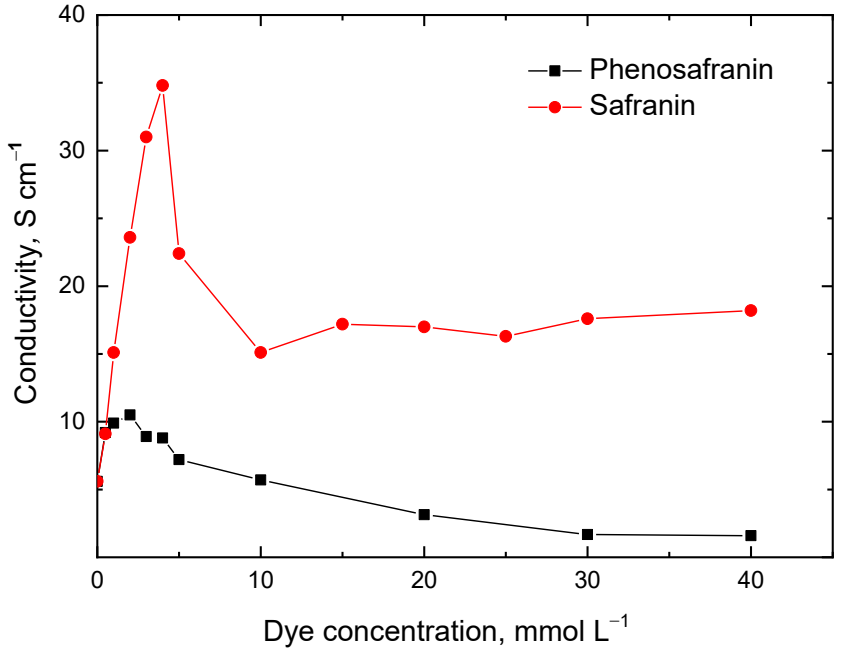

Figure 19. The dependence of polypyrrole conductivity on the molar concentration of safranin or phenosafranin added to the reaction mixture at room temperature. (Appendix 1)

4.2.2. Effect of anionic dye

However, MR sodium salt behaves differently than safranin and phenosafranin, a similar trend of conductivity was obtained by the addition of MR sodium salt to the pyrrole polymerization medium. PPy conductivity increased by increasing MR concentration till the maximum value of 84 S cm^{-1} at 6 mM of the dye, then decreased with a further increase in dye concentration as shown in Figure 20.

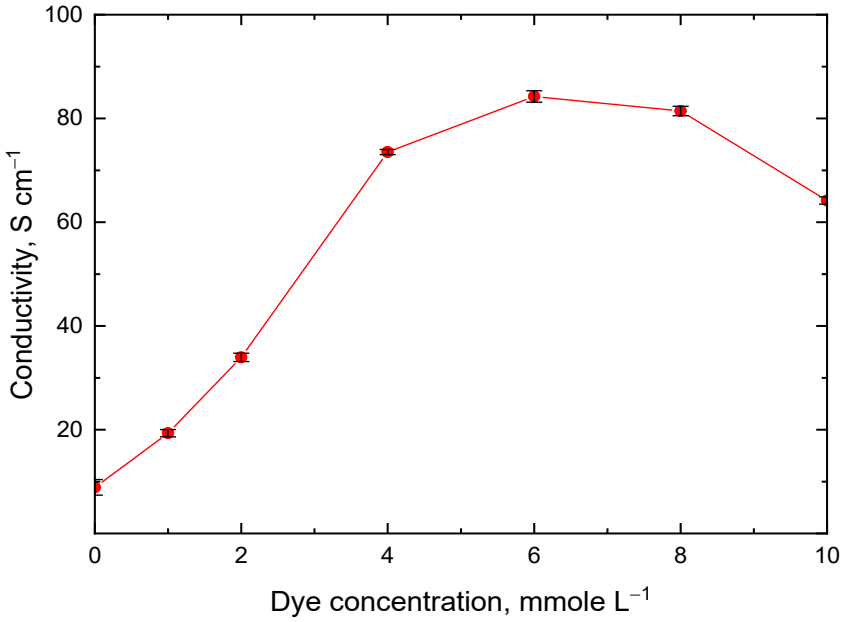

Figure 20. The dependence of polypyrrole conductivity on the molar concentration of methyl red sodium salt in the reaction mixture at room temperature. (Appendix 2)

4.3. Effect of polymerization temperature on polypyrrole morphology and conductivity

Polymerization temperature was found to greatly influence the properties of the chemically [75] and electrochemically polymerized [322] PPy [50]. For the electrochemically prepared PPy conductivity remarkably increased with decreasing the polymerization temperature from 0.04 S cm^{-1} at 60 °C to 26.3 S cm^{-1} at 1 °C [50]. Herein, we study the effect of pyrrole polymerization temperature in the absence or the presence of various organic days on the conductivity of the produced PPy nanostructures (Appendices 2–4).

4.3.1. Neat polypyrrole

The effect of polymerization temperature from +50 to −80 °C was studied for the neat PPy (Appendix 3). Decreasing the polymerization temperature was found to have a positive influence on PPy conductivity. PPy polymerized at a relatively high temperature of 50 °C had the lowest conductivity (~3 S cm^{-1}). By decreasing the temperature of preparation, conductivity

increased to 24 S cm^{-1} at −24 °C (frozen condition), which is fivefold higher than conductivity obtained at room temperature (~ 5 S cm^{-1}) as shown in Figure 21. Neat PPy prepared at −50 and −80 °C showed conductivity of ~ 20 and 22 S cm^{-1}, respectively. While the conductivity did not change compared to its value obtained at −24°C, the yield was highly decreased. FTIR and Raman spectroscopies confirmed the formation of PPy at all polymerization temperatures (50 to –50 °C) (Appendix 3).

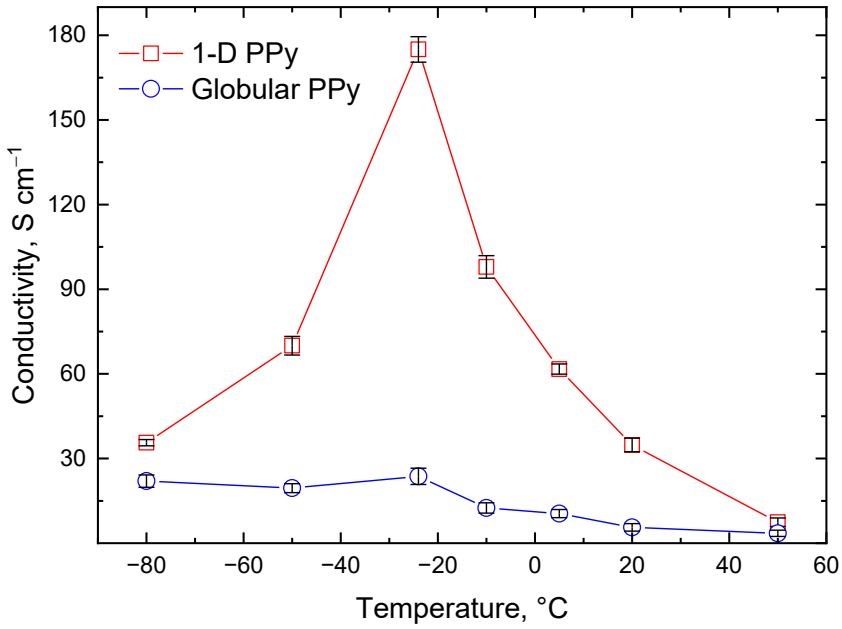

Figure 21. The influence of the polymerization temperature on the conductivity of the one-dimensional polypyrrole prepared in the presence of safranin and the globular polypyrrole prepared without safranin.

4.3.2. Polypyrrole nanostructures

The PPy polymerized in the presence of safranin at frozen state, −24 °C, showed the conductivity of 175 S cm^{-1}, which is the highest conductivity reported in the literature for PPy powder prepared by simple oxidative polymerization approach (Figure 21). The high conductivity of PPy prepared in the frozen condition can be attributed to a higher level of protonation evidenced by Raman spectroscopy (Appendix 3) and a better ordering of PPy chains.

Polypyrrole was also prepared in the presence of other organic dyes; MO and AB in the frozen conditions at −24 °C (Appendix 4). PPy nanotubes prepared in the presence of MO showed a significant increase of conductivity from 55 S cm^{-1} obtained when prepared at room temperature to 109 S cm^{-1} at −24 °C. The same trend was observed for the PPy nanofibers prepared in the presence of AB. The conductivity of 150 S cm^{-1} was reached by frozen-state polymerization, while 32.5 S cm^{-1} was obtained at room temperature. Nonetheless, frozen-state polymerization has not influenced on the morphology of one-dimensional PPy prepared in the presence of dyes, except for a reduction in their dimensions.

Frozen-state polymerization of pyrrole in the presence of MR enhances the conductivity of PPy (104 S cm^{-1} when prepared at −50 °C), however, no one-dimensional morphology was formed (Appendix 2). This confirms that one-dimensional morphologies are not prerequisites for the high conductivity of PPy.

The conductivity of CPs depends on their microscopic (intrinsic) and macroscopic (extrinsic) properties. Microscopic properties are based on the doping level, conjugation length and intra-chain interactions, while the macroscopic properties depend mainly on the inter-chain interactions, morphology and packing of the CPs chains [323]. Frozen-state polymerization was found to influence both micro- and macroscopic properties. It produces PPy chains with higher molecular weight and less defects which leads to improved conductivity.

4.4. Microporous sponge-like polypyrrole–nanofibrillated cellulose aerogels

PPy–NFC was prepared via *in situ* oxidative polymerization of pyrrole with iron(III) chloride in the presence of NFC at frozen conditions. The influence of the NFC content on morphology, conductivity, mechanical properties and specific surface area of PPy–NFC aerogels was studied (Appendix 5).

The SEM investigation of all the PPy–NFC aerogels prepared with various NFC contents show homogenous and highly porous sponge-like three-dimensional networks without any globular PPy aggregates (Figure 22). The porous structure is assigned to the growth of ice crystals during cryopolymerization. Due to the hydrophobic nature of pyrrole monomer, it has a higher affinity to polymerize on the NFC surface than ice crystals. Entangled fibers of the NFC work as a template of three-dimensional networks and PPy works as an adhesive coating to fix them together [324,325]. The hydrogen bonding between nitrogen in PPy chains and

hydroxyl groups on cellulose fibers guarantees the homogenous coating of PPy (FTIR and Raman analysis, Appendix 5). Synthesis of PPy–NFC with low contents of NFC (0.1–0.5 wt%) creates microporous structures with thinner interconnected fibers, while at higher contents of NFC (0.7–2 wt%) the NFC fibers tend to bundle together in thicker aggregates (Figure 22).

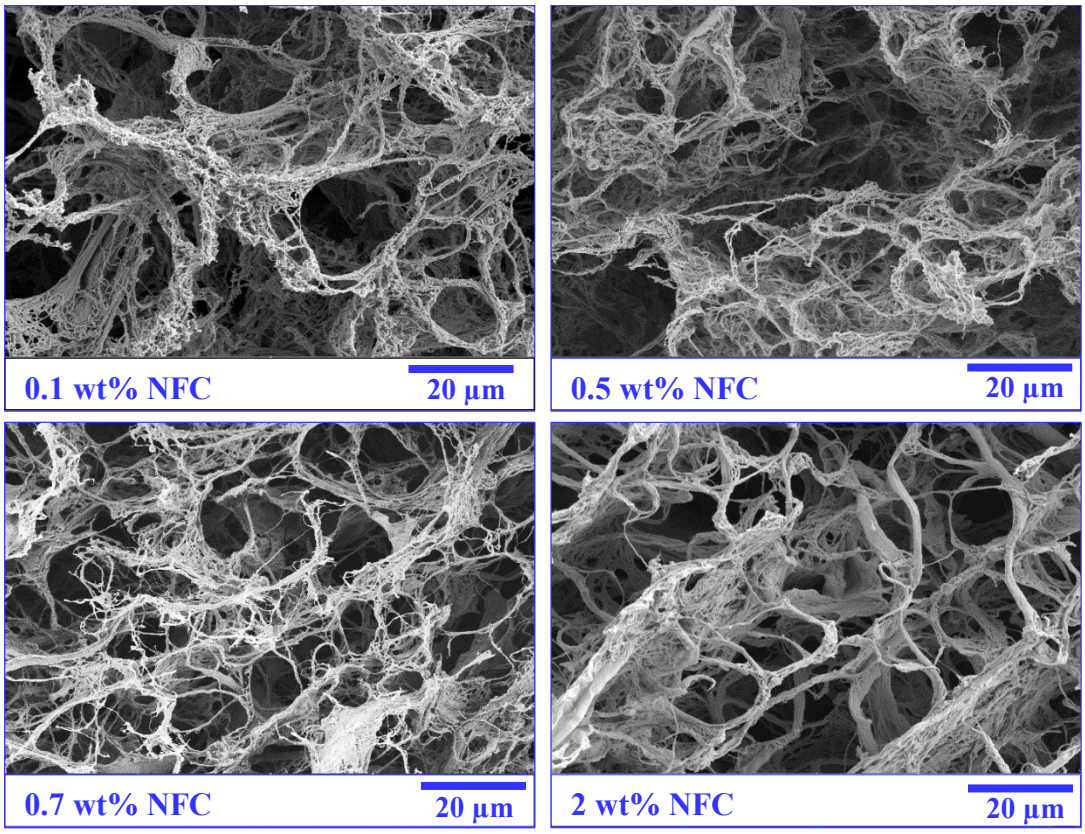

Figure 22. SEM micrographs of polypyrrole–nanofibrillated cellulose aerogels prepared with various contents of nanofibrillated cellulose.

The DC conductivity of the compressed pellets of protonated PPy–NFC aerogels (their corresponding cryogels were washed with 0.2 M HCl solution before freeze-drying to maintain the doping level), and deprotonated PPy–NFC aerogels (their cryogels were washed thoroughly with Milli-Q water before freeze-drying, which leads to partial deprotonation) were compared (Figure 23). The conductivity of protonated PPy–NFC aerogels is almost the same as of the neat PPy prepared in the same condition (frozen-state polymerization) with the value of 24 S cm^{-1} (Appendix 3). Moreover, they all exceeded the conductivity of neat PPy prepared at room temperature (units S cm^{-1}). The highest conductivity of 31 S cm^{-1} was obtained for PPy–NFC

aerogel prepared with 0.7 wt% of NFC, owing to the highest bipolaron to polaron ratio as confirmed by the Raman analysis (Appendix 5). Results also show that PPy–NFC aerogels partially preserve their conductivity at neutral conditions.

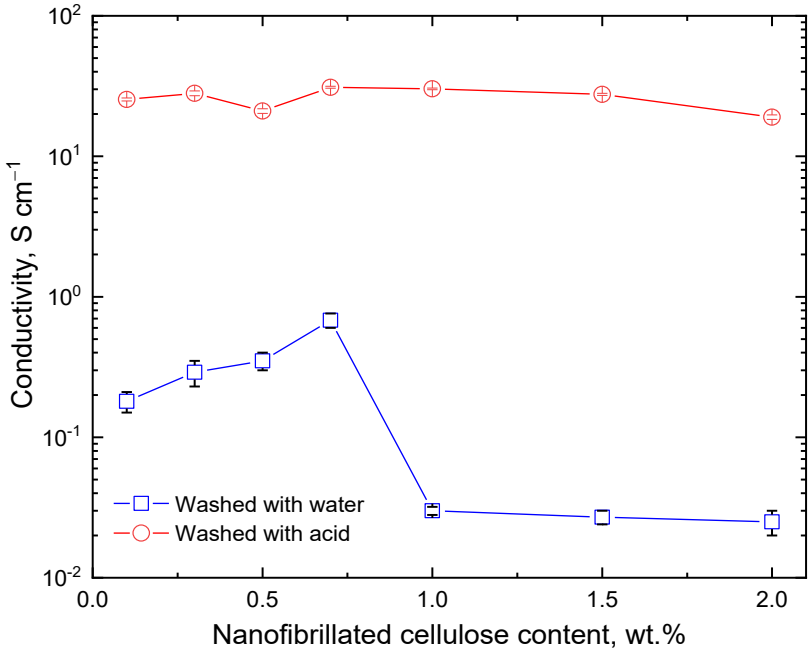

Figure 23. The conductivity of polypyrrole–nanofibrillated cellulose aerogels with varying nanofibrillated cellulose content. Samples have been washed with 0.2 M HCl or Milli-Q water, respectively. (Appendix 5)

All the aerogels have higher specific surface area and higher thermal stability compared to the neat individual components. Also, the mechanical properties were found to be strongly dependent on the contents of the NFC. Tensile modulus proportionally increases with increasing the NFC content as shown in Figure 24.

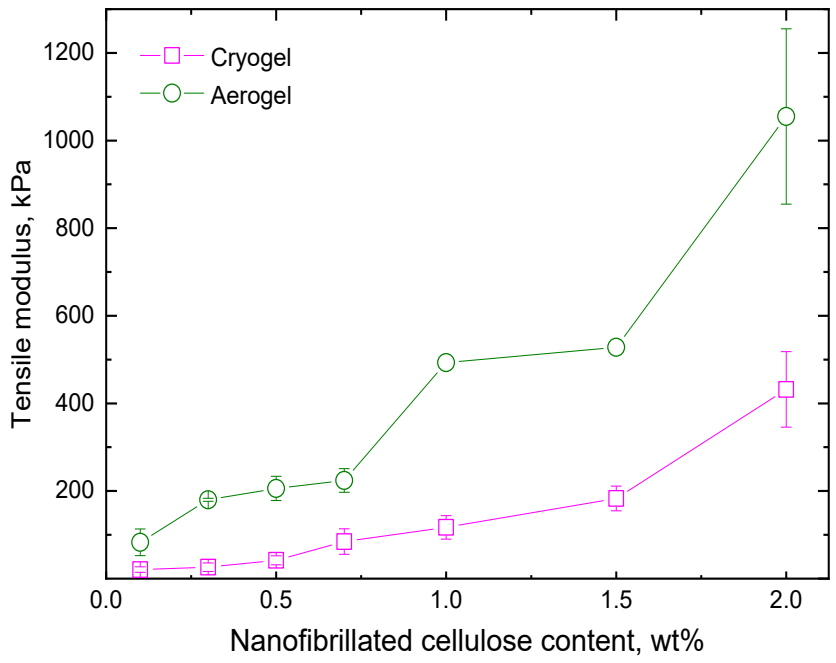

Figure 24. Tensile modulus of polypyrrole–nanofibrillated cellulose cryo- and aerogels with varying nanofibrillated cellulose content. (Appendix 5)

4.5. Nitrogen-enriched carbonaceous materials based on polypyrrole nanotubes

Conducting polymers, such as PANI or PPy can be easily carbonized in an inert atmosphere to nitrogen-enriched carbonaceous materials [326,327]. Thermal treatment of PPy under N_2 atmosphere was found to preserve the initial morphology and substantially increase the specific surface area of the product [326]. This allows tailoring desired morphologies of novel carbon materials, which can be used as cheap alternatives to carbon nanotubes.

Herein, we firstly convert PPy nanotubes (prepared in the presence of MO) to their carbonized analog (Appendix 6). Carbonized PPy was then coated with 20% w/w of neat PPy or PPy prepared in the presence of MO or AB.

By simple pyrolysis at 650 ºC under inert (N_2) atmosphere, PPy nanotubes' original morphology was preserved; however, the nanotubes became shorter due to shrinkage by mass loss on heating (Figure 25). The carbonized PPy nanotubes were then used as a template for the deposition of PPy. The coating of carbonized PPy nanotubes with PPy does not change its morphology, and the TEM analysis showed that all newly produced PPy was deposited on the

surface of the carbonized PPy nanotubes (Appendix 6). The successful coating appeared as an increase in the thickness of the carbonized PPy nanotubes walls.

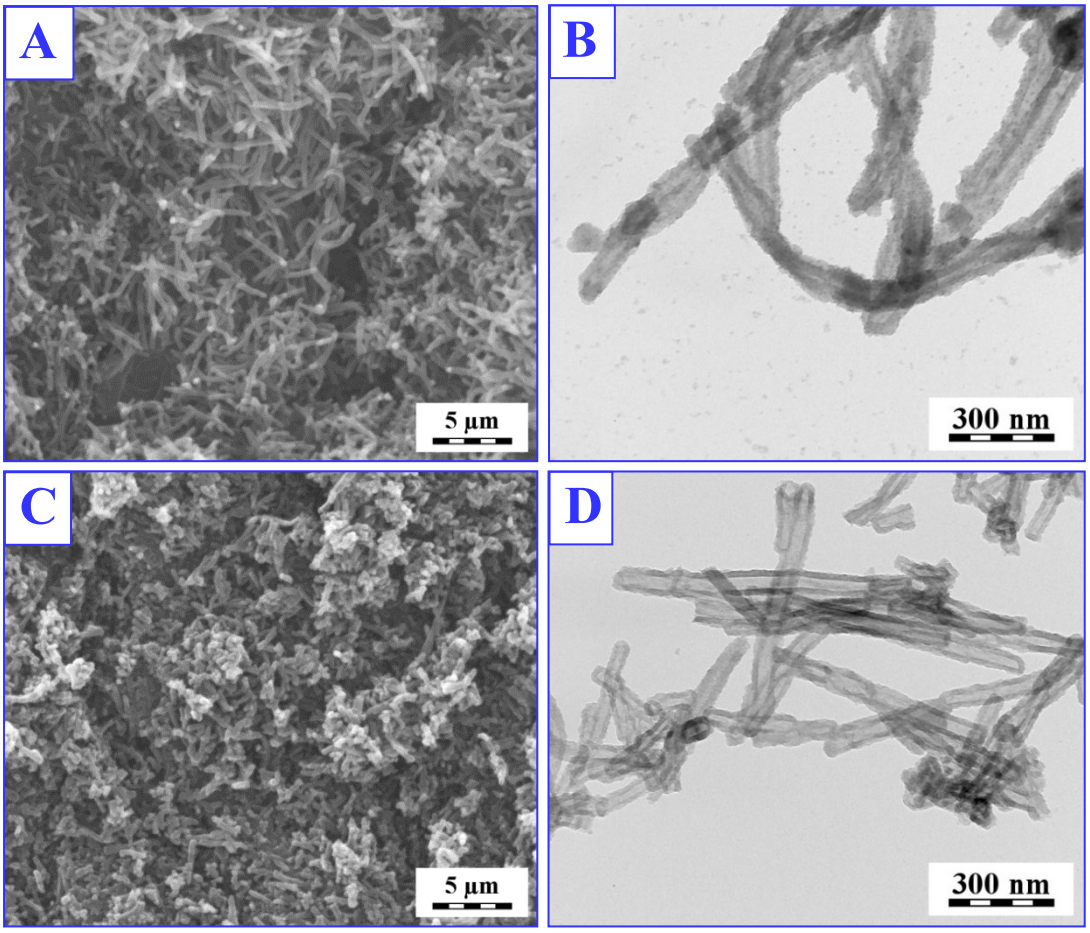

Figure 25. Scanning and transmission electron microscopy images of polypyrrole nanotubes before (A, B) and after (C, D) carbonization at 650 °C.

The conductivity of the precursor PPy nanotubes (before carbonization) was 55 S cm^{-1} or 0.1 S cm^{-1} measured by the DC conductivity of the compressed pellets (by van der Pauw method) or AC conductivity for its powder, respectively. The conductivity of carbonized PPy nanotubes powder dropped to 3×10^{-4} S cm^{-1} (the carbonized productes are not compressible into pellets). Subsequent coating with three types of PPy led to an increase in the conductivity to 3×10^{-2} S cm^{-1} for coating with neat PPy, 8×10^{-2} S cm^{-1} in the presence of AB and 0.15 S cm^{-1} in the presence of MO, which is higher than the conductivity of original PPy nanotubes (Appendix 6).

4.6. Applications of nanostructured conducting polymers composites

Conducting polymers properties such as ease of preparation, low cost, chemical and electrochemical activity and biocompatibility allows a wide range of applications. Composites of CPs are used to enhance their performance and to overcome some of their drawbacks.

In this section, the use of various CPs composites in two main fields of applications is discussed. Carbonized PPy nanotubes and their PPy-coated materials were used as catalysts for ORR. PPDA/γ-Fe_2O_3 composites, PANI/hexaferrite aerogels and PPy–NFC aerogels were used in the field of water treatment for the adsorptive removal of organic dyes and heavy metal ions from water.

4.6.1. Catalytic activity towards oxygen reduction reaction

The oxygen reduction reaction of O_2 to H_2O_2 or H_2O is a very important process in electrochemical energy conversion *e.g.,* in fuel cells [328]. CPs are considered as an interesting alternative to the precious metals *e.g.,* Pt to be used as electrocatalysts [170]. High surface area together with high porosity and electroactivity are important factors to enhance the efficiency of electrocatalysts [329].

Materials obtained by the coating of carbonized PPy nanotubes (Appendix 6) reveal an interesting deactivation effect upon cycling in O_2-saturated alkaline solutions where the measurements were performed using rotating disk electrode technique in KOH solution (Appendix 6). As shown in Figure 26, the ORR process is witnessed by both the reduction of faradaic response in O_2-saturated solution and by the decrease of capacitive response after cycling in the presence of O_2. The deactivation process is assigned to the deprotonation of the PPy shell (coating of the carbonized-PPy nanotubes core) and its irreversible transformation in the presence of the products of O_2 reduction (hydrogen peroxide). The precursor PPy nanotubes (before carbonization) was found to be not active for ORR, which matches the results reported before [330].

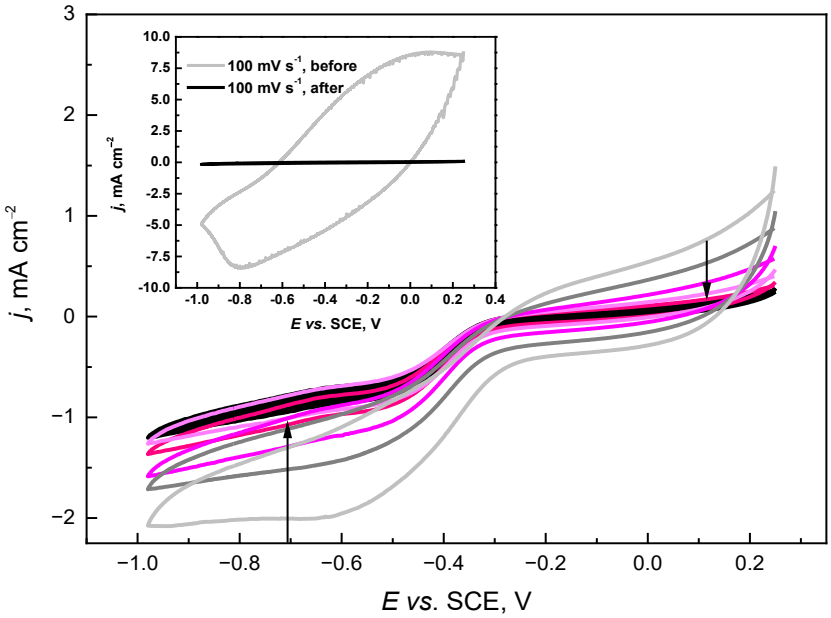

Figure 26. Consecutive cyclic voltammograms of carbonized polypyrrole nanotubes/polypyrrole in O_2-saturated 0.1 M KOH (potential sweep rate 20 mV s^{-1}, electrode rotation rate 600 rpm). Inset depicts baselines recorded in N_2-purged 0.1 M KOH at 100 mV s^{-1} before and after potentiodynamic cycling in O_2-saturated solution.

The results show that the neat carbonized PPy has the best activity among all the tested materials (Figure 27), which is due to the higher nitrogen content on the surface, (observed by XPS, Appendix 6). Also, ORR response was found to increase with increasing the specific surface area.

The selectivity of the various materials used as ORR catalysts was determined using Koutecky-Levich analysis [331]. This analysis allows determining the apparent number of electrons consumed *per* O_2 molecule. The results as presented in Table 2 show that neat carbonized PPy nanotubes are very selective towards the complete reduction of O_2 to H_2O *via* $4e^-$ pathway. The results also suggest the possibility to modulate ORR selectivity by PPy coating shell. Different PPy-coated carbonized PPy nanotubes materials offer different selectivity towards O_2 reduction (Table 2). This effect is probably due to a reduced specific surface area, resulting in a lower number of active sites for O_2 reduction when compared with the neat carbonized PPy nanotubes. Moreover, the formation of molecular shell over

carbonaceous core hinders the effective reduction of O_2. This observation shows that tailoring of the polymeric shell over ORR active carbonaceous core allows for the tuning of the catalyst selectivity and optimizing the performance of the materials for given applications, from fuel alkaline cells to electrochemical synthesis of hydrogen peroxide.

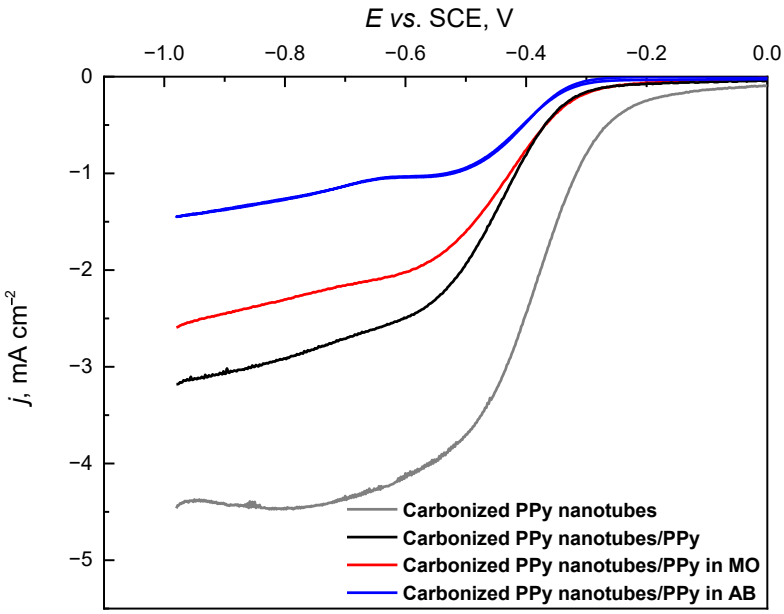

Figure 27. Comparison of oxygen reduction reaction polarization curves recorded under rotating disk electrode conditions (1800 rpm) for the neat carbonized polypyrrole nanotubes and with various coatings in O_2-saturated 0.1 M KOH.

Table 2. Calculated number of electrons *per* O_2 molecule using Koutecky-Levich analysis

E vs SCE/V	Number of electrons *per* O_2 molecule			
	carbonized PPy nanotubes	carbonized PPy nanotubes/PPy	carbonized PPy nanotubes/PPy in MO	carbonized PPy nanotubes/PPy in AB
−0.50	4.20±0.1	2.5±0.1	1.9±0.2	2.20±0.10
−0.60	4.03±0.05	2.5±0.1	1.7±0.2	2.10±0.10
−0.70	3.85±0.02	2.4±0.1	1.7±0.2	2.03±0.08
−0.80	3.55±0.06	2.3±0.1	1.7±0.2	1.92±0.08

4.6.2. Water treatment applications

Dyes, heavy metal ions, pesticides, drugs and personal care products are typical wastewater pollutants that may display eco-toxic hazards and potential bioaccumulation dangers [332,333]. Various techniques *e.g.,* coagulation, flocculation, biodegradation, adsorption, ion exchange, and photocatalytic degradation are used to remove organic and inorganic pollutants from wastewater [334–336]. Among the previously mentioned methods, adsorption is considered a promising technique, due to its high efficiency, low cost and reusability. The adsorption process of most organic contaminants onto the CPs composites is classified as physisorption based on hydrogen bonding, electrostatic or π–π interactions, *etc.*

In this section, various CPs composites *i.e.,* PPDA, PANI and PPy composites have been used as adsorbents for the removal of contaminants (organic dyes and heavy metal ions) from water.

4.6.2.1. Removal of organic dyes

Poly(p-phenylenediamine)/maghemite composite for the removal of Reactive Black 5

Poly(*p*-phenylenediamine) and its composites have been widely utilized for the removal of heavy metals *e.g.,* Cr(VI), Pb(II), As(V), and organic contaminants *e.g.,* organophosphorus pesticides [337,338]. PPDA can be easily prepared and it shows excellent environmental and thermal stability, and biocompatibility [339]. The incorporation of magnetic iron oxide nanoparticles to the PPDA allows for the preparation of hybrid composites with magneto-conductive properties, which allows the easy control by an external magnetic field.

Poly(*p*-phenylenediamine)/maghemite (PPDA/γ-Fe_2O_3) composites were prepared by the oxidative polymerization of *p*-phenylenediamine with APS (as the oxidant) in the presence of various contents of γ-Fe_2O_3 nanoparticles (Appendix 7). The adsorption property of the composites was examined for the removal of RB anionic dye from aqueous solutions.

Results in Appendix 7 show that PPDA/γ-Fe_2O_3 prepared with 25 wt% of γ-Fe_2O_3 has the highest specific surface area of 71 m^2 g^{-1} and the highest adsorption capacity (Q_{max}) of 223 mg g^{-1}. The neat PPDA showed Q_{max} of 185.2 mg g^{-1} while PPDA prepared with 50 wt% of γ-Fe_2O_3 has Q_{max} of 123.2 mg g^{-1}. The results showed that specific surface area and wt% of adsorption-active PPDA phase of the composites plays key role in the adsorption capacity.

PPDA/γ-Fe_2O_3/25 and PPDA/γ-Fe_2O_3/50 contain respectively 93 and 55 wt% of the active PPDA that is effective for the RB adsorption. The γ-Fe_2O_3 nanoparticles have no affinity towards RB dye (Appendix 7). Protonated PPDA can electrostatically adsorb the anionic RB dye in addition to π-π stacking of aromatic rings. The incorporation of γ-Fe_2O_3 not only enhances the adsorption capacity of the composite but also allows easy separation of the composites from the adsorption medium via an external magnetic field (Figure 28).

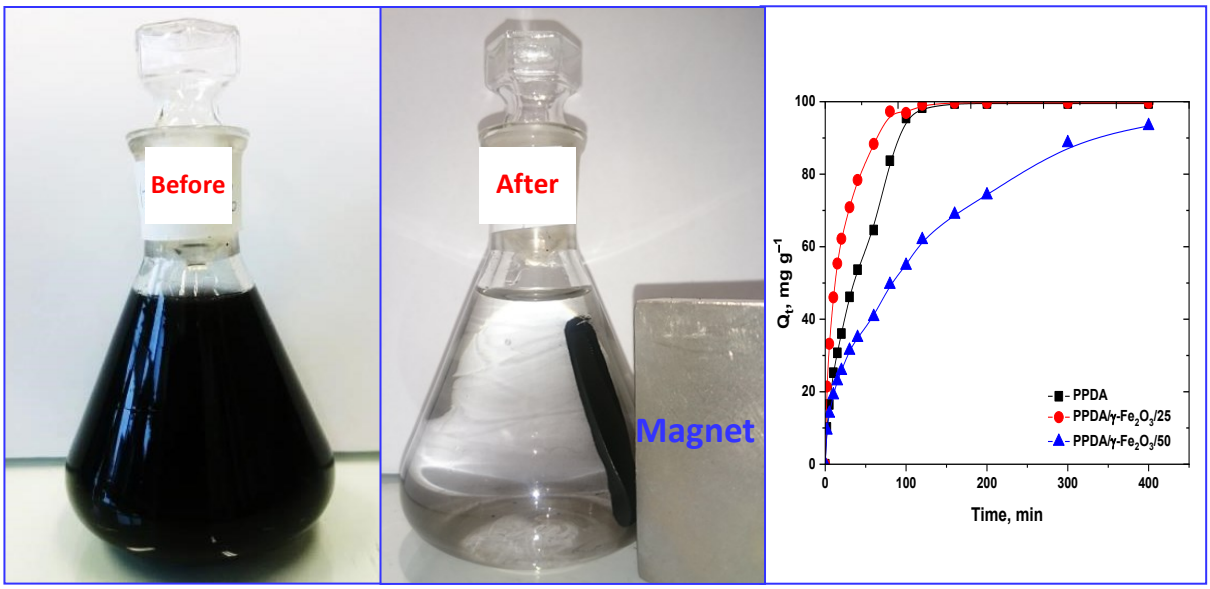

Figure 28. Aqueous solution of Reactive Black 5 (30 mg L^{-1}) before and after the adsorption by poly(*p*-phenylenediamine)/maghemite 50 wt% composite and separation by an external magnet.

Polyaniline/hexaferrite aerogels for the removal of Reactive Black 5

The cryogel of PANI/Ni_2SrCr_xW hexaferrite supported with PVAL has been prepared by a one-step procedure (Appendix 8). The incorporation of magnetic hexaferrite particles into the aerogel matrix (obtained by the freeze-drying of the cryogel) was confirmed with SEM and magnetization measurements (Appendix 8). The results also show that the macroporous PANI aerogels can perfectly host the hexaferrite particles with enhanced coercive force above that of the neat ferrite. The high value of magnetic coercivity allows for the easy separation of the aerogels from solutions. The conductivity and redox properties of PANI have not been directly

exploited in the adsorption study, however, they could be used for the controlled adsorption/desorption by electrochemical switching between the PANI oxidation states.

The results illustrate the efficiency and feasibility of PANI/hexaferrite application in water-pollution treatment on an example of an anionic dye (RB). Figure 29 shows the efficient adsorptive removal of RB dye (55 mg L^{-1}) by the aerogel (50 mg), where the intensive dark color of the dye solution was totally removed (with dye removal of 99%) within 4 h. PANI/hexaferrite aerogel offers a new type of macroporous dye absorbents with good mechanical properties, which can be easily separated from the aqueous medium.

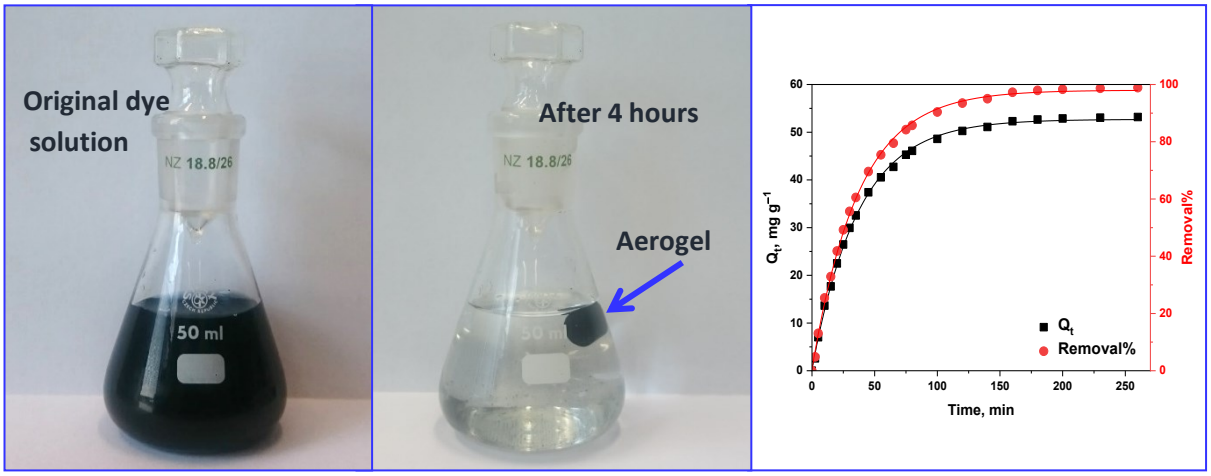

Figure 29. The aqueous solution of Reactive Black 25 (55 mg L^{-1}) becomes nearly colorless after adsorption onto the magnetic PANI/PVAL hexaferrite aerogel for 4 h.

4.6.2.2. Removal of heavy metal ions

Polypyrrole–nanofibrillated cellulose aerogels for the removal of Cr(VI) ions

Cellulose, PPy and their composites have been widely used in water treatment for the removal of heavy metals ions. Cellulose fibers loaded with PPy were used to improve the utilization of waste paper through the "*waste treatment by waste*" strategy for the removal of Cr(VI) from water [228].

Herein, mechanically stable PPy–nanofibrillated cellulose (NFC) aerogels (Appendix 5) are used for the removal of Cr(VI) ions from water. They possess high surface area, oxidation-

reduction properties and straightforward preparation with low cost. Also, they provide an easy separation method from the solution after the adsorption process (Appendix 5). The adsorption of Cr(VI) took place in acidic conditions, where Cr(VI) ions exist in the form of $HCrO_4^-$, which facilitates the electrostatic interactions with the positively charged protonated PPy chains.

Spectroscopic results revealed a dependence of the adsorption capacity on the NFC contents in the PPy–NFC aerogels (Figure 30). However, the pristine NFC revealed no affinity towards Cr(VI). The incorporation of NFC into PPy has led to a significant enhancement of the adsorption capacities of the composites. Among the various PPy–NFC aerogels, PPy–NFC prepared with 2 wt% of NFC has the lowest adsorption capacity of 142.4 mg g^{-1} and the lowest removal efficiency of 75%. PPy–NFC prepared with 0.3 wt% of NFC has shown the highest adsorption capacity of 183.6 mg g^{-1} and removal efficiency of 98%. The high adsorption capacities of PPy–NFC can be assigned to their high specific surface area (34.5 to 67.3 m^2 g^{-1}) (Appendix 5) and the ion exchange capability of PPy.

The adsorption capacity of PPy–NFC prepared with 0.3 wt% NFC aerogels is higher than most of the reported similar materials. PPy/chitin showed a maximum adsorption capacity of 28.9 mg g^{-1} [340], while PPy/chitosan had an adsorption capacity of 78.6 mg g^{-1} [287]. PANI/PVAL aerogel prepared in the same way as PPy–NFC aerogel exhibited only 41.2 mg g^{-1} of maximum adsorption capacity of Cr(VI) ions [281].

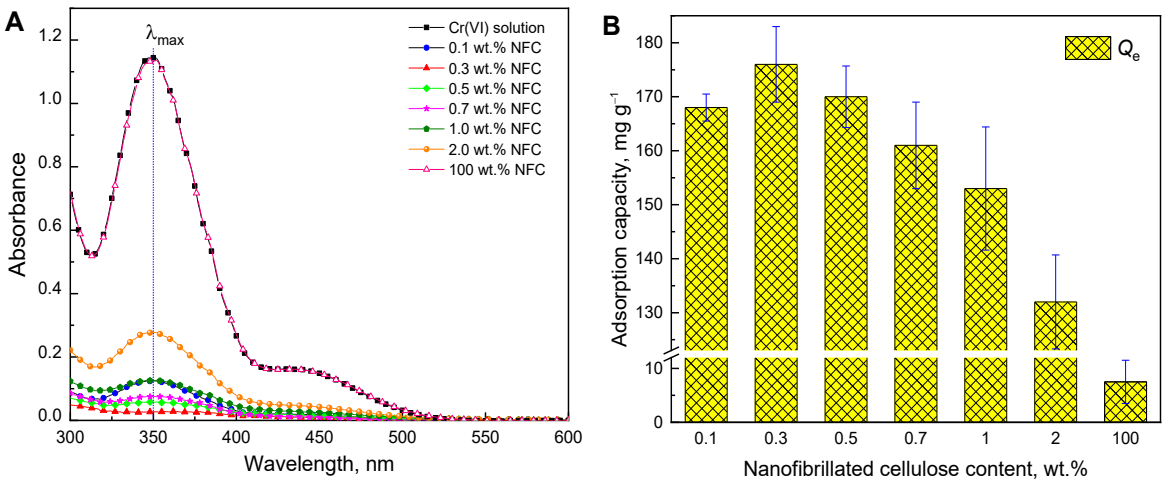

Figure 30. (A) UV-Visible spectra of Cr(VI) ions solutions (35 mg L^{-1}, 50 mL) after adsorption onto the neat nanofibrillated cellulose and polypyrrole–nanofibrillated cellulose aerogels with various nanofibrillated cellulose contents (10 mg), and (B) their corresponding adsorption capacities (Q_e). (Appendix 5)

5. CONCLUSIONS

- Organic cationic dyes, safranin and phenosafranin, have been used as templates for pyrrole polymerization. Their insoluble precipitates when mixing with iron(III) chloride solutions play a major role to convert conventional globular PPy into one-dimensional nanostructures.

- The conductivity of one-dimensional PPy nanostructures prepared in the presence of safranin or phenosafranin was enhanced, and the highest conductivity of 35 S cm^{-1} and 10 S cm^{-1} were obtained when 4 mM safranin and 2 mM phenosafranin were used, respectively, compared with 5 S cm^{-1} obtained for the neat PPy. Enhancement of the conductivity is assigned to the better organization of PPy chains in thin one-dimensional structures than in globules.

- Oxidant-to-pyrrole mole ratio has a significant effect on the conductivity, yield and morphology of PPy.

- The presence of MR sodium salt, anionic dye, during the preparation of PPy has enhanced the conductivity up to 84 S cm^{-1} depending on the dye concentration. The morphology of PPy, however, was neither globular nor nanotubular, and irregular particulate fragments dominated.

- Decreasing the polymerization temperature leads to significant conductivity changes. However, it doesn't drastically affect the morphology, except the dimensions of the PPy fibers or globules. Frozen-state polymerization of pyrrole in the presence of various dyes (safranin, AB and MO) produces one-dimensional nanostructures with high conductivity. The highest conductivity of 175 S cm^{-1} was obtained when PPy was prepared in the presence of safranin at −24°C. One-dimensional morphology of PPy, nanofibers or nanotubes, is not the main prerequisite for the high conductivity, and the conductivity above 100 S cm^{-1} can be achieved even for globular-like morphologies (*e.g.,* PPy prepared in the presence of MR).

- Carbonized PPy nanotubes coated with various types of PPy in the presence of organic dyes were obtained with high specific surface area. The thickness of the PPy coatings proved to have a marked effect on the capacitive performance.

- The incorporation of γ-Fe_2O_3 nanoparticles into the PPDA matrix has enhanced the adsorption capacity and provided an easy way for magnetic separation of the composites. The adsorption process of RB onto PPDA and its composites was found to follow the Langmuir isotherm model with maximum adsorption monolayer capacities of 185, 233 and 123 mg g^{-1} for PPDA, PPDA/γ-Fe_2O_3/25 and PPDA/γ-Fe_2O_3/50, respectively.

- The incorporation of Ni_2SrCr_xW hexaferrite particles into PANI/PVAL cryogels has increased the coercive force of the corresponding aerogels above its neat form value. The magnetic properties allow for the magnetic separation of the aerogel (adsorbent) from the aqueous medium after the adsorption process.

- Pyrrole was polymerized under the frozen conditions in the presence of low contents of NFC to form three-dimensional PPy–NFC cryogels. The sponge-like and lightweight aerogels with excellent mechanical properties and high conductivity were obtained by facile freeze-drying of their corresponding cryogels. Thanks to the high specific surface area and ion exchange capability, PPy–NFC aerogels have shown high adsorption capacities towards Cr(VI) metal ions, and the highest value of 183.6 mg g^{-1} was attained for aerogel with 0.3 wt% of NFC.

REFERENCES:

[1] M. Hess, R.G. Jones, J. Kahovec, T. Kitayama, P. Kratochvíl, P. Kubisa, W. Mormann, R.F.T. Stepto, D. Tabak, J. Vohlídal, Terminology of polymers containing ionizable or ionic groups and of polymers containing ions (IUPAC Recommendations 2006), Pure and Applied Chemistry, 78 (2006) 2067–2074.

[2] K. Potje-Kamloth, Conducting polymer-based Schottky barrier and heterojunction diodes and their sensor application, Handbook of Surfaces and Interfaces of Materials, Elsevier, 2001.

[3] J.C.W. Chien, Polyacetylene: chemistry, physics, and material science, Academic press, 2012.

[4] G. Natta, G. Mazzanti, P. Corradini, Stereospecific polymerization of acetylene, Stereoregular Polymers and Stereospecific Polymerizations, Elsevier, 1967.

[5] D.J. Berets, D.S. Smith, Electrical properties of linear polyacetylene, Transactions of the Faraday Society, 64 (1968) 823–828.

[6] H. Shirakawa, E.J. Louis, A.G. MacDiarmid, C.K. Chiang, A.J. Heeger, Synthesis of electrically conducting organic polymers: halogen derivatives of polyacetylene, $(CH)_x$, Journal of the Chemical Society, Chemical Communications, (1977) 578–580.

[7] A.J. Heeger, Semiconducting and metallic polymers: the fourth generation of polymeric materials (Nobel lecture), Angewandte Chemie International Edition, 40 (2001) 2591–2611.

[8] B. Nordén, E. Krutmeijer, The nobel prize in chemistry, 2000: Conductive polymers, kungl, Vetenskapsakademien, The Royal Swedish Academy of Sciences, (2000) 1–16.

[9] N. Dubey, M. Leclerc, Conducting polymers: efficient thermoelectric materials, Journal of Polymer Science Part B: Polymer Physics, 49 (2011) 467–475.

[10] S. Roth, H. Bleier, Solitons in polyacetylene, Advances in Physics, 36 (1987) 385–462.

[11] G. Kaur, R. Adhikari, P. Cass, M. Bown, P. Gunatillake, Electrically conductive polymers and composites for biomedical applications, RSC Advances, 5 (2015) 37553–37567.

[12] T. Ito, H. Shirakawa, S. Ikeda, Simultaneous polymerization and formation of polyacetylene film on the surface of concentrated soluble Ziegler-type catalyst solution, Journal of Polymer Science: Polymer Chemistry Edition, 12 (1974) 11–20.

[13] T.A. Skotheim (Ed.), Handbook of conducting polymers, CRC press, 1997.

[14] A.F. Diaz, K.K. Kanazawa, Polypyrrole: An electrochemical approach to conducting polymers, Extended Linear Chain Compounds, Springer, 1983.

[15] H.S. Nalwa, Advanced functional molecules and polymers: electronic and photonic properties, CRC Press, 2001.

[16] N.K. Guimard, N. Gomez, C.E. Schmidt, Conducting polymers in biomedical engineering, Progress in Polymer Science, 32 (2007) 876–921.

[17] D.N. Nguyen, H. Yoon, Recent advances in nanostructured conducting polymers: from synthesis to practical applications, Polymers, 8 (2016) 118.

[18] S. Sadki, P. Schottland, N. Brodie, G. Sabouraud, The mechanisms of pyrrole electropolymerization, Chemical Society Reviews, 29 (2000) 283–293.

[19] O.Y. Posudievsky, O.A. Goncharuk, V.D. Pokhodenko, Mechanochemical preparation of conducting polymers and oligomers, Synthetic Metals, 160 (2010) 47–51.

[20] J.K. Koh, J. Kim, B. Kim, J.H. Kim, E. Kim, Highly efficient, iodine-free dye-sensitized solar cells with solid-state synthesis of conducting polymers, Advanced Materials, 23 (2011) 1641–1646.

[21] P.-G. Su, Y.-T. Peng, Fabrication of a room-temperature H_2S gas sensor based on PPy/WO_3 nanocomposite films by in-situ photopolymerization, Sensors and Actuators B: Chemical, 193 (2014) 637–643.

[22] Z. Cui, C. Coletta, A. Dazzi, P. Lefrancois, M. Gervais, S. Néron, S. Remita, Radiolytic method as a novel approach for the synthesis of nanostructured conducting polypyrrole, Langmuir, 30 (2014) 14086–14094.

[23] M. Omastová, M. Mičušík, Polypyrrole coating of inorganic and organic materials by chemical oxidative polymerisation, Chemical Papers, 66 (2012) 392–414.

[24] A. Angeli, L. Alessandri, Sopra il nero pirrolo II. Nota, Gazzetta Chimica Italiana, 46 (1916) 283–300.

[25] N.V. Blinova, J. Stejskal, M. Trchová, J. Prokeš, M. Omastová, Polyaniline and polypyrrole: A comparative study of the preparation, European Polymer Journal, 43 (2007) 2331–2341.

[26] M. Omastová, K. Mosnáčková, M. Trchová, E.N. Konyushenko, J. Stejskal, P. Fedorko, J. Prokeš, Polypyrrole and polyaniline prepared with cerium(IV) sulfate oxidant, Synthetic Metals, 160 (2010) 701–707.

[27] M. Nakata, M. Taga, H. Kise, Synthesis of electrical conductive polypyrrole films by interphase oxidative polymerization–effects of polymerization temperature and oxidizing agents, Polymer Journal, 24 (1992) 437–441.

[28] M. Omastová, K. Mosnáčková, P. Fedorko, M. Trchová, J. Stejskal, Polypyrrole/silver composites prepared by single-step synthesis, Synthetic Metals, 166 (2013) 57–62.

[29] A. Kisiel, D. Korol, A. Michalska, K. Maksymiuk, Polypyrrole nanoparticles of high electroactivity. Simple synthesis methods and studies on electrochemical properties, Electrochimica Acta, 390 (2021) 138787.

[30] S.P. Armes, Optimum reaction conditions for the polymerization of pyrrole by iron(III) chloride in aqueous solution, Synthetic Metals, 20 (1987) 365–371.

[31] A.L. Pang, A. Arsad, M. Ahmadipour, Synthesis and factor affecting on the conductivity of polypyrrole: a short review, Polymers for Advanced Technologies, 32 (2021) 1428–1454.

[32] Y. Li, P. Bober, M. Trchová, J. Stejskal, Polypyrrole prepared in the presence of methyl orange and ethyl orange: nanotubes versus globules in conductivity enhancement, Journal of Materials Chemistry C, 5 (2017) 4236–4245.

[33] C.F. Hsu, L. Zhang, H. Peng, J. Travas-Sejdic, P.A. Kilmartin, Scavenging of DPPH free radicals by polypyrrole powders of varying levels of overoxidation and/or reduction, Synthetic Metals, 158 (2008) 946–952.

[34] J. Stejskal, R.G. Gilbert, Polyaniline. Preparation of a conducting polymer (IUPAC technical report), Pure and Applied Chemistry, 74 (2002) 857–867.

[35] M.M. Ayad, W.A. Amer, M. Whdan, *In situ* polyaniline film formation using ferric chloride as an oxidant, Journal of Applied Polymer Science, 125 (2012) 2695–2700.

[36] P. Bober, M. Trchová, J. Prokeš, M. Varga, J. Stejskal, Polyaniline–silver composites prepared by the oxidation of aniline with silver nitrate in solutions of sulfonic acids, Electrochimica Acta, 56 (2011) 3580–3585.

[37] R.A. de Barros, W.M. de Azevedo, Polyaniline/silver nanocomposite preparation under extreme or non-classical conditions, Synthetic Metals, 158 (2008) 922–926.

[38] Y. Cao, A. Andreatta, A.J. Heeger, P. Smith, Influence of chemical polymerization conditions on the properties of polyaniline, Polymer, 30 (1989) 2305–2311.

[39] Y. Wei, G.W. Jang, C.C. Chan, K.F. Hsueh, R. Hariharan, S.A. Patel, C.K. Whitecar, Polymerization of aniline and alkyl ring-substituted anilines in the presence of aromatic additives, Journal of Physical Chemistry, 94 (1990) 7716–7721.

[40] P. Bober, J. Stejskal, M. Trchova, J. Prokeš, I. Sapurina, Oxidation of aniline with silver nitrate accelerated by *p*-phenylenediamine: a new route to conducting composites, Macromolecules, 43 (2010) 10406–10413.

[41] P. Bober, J. Stejskal, M. Trchová, J. Prokeš, The preparation of conducting polyaniline–silver and poly(*p*-phenylenediamine)–silver nanocomposites in liquid and frozen reaction mixtures, Journal of Solid State Electrochemistry, 15 (2011) 2361–2368.

[42] I. Amer, T. Mokrani, L. Jewell, D.A. Young, H.C.M. Vosloo, Synthesis and characterization of sulfonated poly(*p*-phenylenediamine) prepared by different procedures, Polymer, 66 (2015) 230–239.

[43] F. Cataldo, On the polymerization of *p*-phenylenediamine, European Polymer Journal, 32 (1996) 43–50.

[44] S.-W. Yang, F. Liao, Characterization and morphology control of poly(*p*-phenylenediamine) microstructures in different pH, Nano, 6 (2011) 597–601.

[45] G. Ćirić-Marjanović, B. Marjanović, P. Bober, Z. Rozlívková, J. Stejskal, M. Trchová, J. Prokeš, The oxidative polymerization of *p*-phenylenediamine with silver nitrate: Toward highly conducting micro/nanostructured silver/conjugated polymer composites, Journal of Polymer Science Part A: Polymer Chemistry, 49 (2011) 3387–3403.

[46] R.H. Sestrem, D.C. Ferreira, R. Landers, M.L.A. Temperini, G.M. do Nascimento, Structure of chemically prepared poly-(*para*-phenylenediamine) investigated by spectroscopic techniques, Polymer, 50 (2009) 6043–6048.

[47] X. Li, M. Huang, R. Chen, Y. Jin, Y. Yang, Preparation and characterization of poly(*p*-phenylenediamine-*co*-xylidine), Journal of Applied Polymer Science, 81 (2001) 3107–3116.

[48] M. Ferenets, A. Harlin, Chemical in situ polymerization of polypyrrole on poly(methyl metacrylate) substrate, Thin Solid Films, 515 (2007) 5324–5328.

[49] J. Lei, Z. Cai, C.R. Martin, Effect of reagent concentrations used to synthesize polypyrrole on the chemical characteristics and optical and electronic properties of the resulting polymer, Synthetic Metals, 46 (1992) 53–69.

[50] A. Kassim, Z.B. Basar, H.N.M.E. Mahmud, Effects of preparation temperature on the conductivity of polypyrrole conducting polymer, Journal of Chemical Sciences, 114 (2002) 155–162.

[51] J. Stejskal, I. Sapurina, M. Trchová, E.N. Konyushenko, Oxidation of aniline: Polyaniline granules, nanotubes, and oligoaniline microspheres, Macromolecules, 41 (2008) 3530–3536.

[52] J. Stejskal, A. Riede, D. Hlavatá, J. Prokeš, M. Helmstedt, P. Holler, The effect of polymerization temperature on molecular weight, crystallinity, and electrical conductivity of polyaniline, Synthetic Metals, 96 (1998) 55–61.

[53] A.H. Navarchian, Z. Hasanzadeh, M. Joulazadeh, Effect of polymerization conditions on reaction yield, conductivity, and ammonia sensing of polyaniline, Advances in Polymer Technology, 32 (2013) 21356.

[54] A. Malinauskas, Chemical deposition of conducting polymers, Polymer, 42 (2001) 3957–3972.

[55] P. Bober, J. Stejskal, I. Šeděnková, M. Trchová, L. Martinková, J. Marek, The deposition of globular polypyrrole and polypyrrole nanotubes on cotton textile, Applied Surface Science, 356 (2015) 737–741.

[56] B. Dudem, A.R. Mule, H.R. Patnam, J.S. Yu, Wearable and durable triboelectric nanogenerators via polyaniline coated cotton textiles as a movement sensor and self-powered system, Nano Energy, 55 (2019) 305–315.

[57] J.M. D'Arcy, H.D. Tran, V.C. Tung, A.K. Tucker-Schwartz, R.P. Wong, Y. Yang, R.B. Kaner, Versatile solution for growing thin films of conducting polymers, Proceedings of the National Academy of Sciences, 107 (2010) 19673–19678.

[58] A. Mohammadi, M.-A. Hasan, B. Liedberg, I. Lundström, W.R. Salaneck, Chemical vapour deposition (CVD) of conducting polymers: Polypyrrole, Synthetic Metals, 14 (1986) 189–197.

[59] B. Winther-Jensen, K. West, Vapor-phase polymerization of 3,4-ethylenedioxythiophene: a route to highly conducting polymer surface layers, Macromolecules, 37 (2004) 4538–4543.

[60] J. Stejskal, P. Bober, Conducting polymer colloids, hydrogels, and cryogels: common start to various destinations, Colloid and Polymer Science, 296 (2018) 989–994.

[61] M. Salado, S. Lanceros-Mendez, E. Lizundia, Free-standing intrinsically conducting polymer membranes based on cellulose and poly(vinylidene fluoride) for energy storage applications, European Polymer Journal, 144 (2021) 110240.

[62] Z. Yang, D. Shi, W. Dong, M. Chen, Self-standing hydrogels composed of conducting polymers for all-hydrogel-state supercapacitors, Chemistry–A European Journal, 26 (2020) 1846–1855.

[63] S.K. Jeong, J.S. Suh, E.J. Oh, Y.W. Park, C.Y. Kim, A.G. MacDiarmid, Preparation of polyaniline free standing film by controlled processing and its transport property, Synthetic Metals, 69 (1995) 171–172.

[64] X. Zhang, J. Zhang, W. Song, Z. Liu, Controllable synthesis of conducting polypyrrole nanostructures, The Journal of Physical Chemistry B, 110 (2006) 1158–1165.

[65] H.-Y. Woo, W.-G. Jung, D.-W. Ihm, J.-Y. Kim, Synthesis and dispersion of polypyrrole nanoparticles in polyvinylpyrrolidone emulsion, Synthetic Metals, 160 (2010) 588–591.

[66] J. Stejskal, P. Kratochvíl, M. Helmstedt, Polyaniline dispersions. 5. Poly(vinyl alcohol) and poly(*N*-vinylpyrrolidone) as steric stabilizers, Langmuir, 12 (1996) 3389–3392.

[67] T. Nagaoka, S.M. Ahmed, K. Ogura, Electroactivity of polypyrrole colloids enhanced by quinone mediation, Journal of the Electrochemical Society, 146 (1999) 3378.

[68] O.D. Iakobson, O.L. Gribkova, A.A. Nekrasov, V.A. Tverskoi, V.F. Ivanov, P.V. Mel'nikov, E.A. Polenov, A. v Vannikov, A stable aqueous dispersion of polyaniline and polymeric acid, Protection of Metals and Physical Chemistry of Surfaces, 52 (2016) 1005–1011.

[69] P. Banerjee, Carboxymethylcellulose stabilized polyaniline dispersions and conducting copolymer latex composites, European Polymer Journal, 34 (1998) 841–847.

[70] Q. Tang, J. Wu, H. Sun, J. Lin, S. Fan, D. Hu, Polyaniline/polyacrylamide conducting composite hydrogel with a porous structure, Carbohydrate Polymers, 74 (2008) 215–219.

[71] Y. Tao, J.X. Zhao, C.X. Wu, Polyacrylamide hydrogels with trapped sulfonated polyaniline, European Polymer Journal, 41 (2005) 1342–1349.

[72] Y. Chen, H. Feng, L. Li, S. Shang, M.C.-W. Yuen, Synthesis and properties of polypyrrole/chitosan composite hydrogels, Journal of Macromolecular Science, Part A, 50 (2013) 1225–1229.

[73] T.-S. Tsai, V. Pillay, Y.E. Choonara, L.C. Du Toit, G. Modi, D. Naidoo, P. Kumar, A polyvinyl alcohol-polyaniline based electro-conductive hydrogel for controlled stimuli-actuable release of indomethacin, Polymers, 3 (2011) 150–172.

[74] X. Tang, H. Li, Z. Du, W. Wang, H.Y. Ng, Conductive polypyrrole hydrogels and carbon nanotubes composite as an anode for microbial fuel cells, RSC Advances, 5 (2015) 50968–50974.

[75] G. Qi, L. Huang, H. Wang, Highly conductive free standing polypyrrole films prepared by freezing interfacial polymerization, Chemical Communications, 48 (2012) 8246–8248.

[76] J. Lei, Z. Li, X. Lu, W. Wang, X. Bian, T. Zheng, Y. Xue, C. Wang, Controllable fabrication of porous free-standing polypyrrole films via a gas phase polymerization, Journal of Colloid and Interface Science, 364 (2011) 555–560.

[77] D. Wang, Y.-X. Li, Z. Shi, H.-L. Qin, L. Wang, X.-F. Pei, J. Jin, Spontaneous growth of free-standing polypyrrole films at an air/ionic liquid interface, Langmuir, 26 (2010) 14405–14408.

[78] R. Bouldin, A. Kokil, S. Ravichandran, S. Nagarajan, J. Kumar, L.A. Samuelson, F.F. Bruno, R. Nagarajan, Enzymatic synthesis of electrically conducting polymers, Green Polymer Chemistry: Biocatalysis and Biomaterials, 23 (2010) 315–341.

[79] N. German, A. Popov, A. Ramanaviciene, A. Ramanavicius, Enzymatic formation of polyaniline, polypyrrole, and polythiophene nanoparticles with embedded glucose oxidase, Nanomaterials, 9 (2019) 806.

[80] G.V. Otrokhov, O.V. Morozova, I.S. Vasil'eva, G.P. Shumakovich, E.A. Zaitseva, M.E. Khlupova, A.I. Yaropolov, Biocatalytic synthesis of conducting polymers and prospects for its application, Biochemistry (Moscow), 78 (2013) 1539–1553.

[81] R. Cruz-Silva, J. Romero-García, J.L. Angulo-Sánchez, A. Ledezma-Pérez, E. Arias-Marín, I. Moggio, E. Flores-Loyola, Template-free enzymatic synthesis of electrically conducting polyaniline using soybean peroxidase, European Polymer Journal, 41 (2005) 1129–1135.

[82] W. Liu, J. Kumar, S. Tripathy, K.J. Senecal, L. Samuelson, Enzymatically synthesized conducting polyaniline, Journal of the American Chemical Society, 121 (1999) 71–78.

[83] B. Garcia, F. Fusalba, D. Bélanger, Electrochemical characterization in nonaqueous electrolyte of polyaniline electrochemically prepared from aqueous media, Canadian Journal of Chemistry, 75 (1997) 1536–1541.

[84] S.L. Mu, Y. Kong, J. Wu, Electrochemical polymerization of aniline in phosphoric acid and the properties of polyaniline, Chinese Journal of Polymer Science, 22 (2004) 405–415.

[85] P.C. Pandey, G. Singh, Electrochemical polymerization of aniline in proton-free nonaqueous media: Dependence of microstructure and electrochemical properties of polyaniline on solvent and dopant, Journal of the Electrochemical Society, 149 (2002) D51.

[86] R. Bhadani, M. Kumari, P.P. Baranwal, S.N. Bhadani, Electrochemical polymerization of pyrrole and aniline on some commodity metals, Journal of Polymer Materials, 19 (2002) 93–101.

[87] M. Blomquist, T. Lindfors, L. Vähäsalo, A. Pivrikas, A. Ivaska, Electropolymerization and characterization of poly(*N*-methylaniline) and poly(*N*-butylaniline) in mixtures of aqueous and organic solvents, Synthetic Metals, 156 (2006) 549–557.

[88] Y. Şahin, S. Perçin, M. Şahin, G. Özkan, Electrochemical polymerization of fluoro-and chloro-substituted anilines and copolymers with aniline, Journal of Applied Polymer Science, 91 (2004) 2302–2312.

[89] C.M. Li, C.Q. Sun, W. Chen, L. Pan, Electrochemical thin film deposition of polypyrrole on different substrates, Surface and Coatings Technology, 198 (2005) 474–477.

[90] H.J.N.P.D. Mello, M. Mulato, Influence of galvanostatic electrodeposition parameters on the structure-property relationships of polyaniline thin films and their use as potentiometric and optical pH sensors, Thin Solid Films, 656 (2018) 14–21.

[91] Y.W. Chen-Yang, J.L. Li, T.L. Wu, W.S. Wang, T.F. Hon, Electropolymerization and electrochemical properties of (*N*-hydroxyalkyl)pyrrole/pyrrole copolymers, Electrochimica Acta, 49 (2004) 2031–2040.

[92] H.H. Zhou, J.B. Wen, X.H. Ning, C.P. Fu, J.H. Chen, Y.F. Kuang, Comparison of the growth process and electrochemical properties of polyaniline films prepared by pulse potentiostatic and potentiostatic method on titanium electrode, Journal of Applied Polymer Science, 104 (2007) 458–463.

[93] K.M. Cheung, D. Bloor, G.C. Stevens, Characterization of polypyrrole electropolymerized on different electrodes, Polymer, 29 (1988) 1709–1717.

[94] N.M. Martyak, P. McAndrew, J.E. McCaskie, J. Dijon, Electrochemical polymerization of aniline from an oxalic acid medium, Progress in Organic Coatings, 45 (2002) 23–32.

[95] D. Kumar, R.C. Sharma, Advances in conductive polymers, European Polymer Journal, 34 (1998) 1053–1060.

[96] X.-G. Li, M.-R. Huang, W. Duan, Y.-L. Yang, Novel multifunctional polymers from aromatic diamines by oxidative polymerizations, Chemical Reviews, 102 (2002) 2925–3030.

[97] B. Lakard, G. Herlem, S. Lakard, B. Fahys, Ab initio study of the polymerization mechanism of poly(*p*-phenylenediamine), Journal of Molecular Structure: THEOCHEM. 638 (2003) 177–187.

[98] A.U. Palma-Cando, B.A. Frontana-Uribe, J.L. Maldonado, M.R. Hernández, Control of thickness of PEDOT electrodeposits on glass/ITO electrodes from organic solutions and its use as anode in organic solar cells, Procedia Chemistry, 12 (2014) 92–99.

[99] G. Fomo, T. Waryo, U. Feleni, P. Baker, E. Iwuoha, Electrochemical polymerization, functional polymers, polymers and polymeric composites: A reference series, Springer, Cham, 2019.

[100] Q. Zhang, X. Zhou, H. Yang, Capacitance properties of composite electrodes prepared by electrochemical polymerization of pyrrole on carbon foam in aqueous solution, Journal of Power Sources, 125 (2004) 141–147.

[101] R.B. Moghaddam, P.G. Pickup, Electrochemical impedance study of the polymerization of pyrrole on high surface area carbon electrodes, Physical Chemistry Chemical Physics, 12 (2010) 4733–4741.

[102] C. Bu, Q. Tai, Y. Liu, S. Guo, X. Zhao, A transparent and stable polypyrrole counter electrode for dye-sensitized solar cell, Journal of Power Sources, 221 (2013) 78–83.

[103] Y. Xue, S. Chen, J. Yu, B.R. Bunes, Z. Xue, J. Xu, B. Lu, L. Zang, Nanostructured conducting polymers and their composites: synthesis methodologies, morphologies and applications, Journal of Materials Chemistry C, 8 (2020) 10136–10159.

[104] F. Al-Zohbi, F. Ghamouss, B. Schmaltz, M. Abarbri, M. Zaghrioui, F. Tran-Van, Enhanced storage performance of PANI and PANI/graphene composites synthesized in protic ionic liquids, Materials, 14 (2021) 4275.

[105] X. Zhang, A.G. MacDiarmid, S.K. Manohar, Chemical synthesis of PEDOT nanofibers, Chemical Communications, (2005) 5328–5330.

[106] H. Xia, Q. Wang, Synthesis and characterization of conductive polyaniline nanoparticles through ultrasonic assisted inverse microemulsion polymerization, Journal of Nanoparticle Research, 3 (2001) 399–409.

[107] J. Wen, Y. Tian, Z. Mei, W. Wu, Y. Tian, Synthesis of polypyrrole nanoparticles and their applications in electrically conductive adhesives for improving conductivity, RSC Advances, 7 (2017) 53219–53225.

[108] J. Stejskal, M. Trchová, Conducting polypyrrole nanotubes: a review, Chemical Papers, 72 (2018) 1563–1595.

[109] I.Y. Choi, J. Lee, H. Ahn, J. Lee, H.C. Choi, M.J. Park, High-conductivity two-dimensional polyaniline nanosheets developed on ice surfaces, Angewandte Chemie International Edition, 54 (2015) 10497–10501.

[110] W. Zhong, J. Deng, Y. Yang, W. Yang, Synthesis of large-area three-dimensional polyaniline nanowire networks using a “soft template”, Macromolecular Rapid Communications, 26 (2005) 395–400.

[111] Y. Shi, L. Pan, B. Liu, Y. Wang, Y. Cui, Z. Bao, G. Yu, Nanostructured conductive polypyrrole hydrogels as high-performance, flexible supercapacitor electrodes, Journal of Materials Chemistry A, 2 (2014) 6086–6091.

[112] Y. Zhao, B. Liu, L. Pan, G. Yu, 3D nanostructured conductive polymer hydrogels for high-performance electrochemical devices, Energy & Environmental Science, 6 (2013) 2856–2870.

[113] J. Stejskal, Strategies towards the control of one-dimensional polypyrrole nanomorphology and conductivity, Polymer International, 67 (2018) 1461–1469.

[114] Q.M. Jia, J.B. Li, L.F. Wang, J.W. Zhu, M. Zheng, Electrically conductive epoxy resin composites containing polyaniline with different morphologies, Materials Science and Engineering: A, 448 (2007) 356–360.

[115] X. Zhang, X. Yan, J. Guo, Z. Liu, D. Jiang, Q. He, H. Wei, H. Gu, H.A. Colorado, X. Zhang, Polypyrrole doped epoxy resin nanocomposites with enhanced mechanical properties and reduced flammability, Journal of Materials Chemistry C, 3 (2015) 162–176.

[116] P. Tsotra, K. Friedrich, Thermal, mechanical, and electrical properties of epoxy resin/polyaniline-dodecylbenzenesulfonic acid blends, Synthetic Metals, 143 (2004) 237–242.

[117] J. Stejskal, I. Sapurina, M. Trchová, Polyaniline nanostructures and the role of aniline oligomers in their formation, Progress in Polymer Science, 35 (2010) 1420–1481.

[118] L. Xia, Z. Wei, M. Wan, Conducting polymer nanostructures and their application in biosensors, Journal of Colloid and Interface Science, 341 (2010) 1–11.

[119] J. Jang, H. Yoon, Facile fabrication of polypyrrole nanotubes using reverse microemulsion polymerization, Chemical Communications, 3 (2003) 720–721.

[120] J. Jang, H. Yoon, Formation mechanism of conducting polypyrrole nanotubes in reverse micelle systems, Langmuir, 21 (2005) 11484–11489.

[121] M. Nasrollahzadeh, M. Jahanshahi, M. Salehi, M. Behzad, H. Nasrollahzadeh, Synthesis and characterization of nanostructured polythiophene in aqueous medium by soft-template method, Applied Chemistry, 8 (2013) 31–34.

[122] T. Siva, K. Kamaraj, V. Karpakam, S. Sathiyanarayanan, Soft template synthesis of poly(*o*-phenylenediamine) nanotubes and its application in self healing coatings, Progress in Organic Coatings, 76 (2013) 581–588.

[123] J.F. Hulvat, S.I. Stupp, Liquid-crystal templating of conducting polymers, Angewandte Chemie International Edition, 42 (2003) 778–781.

[124] L. Huang, Z. Wang, H. Wang, X. Cheng, A. Mitra, Y. Yan, Polyaniline nanowires by electropolymerization from liquid crystalline phases, Journal of Materials Chemistry, 12 (2002) 388–391.

[125] M. Trueba, A.L. Montero, J. Rieumont, Pyrrole nanoscaled electropolymerization: effect of the proton, Electrochimica Acta, 49 (2004) 4341–4349.

[126] S.J. Hurst, E.K. Payne, L. Qin, C.A. Mirkin, Multisegmented one-dimensional nanorods prepared by hard-template synthetic methods, Angewandte Chemie International Edition, 45 (2006) 2672–2692.

[127] Z. Zhang, J. Sui, L. Zhang, M. Wan, Y. Wei, L. Yu, Synthesis of polyaniline with a hollow, octahedral morphology by using a cuprous oxide template, Advanced Materials, 17 (2005) 2854–2857.

[128] I. Sapurina, Y. Li, E. Alekseeva, P. Bober, M. Trchova, Z. Moravkova, J. Stejskal, Polypyrrole nanotubes: the tuning of morphology and conductivity, Polymer, 113 (2017) 247–258.

[129] Deepshikha, T. Basu, A review on synthesis and characterization of nanostructured conducting polymers (NSCP) and application in biosensors, Analytical Letters, 44 (2011) 1126–1171.

[130] H. Qiu, M. Wan, Synthesis, characterization, and electrical properties of nanostructural polyaniline doped with novel sulfonic acids (4-{n-[4-(4-nitrophenylazo) phenyloxy] alkyl}

aminobenzene sulfonic acid), Journal of Polymer Science Part A: Polymer Chemistry, 39 (2001) 3485–3497.

[131] Z. Wei, Z. Zhang, M. Wan, Formation mechanism of self-assembled polyaniline micro/nanotubes, Langmuir, 18 (2002) 917–921.

[132] Y. Yang, J. Liu, M. Wan, Self-assembled conducting polypyrrole micro/nanotubes, Nanotechnology, 13 (2002) 771.

[133] M.J. Antony, M. Jayakannan, Self-assembled anionic micellar template for polypyrrole, polyaniline, and their random copolymer nanomaterials, Journal of Polymer Science Part B: Polymer Physics, 47 (2009) 830–846.

[134] M.J. Antony, M. Jayakannan, Amphiphilic azobenzenesulfonic acid anionic surfactant for water-soluble, ordered, and luminescent polypyrrole nanospheres, The Journal of Physical Chemistry B, 111 (2007) 12772–12780.

[135] B.-Z. Hsieh, H.-Y. Chuang, L. Chao, Y.-J. Li, Y.-J. Huang, P.-H. Tseng, T.-H. Hsieh, K.-S. Ho, Formation mechanism of a nanotubular polyanilines prepared by an emulsion polymerization without organic solvent, Polymer, 49 (2008) 4218–4225.

[136] L. Yu, J. Lee, K. Shin, C. Park, R. Holze, Preparation of aqueous polyaniline dispersions by micellar-aided polymerization, Journal of Applied Polymer Science, 88 (2003) 1550–1555.

[137] A. Reung-U-Rai, A. Prom-Jun, W. Prissanaroon-Ouajai, S. Ouajai, Synthesis of highly conductive polypyrrole nanoparticles via microemulsion polymerization, Journal of Metals, Materials and Minerals, 18 (2008) 27–31.

[138] S. Valtera, J. Prokeš, J. Kopecká, M. Vrňata, M. Trchová, M. Varga, J. Stejskal, D. Kopecký, Dye-stimulated control of conducting polypyrrole morphology, RSC Advances, 7 (2017) 51495–51505.

[139] J. Kopecká, D. Kopecký, M. Vrňata, P. Fitl, J. Stejskal, M. Trchová, P. Bober, Z. Morávková, J. Prokeš, I. Sapurina, Polypyrrole nanotubes: mechanism of formation, RSC Advances, 4 (2014) 1551–1558.

[140] P. Bober, Y. Li, U. Acharya, Y. Panthi, J. Pfleger, P. Humpolíček, M. Trchová, J. Stejskal, Acid Blue dyes in polypyrrole synthesis: The control of polymer morphology at nanoscale in the promotion of high conductivity and the reduction of cytotoxicity, Synthetic Metals, 237 (2018) 40–49.

[141] M. Szymczyk, A. El-Shafei, H.S. Freeman, Design, synthesis, and characterization of new iron-complexed azo dyes, Dyes and Pigments, 72 (2007) 8–15.

[142] W. Yan, J. Han, Synthesis and formation mechanism study of rectangular-sectioned polypyrrole micro/nanotubules, Polymer, 48 (2007) 6782–6790.

[143] G. Ćirić-Marjanović, N. v Blinova, M. Trchová, J. Stejskal, Chemical oxidative polymerization of safranines, The Journal of Physical Chemistry B, 111 (2007) 2188–2199.

[144] F. Würthner, T.E. Kaiser, C.R. Saha-Möller, J-aggregates: from serendipitous discovery to supramolecular engineering of functional dye materials, Angewandte Chemie International Edition, 50 (2011) 3376–3410.

[145] X. Lu, W. Zhang, C. Wang, T.-C. Wen, Y. Wei, One-dimensional conducting polymer nanocomposites: Synthesis, properties and applications, Progress in Polymer Science, 36 (2011) 671–712.

[146] T. Hatano, M. Takeuchi, A. Ikeda, S. Shinkai, New morphology-controlled poly(aniline) synthesis using anionic porphyrin aggregate as a template, Chemistry Letters, 32 (2003) 314–315.

[147] Q. Zhou, C.M. Li, J. Li, X. Cui, D. Gervasio, Template-synthesized cobalt porphyrin/polypyrrole nanocomposite and its electrocatalysis for oxygen reduction in neutral medium, The Journal of Physical Chemistry C, 111 (2007) 11216–11222.

[148] J. Feng, W. Yan, L. Zhang, Synthesis of polypyrrole micro/nanofibers via a self-assembly process, Microchimica Acta, 166 (2009) 261–267.

[149] Y. Xue, X. Lu, Y. Xu, X. Bian, L. Kong, C. Wang, Controlled fabrication of polypyrrole capsules and nanotubes in the presence of Rhodamine B, Polymer Chemistry, 1 (2010) 1602–1605.

[150] S. Gupta, U. Acharya, H. Pištěková, O. Taboubi, Z. Morávková, M. Kašparová, P. Humpolíček, P. Bober, Tuning the conductivity, morphology, and capacitance with enhanced antibacterial properties of polypyrrole by acriflavine hydrochloride, ACS Applied Polymer Materials, 3 (2021) 6063–6069.

[151] M. Shi, Y. Zhang, M. Bai, B. Li, Facile fabrication of polyaniline with coral-like nanostructure as electrode material for supercapacitors, Synthetic Metals, 233 (2017) 74–78.

[152] M. Shi, M. Bai, B. Li, Acid Red 27-crosslinked polyaniline with nanofiber structure as electrode material for supercapacitors, Materials Letters, 212 (2018) 259–262.

[153] M. Criado-Gonzalez, A. Dominguez-Alfaro, N. Lopez-Larrea, N. Alegret, D. Mecerreyes, Additive manufacturing of conducting polymers: Recent advances, challenges, and opportunities, ACS Applied Polymer Materials, 3 (2021) 2865–2883

[154] J. Yang, Y. Liu, S. Liu, L. Li, C. Zhang, T. Liu, Conducting polymer composites: material synthesis and applications in electrochemical capacitive energy storage, Materials Chemistry Frontiers, 1 (2017) 251–268.

[155] Y. Gao, K. Ding, X. Xu, Y. Wang, D. Yu, PPy film/TiO_2 nanotubes composite with enhanced supercapacitive properties, RSC Advances, 4 (2014) 40898.

[156] M. Boukriba, F. Sediri, Hydrothermal synthesis and characterization of poly(paraphenylenediamine)/Nb_2O_5 core–shell composite, Ceramics International, 40 (2014) 8499–8505.

[157] W. Ma, Q. Shi, H. Nan, Q. Hu, X. Zheng, B. Geng, X. Zhang, Hierarchical ZnO@MnO_2@PPy ternary core–shell nanorod arrays: an efficient integration of active materials for energy storage, RSC Advances, 5 (2015) 39864–39869.

[158] R.K. Sharma, A.C. Rastogi, S.B. Desu, Manganese oxide embedded polypyrrole nanocomposites for electrochemical supercapacitor, Electrochimica Acta, 53 (2008) 7690–7695.

[159] L. Shao, J.-W. Jeon, J.L. Lutkenhaus, Polyaniline/vanadium pentoxide layer-by-layer electrodes for energy storage, Chemistry of Materials, 24 (2012) 181–189.

[160] R. Srinivasan, E. Elaiyappillai, S. Anandaraj, B. kumar Duvaragan, P.M. Johnson, Study on the electrochemical behavior of $BiVO_4$/PANI composite as a high performance supercapacitor material with excellent cyclic stability, Journal of Electroanalytical Chemistry, 861 (2020) 113972.

[161] R. Gottam, P. Srinivasan, One-step oxidation of aniline by peroxotitanium acid to polyaniline–titanium dioxide: A highly stable electrode for a supercapacitor, Journal of Applied Polymer Science, 132 (2015).

[162] J.-G. Wang, H. Liu, H. Liu, W. Hua, M. Shao, Interfacial constructing flexible V_2O_5@ polypyrrole core–shell nanowire membrane with superior supercapacitive performance, ACS Applied Materials & Interfaces, 10 (2018) 18816–18823.

[163] M. Lee, B.W. Kim, J.D. Nam, Y. Lee, Y. Son, S.J. Seo, In-situ formation of gold nanoparticle/conducting polymer nanocomposites, Molecular Crystals and Liquid Crystals, 407 (2003) 1–6.

[164] L. Yang, Z. Zhang, G. Nie, C. Wang, X. Lu, Fabrication of conducting polymer/noble metal composite nanorings and their enhanced catalytic properties, Journal of Materials Chemistry A, 3 (2015) 83–86.

[165] L. Kergoat, B. Piro, D.T. Simon, M. Pham, V. Noël, M. Berggren, Detection of glutamate and acetylcholine with organic electrochemical transistors based on conducting polymer/platinum nanoparticle composites, Advanced Materials, 26 (2014) 5658–5664.

[166] J. Stejskal, Conducting polymer-silver composites, Chemical Papers, 67 (2013) 814–848.

[167] E. Spain, T.E. Keyes, R.J. Forster, DNA sensor based on vapour polymerised PEDOT films functionalised with gold nanoparticles, Biosensors and Bioelectronics, 41 (2013) 65–70.

[168] Q. Jia, S. Shan, L. Jiang, Y. Wang, D. Li, Synergistic antimicrobial effects of polyaniline combined with silver nanoparticles, Journal of Applied Polymer Science, 125 (2012) 3560–3566.

[169] C.-W. Kuo, L.-M. Huang, T.-C. Wen, A. Gopalan, Enhanced electrocatalytic performance for methanol oxidation of a novel Pt-dispersed poly(3,4-ethylenedioxythiophene)–poly(styrene sulfonic acid) electrode, Journal of Power Sources, 160 (2006) 65–72.

[170] L. Qiu, Y. Peng, B. Liu, B. Lin, Y. Peng, M.J. Malik, F. Yan, Polypyrrole nanotube-supported gold nanoparticles: An efficient electrocatalyst for oxygen reduction and catalytic reduction of 4-nitrophenol, Applied Catalysis A: General, 413 (2012) 230–237.

[171] H.S. Kim, B.H. Sohn, W. Lee, J.-K. Lee, S.J. Choi, S.J. Kwon, Multifunctional layer-by-layer self-assembly of conducting polymers and magnetic nanoparticles, Thin Solid Films, 419 (2002) 173–177.

[172] K. Singh, A. Ohlan, A.K. Bakhshi, S.K. Dhawan, Synthesis of conducting ferromagnetic nanocomposite with improved microwave absorption properties, Materials Chemistry and Physics, 119 (2010) 201–207.

[173] A. Muñoz-Bonilla, J. Sánchez-Marcos, P. Herrasti, Magnetic nanoparticles-based conducting polymer nanocomposites, Conducting polymer hybrids, Springer series on polymer and composite materials, Springer, 2017.

[174] T.K. Mahto, A.R. Chowdhuri, S.K. Sahu, Polyaniline-functionalized magnetic nanoparticles for the removal of toxic dye from wastewater, Journal of Applied Polymer Science. 131 (2014) 40840.

[175] M.B. Gholivand, Y. Yamini, M. Dayeni, S. Seidi, E. Tahmasebi, Adsorptive removal of alizarin red-S and alizarin yellow GG from aqueous solutions using polypyrrole-coated magnetic nanoparticles, Journal of Environmental Chemical Engineering, 3 (2015) 529–540.

[176] L. Bazli, M. Yusuf, A. Farahani, M. Kiamarzi, Z. Seyedhosseini, M. Nezhadmansari, M. Aliasghari, M. Iranpoor, Application of composite conducting polymers for improving the corrosion behavior of various substrates: A Review, Journal of Composites and Compounds, 2 (2020) 228–240.

[177] M. Shabani-Nooshabadi, S.M. Ghoreishi, M. Behpour, Direct electrosynthesis of polyaniline–montmorrilonite nanocomposite coatings on aluminum alloy 3004 and their corrosion protection performance, Corrosion Science, 53 (2011) 3035–3042.

[178] N. Jadhav, T. Matsuda, V. Gelling, Mica/polypyrrole (doped) composite containing coatings for the corrosion protection of cold rolled steel, Journal of Coatings Technology and Research, 15 (2018) 363–374.

[179] G. Contri, G.M.O. Barra, S. Ramoa, C. Merlini, L.G. Ecco, F.S. Souza, A. Spinelli, Epoxy coating based on montmorillonite-polypyrrole: Electrical properties and prospective application on corrosion protection of steel, Progress in Organic Coatings, 114 (2018) 201–207.

[180] M.G. Hosseini, M. Jafari, R. Najjar, Effect of polyaniline–montmorillonite nanocomposite powders addition on corrosion performance of epoxy coatings on Al 5000, Surface and Coatings Technology, 206 (2011) 280–286.

[181] M.G. Hosseini, M. Raghibi-Boroujeni, I. Ahadzadeh, R. Najjar, M.S.S. Dorraji, Effect of polypyrrole–montmorillonite nanocomposites powder addition on corrosion performance of epoxy coatings on Al 5000, Progress in Organic Coatings, 66 (2009) 321–327.

[182] M.R. Arcila-Velez, R.K. Emmett, M. Karakaya, R. Podila, K.P. Díaz-Orellana, A.M. Rao, M.E. Roberts, A facile and scalable approach to fabricating free-standing polymer–Carbon nanotube composite electrodes, Synthetic Metals, 215 (2016) 35–40.

[183] S.W. Lee, B.M. Gallant, H.R. Byon, P.T. Hammond, Y. Shao-Horn, Nanostructured carbon-based electrodes: bridging the gap between thin-film lithium-ion batteries and electrochemical capacitors, Energy & Environmental Science, 4 (2011) 1972–1985.

[184] C. Peng, S. Zhang, D. Jewell, G.Z. Chen, Carbon nanotube and conducting polymer composites for supercapacitors, Progress in Natural Science, 18 (2008) 777–788.

[185] S. Bose, T. Kuila, A.K. Mishra, R. Rajasekar, N.H. Kim, J.H. Lee, Carbon-based nanostructured materials and their composites as supercapacitor electrodes, Journal of Materials Chemistry, 22 (2012) 767–784.

[186] J. Yan, T. Wei, B. Shao, Z. Fan, W. Qian, M. Zhang, F. Wei, Preparation of a graphene nanosheet/polyaniline composite with high specific capacitance, Carbon, 48 (2010) 487–493.

[187] D. Zhang, X. Zhang, Y. Chen, P. Yu, C. Wang, Y. Ma, Enhanced capacitance and rate capability of graphene/polypyrrole composite as electrode material for supercapacitors, Journal of Power Sources, 196 (2011) 5990–5996.

[188] R.B. Choudhary, S. Ansari, M. Majumder, Recent advances on redox active composites of metal-organic framework and conducting polymers as pseudocapacitor electrode material, Renewable and Sustainable Energy Reviews, 145 (2021) 110854.

[189] G. Givaja, P. Amo-Ochoa, C.J. Gómez-García, F. Zamora, Electrical conductive coordination polymers, Chemical Society Reviews, 41 (2012) 115–147.

[190] B. Dhara, S.S. Nagarkar, J. Kumar, V. Kumar, P.K. Jha, S.K. Ghosh, S. Nair, N. Ballav, Increase in electrical conductivity of MOF to billion-fold upon filling the nanochannels with conducting polymer, The Journal of Physical Chemistry Letters, 7 (2016) 2945–2950.

[191] V. Babel, B.L. Hiran, A review on polyaniline composites: Synthesis, characterization, and applications, Polymer Composites, 42 (2021) 3142–3157.

[192] S. Guo, Y. Zhu, Y. Yan, Y. Min, J. Fan, Q. Xu, H. Yun, (Metal-organic framework)-polyaniline sandwich structure composites as novel hybrid electrode materials for high-performance supercapacitor, Journal of Power Sources, 316 (2016) 176–182.

[193] L. Shao, Q. Wang, Z. Ma, Z. Ji, X. Wang, D. Song, Y. Liu, N. Wang, A high-capacitance flexible solid-state supercapacitor based on polyaniline and metal-organic framework (UiO-66) composites, Journal of Power Sources, 379 (2018) 350–361.

[194] M. Rafti, W.A. Marmisollé, O. Azzaroni, Metal-organic frameworks help conducting polymers optimize the efficiency of the oxygen reduction reaction in neutral solutions, Advanced Materials Interfaces, 3 (2016) 1600047.

[195] A. Rußler, K. Sakakibara, T. Rosenau, Cellulose as matrix component of conducting films, Cellulose, 18 (2011) 937–944.

[196] P. Marcasuzaa, S. Reynaud, F. Ehrenfeld, A. Khoukh, J. Desbrieres, Chitosan-*graft*-polyaniline-based hydrogels: elaboration and properties, Biomacromolecules, 11 (2010) 1684–1691.

[197] A.T. Ramaprasad, D. Latha, V. Rao, Synthesis and characterization of polypyrrole grafted chitin, Journal of Physics and Chemistry of Solids, 104 (2017) 169–174.

[198] F.N. Ajjan, M.J. Jafari, T. Rębiś, T. Ederth, O. Inganäs, Spectroelectrochemical investigation of redox states in a polypyrrole/lignin composite electrode material, Journal of Materials Chemistry A, 3 (2015) 12927–12937.

[199] M. Bongo, O. Winther-Jensen, S. Himmelberger, X. Strakosas, M. Ramuz, A. Hama, E. Stavrinidou, G.G. Malliaras, A. Salleo, B. Winther-Jensen, PEDOT: gelatin composites mediate brain endothelial cell adhesion, Journal of Materials Chemistry B, 1 (2013) 3860–3867.

[200] J. Hur, K. Im, S.W. Kim, J. Kim, D.-Y. Chung, T.-H. Kim, K.H. Jo, J.H. Hahn, Z. Bao, S. Hwang, Polypyrrole/agarose-based electronically conductive and reversibly restorable hydrogel, ACS Nano. 8 (2014) 10066–10076.

[201] D. Gan, L. Han, M. Wang, W. Xing, T. Xu, H. Zhang, K. Wang, L. Fang, X. Lu, Conductive and tough hydrogels based on biopolymer molecular templates for controlling in situ formation of polypyrrole nanorods, ACS Applied Materials & Interfaces, 10 (2018) 36218–36228.

[202] D.W. Hatchett, M. Josowicz, Composites of intrinsically conducting polymers as sensing nanomaterials, Chemical Reviews, 108 (2008) 746–769.

[203] S. Saha, P. Sarkar, M. Sarkar, B. Giri, Electroconductive smart polyacrylamide–polypyrrole (PAC–PPy) hydrogel: a device for controlled release of risperidone, RSC Advances, 5 (2015) 27665–27673.

[204] J. Stejskal, P. Kratochvíl, A.D. Jenkins, The formation of polyaniline and the nature of its structures, Polymer, 37 (1996) 367–369.

[205] V. Mottaghitalab, B. Xi, G.M. Spinks, G.G. Wallace, Polyaniline fibres containing single walled carbon nanotubes: Enhanced performance artificial muscles, Synthetic Metals, 156 (2006) 796–803.

[206] A.M. Kenwright, W.J. Feast, P. Adams, A.J. Milton, A.P. Monkman, B.J. Say, Solution-state carbon-13 nuclear magnetic resonance studies of polyaniline, Polymer, 33 (1992) 4292–4298.

[207] G. D'Aprano, M. Leclerc, G. Zotti, Stabilization and characterization of pernigraniline salt: the "acid-doped" form of fully oxidized polyanilines, Macromolecules, 25 (1992) 2145–2150.

[208] R. Jain, R. v Gregory, Solubility and rheological characterization of polyaniline base in *N*-methyl-2-pyrrolidinone and *N,N′*-dimethylpropylene urea, Synthetic Metals. 74 (1995) 263–266.

[209] M. Abe, A. Ohtani, Y. Umemoto, S. Akizuki, M. Ezoe, H. Higuchi, K. Nakamoto, A. Okuno, Y. Noda, Soluble and high molecular weight polyaniline, Journal of the Chemical Society, Chemical Communications, 22 (1989) 1736–1738.

[210] M. Sairam, X.X. Loh, K. Li, A. Bismarck, J.H.G. Steinke, A.G. Livingston, Nanoporous asymmetric polyaniline films for filtration of organic solvents, Journal of Membrane Science, 330 (2009) 166–174.

[211] K. Deshmukh, M.B. Ahamed, R.R. Deshmukh, S.K.K. Pasha, P.R. Bhagat, K. Chidambaram, Biopolymer composites with high dielectric performance: interface engineering, Biopolymer Composites in Electronics, Elsevier, 2017.

[212] M. Neetika, J. Rajni, P.K. Singh, B. Bhattacharya, V. Singh, S.K. Tomar, Synthesis and properties of polyaniline, poly(*o*-anisidine), and poly[aniline-*co*-(*o*-anisidine)] using potassium iodate oxidizing agent, High Performance Polymers, 29 (2017) 266–271.

[213] J. Stejskal, M. Trchová, P. Bober, Z. Morávková, D. Kopecký, M. Vrňata, J. Prokeš, M. Varga, E. Watzlová, Polypyrrole salts and bases: superior conductivity of nanotubes and their stability towards the loss of conductivity by deprotonation, RSC Advances, 6 (2016) 88382–88391.

[214] Q. Pei, R. Qian, Protonation and deprotonation of polypyrrole chain in aqueous solutions, Synthetic Metals, 45 (1991) 35–48.

[215] H. Münstedt, Properties of polypyrroles treated with base and acid, Polymer, 27 (1986) 899–904.

[216] P. Dallas, D. Niarchos, D. Vrbanic, N. Boukos, S. Pejovnik, C. Trapalis, D. Petridis, Interfacial polymerization of pyrrole and in situ synthesis of polypyrrole/silver nanocomposites, Polymer, 48 (2007) 2007–2013.

[217] J. John, P. Saheeda, K. Sabeera, S. Jayalekshmi, Doped polypyrrole with good solubility and film forming properties suitable for device applications, Materials Today: Proceedings, 5 (2018) 21140–21146.

[218] R. Qian, W.R. Salaneck, I. LundstrGm, B. Ranby, eds., Conjugated Polymers and Related Materials, Oxford University Press, London, 1993.

[219] Y. Murakami, T. Yamamoto, Synthesis of new polypyrroles by oxidative polymerization of *N*-(benzylideneamino)pyrroles and properties of the polymers, Polymer Journal, 31 (1999) 476–478.

[220] H.-K. Lin, S.-A. Chen, Synthesis of new water-soluble self-doped polyaniline, Macromolecules, 33 (2000) 8117–8118.

[221] J.Y. Lee, D.Y. Kim, C.Y. Kim, Synthesis of soluble polypyrrole of the doped state in organic solvents, Synthetic Metals, 74 (1995) 103–106.

[222] Y. Shen, M. Wan, In situ doping polymerization of pyrrole with sulfonic acid as a dopant, Synthetic Metals, 96 (1998) 127–132.

[223] Y. Cao, P. Smith, A.J. Heeger, Counter-ion induced processibility of conducting polyaniline and of conducting polyblends of polyaniline in bulk polymers, Synthetic Metals, 48 (1992) 91–97.

[224] H.K. Lim, S.O. Lee, K.J. Song, S.G. Kim, K.H. Kim, Synthesis and properties of soluble polypyrrole doped with dodecylbenzenesulfonate and combined with polymeric additive poly(ethylene glycol), Journal of Applied Polymer Science, 97 (2005) 1170–1175.

[225] R.L. Elsenbaumer, K.Y. Jen, R. Oboodi, Processible and environmentally stable conducting polymers, Synthetic Metals, 15 (1986) 169–174.

[226] T.K. Das, S. Prusty, Review on conducting polymers and their applications, Polymer-Plastics Technology and Engineering, 51 (2012) 1487–1500.

[227] B.L. Guo, P.X. Ma, Conducting polymers for tissue engineering, Biomacromolecules, 19 (2018) 1764–1782.

[228] Y. Li, Conducting polymers, Organic optoelectronic materials, Springer, 2015.

[229] C. Tang, N. Chen, X. Hu, Conducting polymer nanocomposites: recent developments and future prospects, Conducting Polymer Hybrids, Springer, 2017.

[230] T.-H. Le, Y. Kim, H. Yoon, Electrical and electrochemical properties of conducting polymers, Polymers, 9 (2017) 150.

[231] A. R Murad, A. Iraqi, S.B. Aziz, S. N Abdullah, M.A. Brza, Conducting polymers for optoelectronic devices and organic solar cells: A review, Polymers, 12 (2020) 2627.

[232] P. Sengodu, A.D. Deshmukh, Conducting polymers and their inorganic composites for advanced Li-ion batteries: a review, RSC Advances, 5 (2015) 42109–42130.

[233] A. Mirmohseni, R. Solhjo, Preparation and characterization of aqueous polyaniline battery using a modified polyaniline electrode, European Polymer Journal, 39 (2003) 219–223.

[234] T.F. Otero, I. Cantero, Conducting polymers as positive electrodes in rechargeable lithium-ion batteries, Journal of Power Sources, 81 (1999) 838–841.

[235] C. Wang, W. Zheng, Z. Yue, C.O. Too, G.G. Wallace, Buckled, stretchable polypyrrole electrodes for battery applications, Advanced Materials, 23 (2011) 3580–3584.

[236] D. Khokhar, S. Jadoun, R. Arif, S. Jabin, Functionalization of conducting polymers and their applications in optoelectronics, Polymer-Plastics Technology and Materials, 60 (2021) 463–485.

[237] V. Koncar, C. Cochrane, M. Lewandowski, F. Boussu, C. Dufour, Electro-conductive sensors and heating elements based on conductive polymer composites, International Journal of Clothing Science and Technology, 21 (2009) 82–92.

[238] C.Z. Zhu, G.H. Yang, H. Li, D. Du, Y.H. Lin, Electrochemical sensors and biosensors based on nanomaterials and nanostructures, Analytical Chemistry, 87 (2015) 230–249.

[239] M. Trojanowicz, Application of conducting polymers in chemical analysis, Microchimica Acta, 143 (2003) 75–91.

[240] D. Jiang, V. Murugadoss, Y. Wang, J. Lin, T. Ding, Z. Wang, Q. Shao, C. Wang, H. Liu, N. Lu, Electromagnetic interference shielding polymers and nanocomposites-a review, Polymer Reviews, 59 (2019) 280–337.

[241] Y. Li, X. Wang, Intrinsically conducting polymers and their composites for anticorrosion and antistatic applications, Semiconducting polymer composites, Wiley-VCH Verlag GmbH & Co. KGaAs, 2013.

[242] P.P. Deshpande, N.G. Jadhav, V.J. Gelling, D. Sazou, Conducting polymers for corrosion protection: a review, Journal of Coatings Technology and Research, 11 (2014) 473–494.

[243] R. Hasanov, S. Bilgiç, Monolayer and bilayer conducting polymer coatings for corrosion protection of steel in 1 M H_2SO_4 solution, Progress in Organic Coatings, 64 (2009) 435–445.

[244] J. Pellegrino, The use of conducting polymers in membrane-based separations, Advanced Membrane Technology, 984 (2003) 289–305.

[245] J. Arroyo, M. Akieh-Pirkanniemi, G. Lisak, R.-M. Latonen, J. Bobacka, Electrochemically controlled transport of anions across polypyrrole-based membranes, Journal of Membrane Science, 581 (2019) 50–57.

[246] V. Krikstolaityte, R. Ding, T. Ruzgas, S. Björklund, G. Lisak, Characterization of nano-layered solid-contact ion selective electrodes by simultaneous potentiometry and quartz crystal microbalance with dissipation, Analytica Chimica Acta, 1128 (2020) 19–30.

[247] Y.H. Cheong, L. Ge, G. Lisak, Highly reproducible solid contact ion selective electrodes: emerging opportunities for potentiometry–a review, Analytica Chimica Acta, 1162 (2021) 338304.

[248] A. Malinauskas, Electrocatalysis at conducting polymers, Synthetic Metals, 107 (1999) 75–83.

[249] A. Taghizadeh, M. Taghizadeh, M. Jouyandeh, M.K. Yazdi, P. Zarrintaj, M.R. Saeb, E.C. Lima, V.K. Gupta, Conductive polymers in water treatment: A review, Journal of Molecular Liquids, 312 (2020) 113447.

[250] A.A. Entezami, B. Massoumi, Artificial muscles, biosensors and drug delivery systems based on conducting polymers: A review, Iranian Polymer Journal (English), 15 (2006) 13–30.

[251] M. Talikowska, X. Fu, G. Lisak, Application of conducting polymers to wound care and skin tissue engineering: A review, Biosensors and Bioelectronics, 135 (2019) 50–63.

[252] A.H. Ismail, N.A.M. Yahya, M.H. Yaacob, M.A. Mahdi, Y. Sulaiman, Optical ammonia gas sensor of poly(3,4-polyethylenedioxythiophene), polyaniline and polypyrrole: A comparative study, Synthetic Metals, 260 (2020) 116294.

[253] Rajesh, T. Ahuja, D. Kumar, Recent progress in the development of nano-structured conducting polymers/nanocomposites for sensor applications, Sensors and Actuators B: Chemical, 136 (2009) 275–286.

[254] M.M. Ayad, N.A. Salahuddin, I.M. Minisy, W.A. Amer, Chitosan/polyaniline nanofibers coating on the quartz crystal microbalance electrode for gas sensing, Sensors and Actuators B: Chemical, 202 (2014) 144–153.

[255] A. Malinauskas, R. Garjonyte, R. Mazeikiene, I. Jureviciute, Electrochemical response of ascorbic acid at conducting and electrogenerated polymer modified electrodes for electroanalytical applications: a review, Talanta, 64 (2004) 121–129.

[256] S.S. Kumar, J. Mathiyarasu, K.L. Phani, Y.K. Jain, V. Yegnaraman, Determination of uric acid in the presence of ascorbic acid using poly(3,4-ethylenedioxythiophene)-modified electrodes, Electrocanalysis, 17 (2005) 2281–2286.

[257] H. Zejli, P. Sharrock, J. de Cisneros, I. Naranjo-Rodriguez, K.R. Temsamani, Voltammetric determination of trace mercury at a sonogel-carbon electrode modified with poly-3-methylthiophene, Talanta, 68 (2005) 79–85.

[258] S. Nambiar, J.T.W. Yeow, Conductive polymer-based sensors for biomedical applications, Biosensors and Bioelectronics, 26 (2011) 1825–1832.

[259] M. Gerard, A. Chaubey, B.D. Malhotra, Application of conducting polymers to biosensors, Biosensors and Bioelectronics, 17 (2002) 345–359.

[260] D. Melling, J.G. Martinez, E.W.H. Jager, Conjugated polymer actuators and devices: progress and opportunities, Advanced Materials, 31 (2019) 1808210.

[261] E. Smela, O. Inganas, I. Lundstrom, Conducting polymers as artificial muscles: challenges and possibilities, Journal of Micromechanics and Microengineering, 3 (1993) 203–205.

[262] A.S. Hutchison, T.W. Lewis, S.E. Moulton, G.M. Spinks, G.G. Wallace, Development of polypyrrole-based electromechanical actuators, Synthetic Metals, 113 (2000) 121–127.

[263] M.A. Careem, K.P. Vidanapathirana, S. Skaarup, K. West, Dependence of force produced by polypyrrole-based artificial muscles on ionic species involved, Solid State Ionics, 175 (2004) 725–728.

[264] M. Onoda, Y. Kato, H. Shonaka, K. Tada, Artificial muscle using conducting polymers, Electrical Engineering in Japan, 149 (2004) 7–13.

[265] P. Marque, J. Roncali, Structural effect on the redox thermodynamics of poly(thiophenes), Journal of Physical Chemistry, 94 (1990) 8614–8617.

[266] J. Foroughi, G.M. Spinks, G.G. Wallace, High strain electromechanical actuators based on electrodeposited polypyrrole doped with di-(2-ethylhexyl) sulfosuccinate, Sensors and Actuators B: Chemical, 155 (2011) 278–284.

[267] C. Wei, S. German, S. Basak, K. Rajeshwar, Reduction of hexavalent chromium in aqueous solutions by polypyrrole, Journal of the Electrochemical Society, 140 (1993) L60.

[268] A. Malinauskas, R. Holze, An in situ UV-Vis spectroelectrochemical investigation of the dichromate reduction at a polyaniline-modified electrode, Berichte Der Bunsengesellschaft Für Physikalische Chemie, 102 (1998) 982–984.

[269] M.A. Del Valle, F.R. Díaz, M.E. Bodini, T. Pizarro, R. Córdova, H. Gómez, R. Schrebler, Polythiophene, polyaniline and polypyrrole electrodes modified by electrodeposition of Pt and Pt+Pb for formic acid electrooxidation, Journal of Applied Electrochemistry, 28 (1998) 943–946.

[270] R.C.M. Jakobs, L.J.J. Janssen, E. Barendrecht, Oxygen reduction at polypyrrole electrodes–I. Theory and evaluation of the rrde experiments, Electrochimica Acta, 30 (1985) 1085–1091.

[271] Y. Yuan, S. Zhou, L. Zhuang, Polypyrrole/carbon black composite as a novel oxygen reduction catalyst for microbial fuel cells, Journal of Power Sources, 195 (2010) 3490–3493.

[272] M. Sevilla, L. Yu, T.P. Fellinger, A.B. Fuertes, M.-M. Titirici, Polypyrrole-derived mesoporous nitrogen-doped carbons with intrinsic catalytic activity in the oxygen reduction reaction, RSC Advances, 3 (2013) 9904–9910.

[273] J. Quílez-Bermejo, E. Morallón, D. Cazorla-Amorós, Polyaniline-derived *N*-doped ordered mesoporous carbon thin films: efficient catalysts towards oxygen reduction reaction, Polymers, 12 (2020) 2382.

[274] H. Begum, M.S. Ahmed, Y.-B. Kim, Nitrogen-rich graphitic-carbon@graphene as a metal-free electrocatalyst for oxygen reduction reaction, Scientific Reports, 10 (2020) 1–10.

[275] R. Kumar, J. Travas-Sejdic, L.P. Padhye, Conducting polymers-based photocatalysis for treatment of organic contaminants in water, Chemical Engineering Journal Advances, 14 (2020) 100047.

[276] K.M. Emran, S.M. Ali, A.L. Al-Oufi, The electrocatalytic activity of polyaniline/TiO_2 nanocomposite for congo red degradation in aqueous solutions, International Journal of Electrochemical Science, 13 (2018) 5085–5095.

[277] J. Stejskal, Interaction of conducting polymers, polyaniline and polypyrrole, with organic dyes: polymer morphology control, dye adsorption and photocatalytic decomposition, Chemical Papers, 74 (2020) 1–54.

[278] V.K. Gupta, Application of low-cost adsorbents for dye removal – a review, Journal of Environmental Management, 90 (2009) 2313–2342.

[279] I.M. Minisy, N.A. Salahuddin, M.M. Ayad, Adsorption of methylene blue onto chitosan–montmorillonite/polyaniline nanocomposite, Applied Clay Science, 203 (2021) 105993.

[280] I.M. Minisy, N.A. Salahuddin, M.M. Ayad, Chitosan/polyaniline hybrid for the removal of cationic and anionic dyes from aqueous solutions, Journal of Applied Polymer Science, 136 (2019) 47056.

[281] S. Zaghlol, W.A. Amer, M.H. Shaaban, M.M. Ayad, P. Bober, J. Stejskal, Conducting macroporous polyaniline/poly(vinyl alcohol) aerogels for the removal of chromium(VI) from aqueous media, Chemical Papers, 74 (2020) 3183–3193.

[282] Y. Xu, Z. Sui, B. Xu, H. Duan, X. Zhang, Emulsion template synthesis of all conducting polymer aerogels with superb adsorption capacity and enhanced electrochemical capacitance, Journal of Materials Chemistry, 22 (2012) 8579–8584.

[283] W. Sun, W. Zhang, H. Li, Q. Su, P. Zhang, L. Chen, Insight into the synergistic effect on adsorption for Cr(VI) by a polypyrrole-based composite, RSC Advances, 10 (2020) 8790–8799.

[284] X. Han, L. Gai, H. Jiang, L. Zhao, H. Liu, W. Zhang, Core–shell structured Fe_3O_4/PANI microspheres and their Cr(VI) ion removal properties, Synthetic Metals, 171 (2013) 1–6.

[285] M. Bhaumik, A. Maity, V.V. Srinivasu, M.S. Onyango, Enhanced removal of Cr(VI) from aqueous solution using polypyrrole/Fe_3O_4 magnetic nanocomposite, Journal of Hazardous Materials, 190 (2011) 381–390.

[286] J. Feng, N. Sun, D. Wu, H. Yang, H. Xu, W. Yan, Preparation of Fe_3O_4/TiO_2/polypyrrole ternary magnetic composite and using as adsorbent for the removal of acid red G, Journal of Polymers and the Environment, 25 (2017) 781–791.

[287] R. Karthik, S. Meenakshi, Removal of hexavalent chromium ions from aqueous solution using chitosan/polypyrrole composite, Desalination and Water Treatment, 56 (2015) 1587–1600.

[288] L. Zhang, W. Niu, J. Sun, Q. Zhou, Efficient removal of Cr(VI) from water by the uniform fiber ball loaded with polypyrrole: Static adsorption, dynamic adsorption and mechanism studies, Chemosphere, 248 (2020) 126102.

[289] R. Bhatt, P. Padmaja, Spectroscopic signature of branched polyaniline nanotubules decorated with nanospheres as an adsorbent for chromium, Journal of Environmental Chemical Engineering, 6 (2018) 6797–6806.

[290] M. Bhaumik, A. Maity, V.V. Srinivasu, M.S. Onyango, Removal of hexavalent chromium from aqueous solution using polypyrrole-polyaniline nanofibers, Chemical Engineering Journal, 181 (2012) 323–333.

[291] N.H. Kera, M. Bhaumik, K. Pillay, S.S. Ray, A. Maity, Selective removal of toxic Cr(VI) from aqueous solution by adsorption combined with reduction at a magnetic nanocomposite surface, Journal of Colloid and Interface Science, 503 (2017) 214–228.

[292] E. da S. Reis, F.D.S. Gorza, G. da C. Pedro, B.G. Maciel, R.J. da Silva, G.P. Ratkovski, C.P. de Melo, (Maghemite/chitosan/polypyrrole) nanocomposites for the efficient removal of Cr(VI) from aqueous media, Journal of Environmental Chemical Engineering, 9 (2021) 104893.

[293] J. Chen, M. Yu, C. Wang, J. Feng, W. Yan, Insight into the synergistic effect on selective adsorption for heavy metal ions by a polypyrrole/TiO_2 composite, Langmuir, 34 (2018) 10187–10196.

[294] R. Das, S. Giri, A.M. Muliwa, A. Maity, High-performance Hg(II) removal using thiol-functionalized polypyrrole (PPy/MAA) composite and effective catalytic activity of Hg(II)-adsorbed waste material, ACS Sustainable Chemistry & Engineering, 5 (2017) 7524–7536.

[295] Q. Lü, M. Huang, X. Li, Synthesis and heavy-metal-ion sorption of pure sulfophenylenediamine copolymer nanoparticles with intrinsic conductivity and stability, Chemistry–A European Journal, 13 (2007) 6009–6018.

[296] J. Wang, B. Deng, H. Chen, X. Wang, J. Zheng, Removal of aqueous Hg(II) by polyaniline: sorption characteristics and mechanisms, Environmental Science & Technology, 43 (2009) 5223–5228.

[297] M.I. Din, S. Ata, I.U. Mohsin, A. Rasool, A.A. Aziz, Evaluation of conductive polymers as an adsorbent for eradication of As(III) from aqueous solution using inductively coupled plasma optical emission spectroscopy (ICP-OES), International Journal of Science and Engineering, 6 (2014) 154–162.

[298] M. Bhaumik, C. Noubactep, V.K. Gupta, R.I. McCrindle, A. Maity, Polyaniline/Fe^0 composite nanofibers: An excellent adsorbent for the removal of arsenic from aqueous solutions, Chemical Engineering Journal, 271 (2015) 135–146.

[299] R. Khalili, F. Shabanpour, H. Eisazadeh, Synthesis of polythiophene/Sb_2O_3 nanocomposite using sodium dodecylbenzenesulfonate for the removal of Pb(II), Advances in Polymer Technology, 33 (2014) 21389.

[300] J. Han, J. Dai, R. Guo, Highly efficient adsorbents of poly(*o*-phenylenediamine) solid and hollow sub-microspheres towards lead ions: a comparative study, Journal of Colloid and Interface Science, 356 (2011) 749–756.

[301] J. Chen, J. Feng, W. Yan, Facile synthesis of a polythiophene/TiO_2 particle composite in aqueous medium and its adsorption performance for Pb(II), RSC Advances, 5 (2015) 86945–86953.

[302] M. Huang, Q. Peng, X. Li, Rapid and effective adsorption of lead ions on fine poly(phenylenediamine) microparticles, Chemistry–A European Journal, 12 (2006) 4341–4350.

[303] T. Yao, W. Jia, X. Tong, Y. Feng, Y. Qi, X. Zhang, J. Wu, One-step preparation of nanobeads-based polypyrrole hydrogel by a reactive-template method and their applications in adsorption and catalysis, Journal of Colloid and Interface Science, 527 (2018) 214–221.

[304] E.A. El-Sharkaway, R.M. Kamel, I.M. El-Sherbiny, S.S. Gharib, Removal of methylene blue from aqueous solutions using polyaniline/graphene oxide or polyaniline/reduced graphene oxide composites, Environmental Technology, 41 (2020) 2854–2862.

[305] B. Yan, Z. Chen, L. Cai, Z. Chen, J. Fu, Q. Xu, Fabrication of polyaniline hydrogel: synthesis, characterization and adsorption of methylene blue, Applied Surface Science, 356 (2015) 39–47.

[306] W.A. Amer, M.M. Omran, A.F. Rehab, M.M. Ayad, Acid green crystal-based in situ synthesis of polyaniline hollow nanotubes for the adsorption of anionic and cationic dyes, RSC Advances, 8 (2018) 22536–22545.

[307] S. Kalotra, R. Mehta, Carbon aerogel and polyaniline/carbon aerogel adsorbents for Acid Green 25 dye: synthesis, characterization and an adsorption study, Chemical Engineering Communications, (2021). DOI: 10.1080/00986445.2021.1919650

[308] V. Janaki, B.-T. Oh, K. Shanthi, K.-J. Lee, A.K. Ramasamy, S. Kamala-Kannan, Polyaniline/chitosan composite: an eco-friendly polymer for enhanced removal of dyes from aqueous solution, Synthetic Metals, 162 (2012) 974–980.

[309] X. Li, H. Lu, Y. Zhang, F. He, Efficient removal of organic pollutants from aqueous media using newly synthesized polypyrrole/CNTs-$CoFe_2O_4$ magnetic nanocomposites, Chemical Engineering Journal, 316 (2017) 893–902.

[310] A. Karamipour, N. Rasouli, M. Movahedi, H. Salavti, A kinetic study on adsorption of congo red from aqueous solution by ZnO-$ZnFe_2O_4$-polypyrrole magnetic nanocomposite, Physical Chemistry Research, 4 (2016) 291–301.

[311] P. Kharazi, R. Rahimi, M. Rabbani, Copper ferrite-polyaniline nanocomposite: structural, thermal, magnetic and dye adsorption properties, Solid State Sciences, 93 (2019) 95–100.

[312] L. Ai, J. Jiang, R. Zhang, Uniform polyaniline microspheres: a novel adsorbent for dye removal from aqueous solution, Synthetic Metals, 160 (2010) 762–767.

[313] P.E. Díaz-Flores, C.J. Guzmán-Álvarez, V.M. Ovando-Medina, H. Martínez-Gutiérrez, O. Gonzalez-Ortega, Synthesis of α-cellulose/magnetite/polypyrrole composite for the removal of reactive black 5 dye from aqueous solutions, Desalination and Water Treatment, 155 (2019) 350–363.

[314] M. Bhaumik, R.I. McCrindle, A. Maity, S. Agarwal, V.K. Gupta, Polyaniline nanofibers as highly effective re-usable adsorbent for removal of reactive black 5 from aqueous solutions, Journal of Colloid and Interface Science, 466 (2016) 442–451.

[315] F. Mohamed, M.R. Abukhadra, M. Shaban, Removal of safranin dye from water using polypyrrole nanofiber/Zn-Fe layered double hydroxide nanocomposite (PPy NF/Zn-Fe LDH) of enhanced adsorption and photocatalytic properties, Science of the Total Environment, 640 (2018) 352–363.

[316] S. Majumdar, A. Baishya, D. Mahanta, Kinetic and equilibrium modeling of anionic dye adsorption on polyaniline emeraldine salt: batch and fixed bed column studies, Fibers and Polymers, 20 (2019) 1226–1235.

[317] Y. Meng, L. Zhang, L. Chai, W. Yu, T. Wang, S. Dai, H. Wang, Facile and large-scale synthesis of poly(*m*-phenylenediamine) nanobelts with high surface area and superior dye adsorption ability, RSC Advances, 4 (2014) 45244–45250.

[318] M. Trchová, J. Stejskal, Polyaniline: The infrared spectroscopy of conducting polymer nanotubes (IUPAC Technical Report), Pure and Applied Chemistry, 83 (2011) 1803–1817.

[319] L.J. Pauw, A method of measuring specific resistivity and Hall effect of discs of arbitrary shape, Philips Research Reports, 13 (1958) 1–9.

[320] J. Stejskal, J. Prokeš, Conductivity and morphology of polyaniline and polypyrrole prepared in the presence of organic dyes, Synthetic Metals, 264 (2020) 116373.

[321] M. Omastova, M. Trchová, J. Kovářová, J. Stejskal, Synthesis and structural study of polypyrroles prepared in the presence of surfactants, Synthetic Metals, 138 (2003) 447–455.

[322] C.O. Yoon, H.K. Sung, J.H. Kim, E. Barsoukov, J.H. Kim, H. Lee, The effect of low-temperature conditions on the electrochemical polymerization of polypyrrole films with high density, high electrical conductivity and high stability, Synthetic Metals, 99 (1999) 201–212.

[323] U. Acharya, P. Bober, M. Trchová, A. Zhigunov, J. Stejskal, J. Pfleger, Synergistic conductivity increase in polypyrrole/molybdenum disulfide composite, Polymer, 150 (2018) 130–137.

[324] L. Yue, Y. Xie, Y. Zheng, W. He, S. Guo, Y. Sun, T. Zhang, S. Liu, Sulfonated bacterial cellulose/polyaniline composite membrane for use as gel polymer electrolyte, Composites Science and Technology, 145 (2017) 122–131.

[325] Q. Ding, X. Xu, Y. Yue, C. Mei, C. Huang, S. Jiang, Q. Wu, J. Han, Nanocellulose-mediated electroconductive self-healing hydrogels with high strength, plasticity, viscoelasticity, stretchability, and biocompatibility toward multifunctional applications, ACS Applied Materials & Interfaces, 10 (2018) 27987–28002.

[326] J. Kopecká, M. Mrlík, R. Olejník, D. Kopecký, M. Vrňata, J. Prokeš, P. Bober, Z. Morávková, M. Trchová, J. Stejskal, Polypyrrole nanotubes and their carbonized analogs: synthesis, characterization, gas sensing properties, Sensors, 16 (2016) 1917.

[327] M. Trchová, E.N. Konyushenko, J. Stejskal, J. Kovářová, G. Ćirić-Marjanović, The conversion of polyaniline nanotubes to nitrogen-containing carbon nanotubes and their comparison with multi-walled carbon nanotubes, Polymer Degradation and Stability, 94 (2009) 929–938.

[328] P. Dange, N. Savla, S. Pandit, R. Bobba, S.P. Jung, P.K. Gupta, M. Sahni, R. Prasad, A Comprehensive review on oxygen reduction reaction in microbial fuel cells, Journal of Renewable Materials, 10 (2022) 665–697.

[329] A.P. Mártire, G.M. Segovia, O. Azzaroni, M. Rafti, W. Marmisollé, Layer-by-layer integration of conducting polymers and metal organic frameworks onto electrode surfaces: Enhancement of the oxygen reduction reaction through electrocatalytic nanoarchitectonics, Molecular Systems Design & Engineering, 4 (2019) 893–900.

[330] G. Ciric-Marjanovic, S. Mentus, I. Pasti, N. Gavrilov, J. Krstic, J. Travas-Sejdic, L.T. Strover, J. Kopecká, Z. Moravková, M. Trchová, J. Stejskal, Synthesis, characterization, and electrochemistry of nanotubular polypyrrole and polypyrrole-derived carbon nanotubes. The Journal of Physical Chemistry C, 118 (2014) 14770–14784.

[331] A.J. Bard, L.R. Faulkner, Electrochemical methods fundamentals and applications, Surface Technology, 20 (1983) 91–92.

[332] E. Wołejko, A. Jabłońska-Trypuć, A. Butarewicz, U. Wydro, Heavy metals, hydrocarbons, radioactive materials, xenobiotics, pesticides, hazardous chemicals, explosives, pharmaceutical waste and dyes bioremediation, Rhizomicrobiome Dynamics in Bioremediation, CRC Press, (2021).

[333] M. Wagner, K.-Y.A. Lin, W.-D. Oh, G. Lisak, Metal-organic frameworks for pesticidal persistent organic pollutants detection and adsorption–a mini review, Journal of Hazardous Materials, 413 (2021) 125325.

[334] V.D. Gosavi, S. Sharma, A general review on various treatment methods for textile wastewater, Journal of Environmental Science, Computer Science and Engineering & Technology, 3 (2014) 29–39.

[335] V. Katheresan, J. Kansedo, S.Y. Lau, Efficiency of various recent wastewater dye removal methods: A review, Journal of Environmental Chemical Engineering, 6 (2018) 4676–4697.

[336] T.C. Egbosiuba, M.C. Egwunyenga, J.O. Tijani, S. Mustapha, A.S. Abdulkareem, A.S. Kovo, V. Krikstolaityte, A. Veksha, M. Wagner, G. Lisak, Activated multi-walled carbon nanotubes decorated with zero valent nickel nanoparticles for arsenic, cadmium and lead adsorption from wastewater in a batch and continuous flow modes, Journal of Hazardous Materials, 423 (2022) 126993.

[337] L. Mdlalose, M. Balogun, K. Setshedi, M. Tukulula, L. Chimuka, A. Chetty, Synthesis, characterization and optimization of poly(*p*-phenylenediamine)-based organoclay composite for Cr(VI) remediation, Applied Clay Science, 139 (2017) 72–80.

[338] A. Targhoo, A. Amiri, M. Baghayeri, Magnetic nanoparticles coated with poly(*p*-phenylenediamine-*co*-thiophene) as a sorbent for preconcentration of organophosphorus pesticides, Microchimica Acta, 185 (2018) 1–8.

[339] J. Stejskal, Polymers of phenylenediamines, Progress in Polymer Science, 41 (2015) 1–31.

[340] R. Karthik, S. Meenakshi, Synthesis, characterization and Cr(VI) uptake studies of polypyrrole functionalized chitin, Synthetic Metals, 198 (2014) 181–187.

List of Appendices

Appendix 1 **I.M. Minisy**, P. Bober, U. Acharya, M. Trchová, J. Hromádková, J. Pfleger, J. Stejskal, Cationic dyes as morphology-guiding agents for one-dimensional polypyrrole with improved conductivity, *Polymer*, 174 (2019) 11–17.

Appendix 2 **I.M. Minisy**, P. Bober, I. Šeděnková, J. Stejskal, Methyl red dye in the tuning of polypyrrole conductivity, *Polymer*, 207 (2020) 122854:1–9.

Appendix 3 **I.M. Minisy**, U. Acharya, L. Kobera, M. Trchova, C. Unterweger, S. Breitenbach, J. Brus, J. Pfleger, J. Stejskal, P. Bober, Highly conducting 1-D polypyrrole prepared in the presence of safranin, *Journal of Materials Chemistry C*, 8 (2020) 12140–12147.

Appendix 4 **I.M. Minisy**, P. Bober, Frozen-state polymerization as a tool in conductivity enhancement of polypyrrole, *Macromolecular Rapid Communications*, 41(17) (2020) 2000364:1–5.

Appendix 5 **I.M. Minisy,** U. Acharya, S. Veigel, Z. Morávková, O. Taboubi, J. Hodan, S. Breitenbach, C. Unterweger, W. Gindl-Altmutter, P. Bober, Sponge-like polypyrrole–nanofibrillated cellulose aerogels: Synthesis and application, *Journal of Materials Chemistry C*, 9 (2021) 12615-12623.

Appendix 6 **I.M. Minisy**, N. Gavrilov, U. Acharya, Z. Morávková, C. Unterweger, M. Mičušík, S.K. Filippov, J. Kredatusová, I.A. Pašti, S. Breitenbach, G. Ćirić-Marjanović, J. Stejskal, P. Bober, Tailoring of carbonized polypyrrole nanotubes core by different polypyrrole shells for oxygen reduction reaction selectivity modification, *Journal of Colloid and Interface Science*, 551 (2019) 184–194.

Appendix 7 **I.M. Minisy**, B.A. Zasońska, E. Petrovský, P. Veverka, I. Šeděnková, J. Hromádková, P. Bober, Poly(*p*-phenylenediamine)/maghemite composite as highly effective adsorbent for anionic dye removal, *Reactive and Functional Polymers*, 146 (2020) 104436.

Appendix 8 P. Bober, **I.M. Minisy**, U. Acharya, J. Pfleger, V. Babayan, N. Kazantseva, J. Hodan, J. Stejskal, Conducting polymer composite aerogel with magnetic properties for organic dye removal, *Synthetic Metals*, 260 (2020) 116266.